

Copyright
by
Mandana Ashouripashaki
2012

**The Thesis Committee for Mandana Ashouripashaki
certifies that this is the approved version of the following thesis:**

**Formation and Decomposition of 1-Nitrosopiperazine in the CO₂
Capture Process**

**APPROVED BY
SUPERVISING COMMITTEE:**

Supervisor:

Gary T. Rochelle

Howard M. Liljestrand

**Formation and Decomposition of 1-Nitrosopiperazine in the CO₂
Capture Process**

by

Mandana Ashouripashaki, M.S.E.

Thesis

Presented to the Faculty of the Graduate School of

The University of Texas at Austin

in Partial Fulfillment

of the Requirements

for the Degree of

Masters of Science in Engineering

The University of Texas at Austin

December 2012

Dedication

To my beloved son, Hesam

Acknowledgments

I would like to express my sincere thanks to Prof. Rochelle, who under his great supervision and supportive encouragement I was able to do current thesis. I truly appreciate the time and effort that he spend to mentor and motivate me during this work. His patience and genuinely caring character was very impressive to me and helped me to finish this project. Being part of his research group is one of the best opportunities in my career.

I would like to thank the Luminant Carbon Management Program (LCPM) that kindly funded this work and their association to support our research group is really appreciated.

I like to thank Dr. Liljestrand who took time to read this thesis and also he provided me Lab space and apparatuses for the first phase of this research.

I really would like to thank Maeve Cooney who always was ready to help and rather than doing administrative work was a great listener and advisor.

I would like to acknowledge all members of the Rochelle research group Fred, Stephanie Freeman, Thu Nguyen, Alex Voice, Jorge Plaza, Alex Voice, Eric Chen, Humera Rafque, Sepideh Ziaii, Qing Xu, Xi Chen, Steven Fulk, Peter Frailie, Lynn Li, Omkar Namjoshi, Nathan Fine, Chao Wang, Stuart Cohen, and David Van Wagener, and other group members who may I missed. Also thanks to Dr. Hector Garcia and Dr. Chai Chen who helped me with LC-MS.

Finally, I would like to appreciate all help and support from my family especially my son Hesam who always was patient and understood me.

Abstract

Formation and Decomposition of 1-Nitrosopiperazine in the CO₂ Capture Process

Mandana Ashouripashaki, M.S.E.

The University of Texas at Austin, 2012

Supervisor: Gary T Rochelle

Piperazine (PZ) is a cyclic diamine, which means it can absorb two moles of CO₂ per mole of amine and potentially has a higher capacity for CO₂ capture than monoethanolamine, the current solvent of choice for flue gas treatment. Nitrosamines are formed from the reaction between secondary or tertiary amines and nitrites or nitrogen oxides. Over 80% of nitrosamines are carcinogenic. The reaction of PZ and nitrite can form 1-nitrosopiperazine (also mononitrosopiperazine, MNPZ) and N-N, dinitrosopiperazine (DNPZ). Carcinogenicity of DNPZ is almost 20 times as that of MNPZ. There is also a possibility of nitrosamine formation of PZ in the CO₂ capture process because of NO_x in input flue gas, with the oxidative and thermal degradation products of PZ.

Analytical methods were developed in order to perform kinetic studies of the reaction between a nitrite solution and PZ over a range of temperature from 20 to 150 °C at two different PZ concentrations, 8 and 2 mol/kg of solution, and three levels of CO₂ loading, 0.3, 0.2, and 0.1 mole CO₂/mole of alkalinity.

At less than 75 °C, nitrite reacts with PZ and disappears during the reaction to an equilibrium concentration while at the higher temperature; the concentration of nitrite quickly decreases to a very low value.

There is no evidence of DNPZ as a reaction product in all reaction conditions, but MNPZ is formed at the temperature greater than 75 °C. The MNPZ concentration approaches a maximum value consistent with the material balance and nitrite disappearance. By developing the time of reaction at the higher temperature a decomposition of MNPZ has been observed, by either the reverse of the formation reaction or decomposition to other compounds. By increasing the temperature, the maximum value of MNPZ concentration is achieved more quickly and the rate of MNPZ decomposition increases. Reactions follow the same trend at both PZ concentration and at the three different degrees of CO₂ loading. A model has been established considering temperature, PZ concentration, and CO₂ loading. The calculated activation energies of MNPZ production and decomposition were determined. MNPZ decomposition is more rapid than PZ degradation.

Table of Contents

List of Tables	x
List of Figures	xi
Chapter 1: Introduction	1
1.1 Scope of work	3
1.2 Properties of Piperazine (PZ).....	3
1.3 PZ Risk assessment.....	5
1.4 Properties of MNPZ and DNPZ.....	6
1.5 Nitrosopiperazine risk assessment	6
Chapter 2: Nitrosamine Formation	8
2.1 Nitrosamine Chemistry	12
2.1.1 N-Nitroso Compounds	13
2.1.2 S-Nitroso Compounds.....	18
2.2 Nitrosamine inhibitors	20
2.2.1 Inhibition by Ascorbic Acid.....	21
2.2.2 Inhibition by Phenols	22
2.2.3 Inhibition by Sulfur Compounds	23
2.2.4 Inhibition by some other components.....	23
2.3 N-Nitroso compound destruction.....	24
Chapter 3: Nitrosopiperazine Formation and Detection	26
3.1 Standard sample of Dinitrosopiperazine.....	26
3.1.1 Nitrosation in presence of hydrochloric acid	26
3.1.2 Nitrosation of piperazine citrate in presence of formaldehyde ...	29
3.1.3 Nitrosation of piperazine in the presence of formaldehyde	31
3.2 Quantifying Mononitrosopiperazine by HPLC.....	34
Chapter 4: Reaction of Piperazine (PZ) and Nitrite.....	36
4.1 Effect of Nitrite concentration	36
4.2 Effect of Temperature	37

4.3 Effect of PZ concentration	38
4.4 The Effect of pH	39
4.5 Effect of Formaldehyde	40
4.6 Kinetics of the reaction between nitrite and loaded piperazine	41
4.5 Reaction of NO ₂ and nitrite with loaded piperazine	45
4.6 Reaction of nitrite with loaded piperazine at high temperature	49
Chapter 5: Nitrosopiperazine Formation and Decomposition Modeling.....	56
Chapter 6: Conclusions and Recommendations	66
6.1 Temperature effect	66
6.2 The effect of UV light.....	66
Appendix A.....	68
METHOD DEVELOPMENT FOR DETECTING AND MEASURING DNPZ AND MNPZ	68
A.1 Direct injection of dinitrosopiperazine (DNPZ) to Mass Spectrometry	68
A.2 Quantifying DNPZ by Liquid chromatography and Mass Spectrometry (LC-MS).....	75
A.3 Detecting MNPZ and DNPZ in a solution of PZ.....	85
A.4 Detecting MNPZ and DNPZ in aqueous PZ using HPLC with UV detection	90
A.5 Comparing the results of LC-MS and HPLC for unknown samples	91
Appendix B	96
B.1 data for reaction rate of nitrite consumption during the reaction with pz	96
B.2 High temperature experimental data	98
REFERENCES	102
Vita.....	107

List of Tables

Table 1.1:	Summary of Physico-Chemical Properties of Piperazine, Kemi 2005.4	
Table 1.2:	Summary of Physico-Chemical Properties of NitrosoPiperazines6	
Table 3.3:	The effect of formaldehyde on dinitrosopiperazine production by the reaction between PZ citrate and sodium nitrite in the range of absorber temperatures30	
Table 3.4:	The effect of formaldehyde concentration on nitrosation reaction between PZ and sodium nitrite at different temperatures33	
Table 4.1:	Reaction conditions and rate constant of reaction between PZ and nitrite for the experiments performed in glass reactor.....45	
Table 5.1:	Reaction rate constants for different temperatures65	

List of Figures

Figure 3.1: N, N-dinitrosopiperazine production respect to the amount of hydrochloric acid in the reaction between piperazine citrate and piperazine with sodium nitrite.	29
Figure 3.2: Nitrosation PZ citrate with formaldehyde present in absorber temperature range.....	30
Figure 3.3: Nitrosation reaction of PZ in different concentrations of formaldehyde as indicated by pH.....	34
Figure 3.4: Calibration curve for standard MNPZ, with a detection limit of 4×10^{-4} mmol/kg	35
Figure 4.1: Nitrite concentration change in the reaction at 60°C and different initial nitrite concentration, (5 mmol/kg, 20 mmol/kg, and 50 mmol/kg) ..	37
Figure 4.2: Nitrite concentration changes in different temperature (21, 60, and 75°C) over a 5 days reaction time	38
Figure 4.3: Nitrite concentration changes in different PZ concentrations (2 and 8 molal) over a 6 days reaction time and 60°C	39
Figure 4.4: Effect of acidity (pH) on nitrite consumption during the reaction with 8 m PZ at 60°C	40
Figure 4.5: Effect of 50 mM formaldehyde on nitrite consumption during the reaction with 8 m PZ at 60°C	41
Figure 4.6: Natural log of reaction rate constant in terms of $1/T$ to calculate the activation energy of reaction.....	42
Figure 4.7: Reaction rate of PZ and nitrite under different conditions with respect to temperature ($1/T$)	44

Figure 4.8: Nitrite disappearance rate in an aerated reactor from the reaction of 8 m PZ and 50 mmolal/kg nitrite at 55 °C during 7 days	46
Figure 4.9: Nitrite accumulation and MNPZ production from the reaction of 8 m loaded PZ and 50 ppm NO ₂ in a low gas flow experiment with 98% O ₂ , 2% CO ₂ , and 50 ppm NO ₂ at 55 °C.	47
Figure 4.10: The reaction of 8 m loaded PZ and 50 ppm NO ₂ in high gas flow experiment with 98% O ₂ , 2% CO ₂ , and 50 ppm NO ₂ at 55 °C.....	48
Figure 4.11: Nitrite consumption and MNPZ production from the reaction of 8 m loaded PZ and 50 mmol/kg nitrite in a low gas flow experiment , 100 mL/min of 98% O ₂ , 2% CO ₂ . 55°C.	49
Figure 4.12: Nitrite consumption from the reaction of 8 m PZ, 0.3 mol CO ₂ /equiv N, and 50 mmol/kg of nitrite at high temperature	50
Figure 4.13: MNPZ production from the reaction of 8 mPZ, 0.3 mol CO ₂ /equiv N, and 50 mmol/kg nitrite at high temperature.....	51
Figure 4.14: Nitrite consumption from the reaction of 2 m PZ, 0.3 mol CO ₂ /equiv N and 50 mmol/kg nitrite at high temperature.....	52
Figure 4.15: MNPZ from the reaction of 2 mPZ, 0.3 mol CO ₂ /equiv N and 50 mmol/kg of nitrite at high temperature.	52
Figure 4.16: Nitrite consumption from the reaction of 8 m loaded PZ, 0.1 mol CO ₂ /equiv N , and 50 mmol/kg nitrite at high temperature.....	53
Figure 4.17: MNPZ production from the reaction of 8 mPZ, 0.1 mol CO ₂ /equiv N and 50 mmol/kg of nitrite at high temperature.	54
Figure 4.18: Nitrite consumption from the reaction of 8 m loaded PZ, 0.2 mol CO ₂ /equiv N , and 50 mmol/kg nitrite at high temperature.....	54

Figure 4.19: MNPZ production from the reaction of 8 m loaded PZ, 0.2 mol CO ₂ /equiv N, and 50 mmol/kg nitrite at high temperature	55
Figure 5.1: Nitrite consumption data point and best fit curves from the reaction of 8 m loaded PZ, 0.2 mol CO ₂ /equiv N, and 50 mmol/kg nitrite at the absorber temperature range.....	57
Figure 5.2: Reaction rate constant for nitrite consumption during the reaction of 8 m loaded PZ, 0.2 mol CO ₂ /equiv N, and 50 mmol/kg nitrite at the absorber temperature range.....	58
Figure 5.3: Nitrite consumption data point and fitted equation from the reaction of 8 m loaded PZ, 0.2 mol CO ₂ /equiv N, and 50 mmol/kg nitrite at the transition temperature range.	59
Figure 5.4: Reaction rate constant for nitrite consumption during the reaction of 8 m loaded PZ, 0.2 mol CO ₂ /equiv N, and 50 mmol/kg nitrite at the absorber temperature range.....	60
Figure 5.5: Reaction rate constant for reverse reaction during the reaction of 8 m loaded PZ, 0.2 mol CO ₂ /equiv N, and 50 mmol/kg nitrite at the transition temperature range.....	61
Figure 5.6: Reaction rate constant for MNPZ decomposition during the reaction of 8 m loaded PZ, 0.2 mol CO ₂ /equiv N, and 50 mmol/kg nitrite at the transition temperature range.	62
Figure 5.7: Nitrite and MNPZ concentration change data point and fitted equation from the reaction of 8 m loaded PZ, 0.2 mol CO ₂ /equiv N, and 50 mmol/kg nitrite at the stripper temperature range.....	63

Figure 5.8: Reaction rate constant for nitrite consumption during the reaction of 8 m loaded PZ, 0.2 mol CO ₂ /equiv N, and 50 mmol/kg nitrite at the stripper temperature range.....	64
Figure 5.9: Reaction rate constant for MNPZ decomposition during the reaction of 8 m loaded PZ, 0.2 mol CO ₂ /equiv N, and 50 mmol/kg nitrite at the stripper temperature range.	65
Figure A.1: Mass spectrum of a sample of DNPZ and methanol (relative abundance in terms of m/z).....	70
Figure A.2: Mass spectrum of a sample of DNPZ in methanol and water (Relative abundance in terms of m/z).....	71
Figure A.3: Mass spectrum of fragmentation of a sample of DNPZ in methanol and water by collision energy of 10. (Relative abundance in terms of m/z)	72
Figure A.4: Mass spectrum of fragmentation of a sample of DNPZ in methanol and water by collision energy of 20. (Relative abundance in terms of m/z)	73
Figure A.5: Mass spectrum of fragmentation of a sample of DNPZ in methanol and water by collision energy of 30. (Relative abundance in terms of m/z)	74
Figure A.6: Chromatogram of a sample of DNPZ in methanol and water analyzed by LC-MS	75
Figure A.7: Chromatogram of a sample of DNPZ in methanol and water analyzed by LC-MS in mass range of MNPZ (116)	76
Figure A.8: Chromatogram of a sample of DNPZ in methanol and water analyzed by LC-MS in mass range of PZ (87).....	77

Figure A.9: Chromatogram of a sample of PZ in methanol and water analyzed by LC-MS in mass range of PZ (87).....	78
Figure A.10: Chromatogram of a sample of PZ in methanol and water analyzed by LC-MS in mass range of MNPZ (116)	79
Figure A.11: Chromatogram of a sample of PZ and DNPZ in methanol and water analyzed by LC-MS in mass range of PZ (87)	80
Figure A.12: Chromatogram of a sample of PZ in methanol and water analyzed by LC-MS in mass range of DNPZ (145).....	81
Figure A.13: Chromatogram of a sample of PZ in methanol and water analyzed by LC-MS in mass range of MNPZ (116)	82
Figure A.14: Chromatogram of a sample of piperazine in methanol and water analyzed by LC-MS in mass range of PZ (87)	83
Figure A.15: Calibration curve for standard DNPZ, with a detection limit of 9×10^{-5} mmol/kg	84
Figure A.17: Chromatogram of MNPZ, DNPZ, and PZ when the mobile phase contains 40% methanol and 60% water	86
Figure A.18: Chromatogram of MNPZ, DNPZ, and PZ when the mobile phase contains 20% methanol and 80% water	87
Figure A.19: Chromatogram of MNPZ, DNPZ, and PZ when the mobile phase contains 10% methanol and 90% water	87
Figure A.20: Chromatogram of the reaction product of 8 m loaded PZ and 50 mmol/kg NaNO ₂ at 60 °C.	88
Figure A.21: Concentrations of MNPZ and DNPZ in reaction products of 8 m loaded PZ and 50 mmol/kg nitrite at 60 °C.	89
Figure A.22: Chromatogram of 500 ppm of MNPZ, DNPZ, and PZ, using HPLC91	

Figure A.23: Chromatogram of reaction products of HGF experiments at the t=0, 3 ,
and 5 days of the reaction, analyzed by LC-MS92

Figure A.24: Chromatogram of reaction products of HGF experiments at t=0, 3, and 5
days, analyzed by HPLC/UV93

Figure A.25: Chromatogram of reaction products of LGF experiments at the t=0, 3,
and 15 days of reaction, analyzed by LC-MS. as before, show the times.
.....94

Figure A.26: Chromatogram of reaction products of LGF experiments at the t=0, 3,
and 15 days of reaction, analyzed by HPLC.....95

Chapter 1: Introduction

Global warming is a worldwide policy issue and almost 98% of CO₂ emissions come from burning fossil fuels. Aqueous absorption/stripping are used generally in gas processing to remove acid gases such as carbon dioxide and hydrogen sulfide from the process gas stream. Aqueous monoethanolamine (MEA) is the present solvent of choice for flue gas treatment. In this research, piperazine (PZ) is the amine of interest. PZ is a cyclic diamine, which means it can absorb two moles of CO₂ per mole of amine and therefore potentially has a higher capacity for CO₂ capture than a monoamine. It also has a fast CO₂ absorption rate that is comparable to or even faster than that of MEA.

However the probability of producing nitrosamines from the secondary amine piperazine is not negligible in flue gas processing. Nitrosamines are formed from the reaction between secondary or tertiary amines and nitrites or nitrogen oxides. Over 80% of nitrosamines are thought to be carcinogenic.

Since the discovery of the carcinogenicity of nitrosodimethylamine (NDMA) by Magee and Barnes (1956), significant interest has been shown to the formation and characteristic carcinogenicity of several nitrosamines. Diethylamine, dimethylamine, methylaniline, methyl urea, morpholine, N-methylpiperazine, and piperazine are the most common secondary amines found in the literature in nitrosamine studies. Many of these investigations focused on the carcinogenicity of nitrosamines and their characteristic in vivo condition and human health (Mizgireuv et al., 2004; Fukushima et al., 2005; Tanaka et al., 1988; Anderson et al., 1992, Tannenbaum et al.; 1991, Kunisaki and Hayashi, 1979; Mitch and Sedlak, 2002; and many other investigators). A more detailed literature review is presented in the second chapter of this work.

The majority of nitrosamine studies have been done in acidic environments, while the CO₂ capture process operates in an alkaline environment. Primary investigations showed that there is no evidence of nitrosation under basic conditions but there are some catalysts that accelerate nitrosation in such environments (Keefer and Roller, 1973; 1974; Archer et al., 1975; Challis and Kyrtoloulos, 1977; Challis and Butler, 1968; and Challis et al., 1978).

The importance of nitrosamine formation in CO₂ capture became of concern when monoamines were replaced with the promising secondary amines such as piperazine (PZ) have been used for this process. However Strazisar et al. (2003) reported nitrosamine formation in lean MEA in a carbon capture plant at Trona, CA, but due to its low boiling point, it disappeared. DEA produced from MEA during the CO₂ scrubbing process generates nitrosamine (Fostas et al. 2011). Nitrosodimethylamine can be destroyed by UV radiation, and the reductants ascorbic acid and sulfite can reduce nitrosamine formation (Schallert, 2011).

Nitrosopiperazine can be produced by reaction of piperazine and a high concentration of nitrite in 60°C (Jackson and Ataalla, 2011). They found mononitrosopiperazine and dinitrosopiperazine in reaction products while UV radiation could degrade these nitrosamines.

In the CO₂ capture and recovery steps; there are a wide range of temperatures. This work focused on the reaction between piperazine (PZ) and nitrite at different temperatures in order to provide information about the probability of producing nitrosamines during CO₂ capture.

1.1 SCOPE OF WORK

Nitrogen compounds in capture plants come from different sources including the input flue gas, oxidative degradation of the liquid organic amine, and thermal degradation of the organic amine. With the presence of both nitrogen oxides and reduced organic amines, there is a possibility of the formation of nitrosamines, especially in systems using secondary or tertiary amines. In this work, kinetic studies of the reaction between nitrite and PZ has been performed over the range of temperature from 20 to 150°C at two different PZ concentrations, 8 and 2 mol/kg solution, and three CO₂ loadings, 0.3, 0.2, and 0.1 mol CO₂/mol alkalinity. Nitrite consumption during the reaction has been monitored by Ion Chromatography (IC), DNPZ has been screened by Liquid Chromatography followed by Mass Spectrometer (LC-MS), and MNPZ has been measured by High Performance Liquid Chromatography (HPLC).

Nitrite consumption during the reaction is modeled as a first order reaction in nitrite at all temperatures. The developed method shows the absence of DNPZ as a reaction product but MNPZ is formed at temperatures greater than 75°C. The decomposition rate of MNPZ has been observed to increase as the temperature increases. Reaction of PZ and nitrite follows the same trend with different concentrations of PZ as well as different CO₂ loadings.

1.2 PROPERTIES OF PIPERAZINE (PZ)

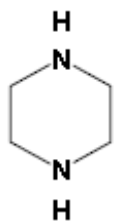
Piperazine is an organic compound that consists of a six-membered ring containing two opposing nitrogen atoms. PZ exists as small alkaline deliquescent crystals with a saline taste. At room temperature, anhydrous PZ forms white or translucent, rhomboid, or flake like crystals that are highly hygroscopic. PZ base is

available either as colorless, hygroscopic, crystalline chips or as a solution in water. The concentration is usually 64-69%.

PZ is highly basic (pH > 12 for concentrated solutions), with two dissociation constants, pK_{a1} is 5.3 and pK_{a2} is 9.7 (Kemi, 2003). PZ hexahydrate is soluble in water.

Reactions of the PZ base with acids are exothermic. PZ absorbs CO₂ from the atmosphere. In acid solution, piperazine is converted to N-Mononitrosopiperazine (MNPZ) and N, N-Dinitrosopiperazine (DNPZ) in the presence of nitrite. Table 1-1 shows a summary of PZ physical-chemical properties.

Table 1.1: Summary of Physico-Chemical Properties of Piperazine, Kemi 2005.

Property	Significance
Chemical Formula and Shape	$ \begin{array}{c} \text{H} \\ \\ \text{N} \\ \\ \text{C}_4\text{H}_{10}\text{N}_2 \\ \\ \text{N} \\ \\ \text{H} \end{array} $ 
Melting Point	107°C
Boiling Point	147.7°C
Density	1.1 g/cm ³ at 20°C
Vapor Pressure	0.44 mbar (44 Pa) at 24.2°C
Solubility	150 g/l at 20°C and pH 12 Piperazine salts differ in solubility from very slightly soluble to freely soluble in water
Partition Coefficient n-octanol/water	-1.24 at 25°C
Flash point	65°C

1.3 PZ RISK ASSESSMENT

PZ can be assumed to be rapidly photolysed in the atmosphere; the half-life is calculated to be 0.8 hours. (MSDS, 2010) In natural water it is considered to be stable towards photolysis. From laboratory studies, it can be expected that PZ is hydrolytically stable under environmentally relevant conditions. PZ is not readily biodegradable but as an organic amine is considered to be inherently degradable.

Humans may be exposed from different sources: 1) at the workplace; at the sites manufacturing PZ, at the sites of industrial use of PZ and PZ salts and at the industrial sites handling end-uses of products containing PZ and PZ derivatives; 2) from use of consumer products; and, 3) indirectly via the environment, food, soil, water and air. PZ is used in veterinary pharmaceuticals as anthelmintics, i.e., drugs that act against infections caused by parasitic worms. PZ is also used as hardener for pre-polymers for glue, in gas washer formulations, as intermediates for urethane catalysts, and as an intermediate for a number of pharmaceuticals (Kemi, 2003).

Humans can be exposed via inhalation, oral and dermal routes. The forms of PZ which humans can be exposed by inhalation are as vapor, aerosol of condensed PZ (mist), airborne solid PZ, and salts of PZ. Dermal exposure may occur at contact with the pure substance or PZ salts and at contact with products containing PZ (Kemi, 2005).

PZ in concentrated aqueous solutions has strongly irritating properties on the skin and eyes. Exposure to PZ and its salts has been demonstrated to cause allergic dermatitis as well as respiratory sensitization in humans. The genotoxic and carcinogenic properties have been investigated both in vitro (in the Ames test, in a nonstandard study on *Saccharomyces cerevisiae* and in Chinese hamster ovary cells) and in vivo, in a micronuclei assay on mice, all with negative results. Neither animal nor human have shown solid indications of a carcinogenic effect of PZ (Kemi, 2005).

1.4 PROPERTIES OF MNPZ AND DNPZ

PZ can nitrosate to form N-mononitrosopiperazine (MNPZ) and N, N'-dinitrosopiperazine (DNPZ) in vitro (Tricker et al. 1991). Nitrosation of PZ to MNPZ in the presence of nitrite is a rapid reaction, whereas the DNPZ is formed at a slower rate. MNPZ and DNPZ both are non-volatile (Kemi, 2003).

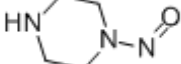
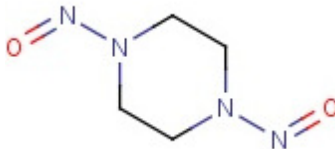
Property	Mononitrosopiperazine	Dinitrosopiperazine
Chemical Formula and Shape	C ₄ H ₉ N ₃ O 	C ₄ H ₈ N ₄ O ₂ 
Melting Point	Does not apply	158°C
Boiling Point	264.5°C	No data
Density	1.34 g/cm ³ at 20°C	1.42 g/cm ³ at 20°C
Vapor Pressure	0.44 mbar (44 Pa) at 24.2°C	No data
Solubility	Soluble in alcohol, acetone, and water	0.58 g/L in water at 20°C Soluble in alcohol, acetone, dimethylsulfoxide, hexane.
Flash point	113.8°C	Does not apply
Explosivity	Does not apply	Does not apply

Table 1.2: Summary of Physico-Chemical Properties of NitrosoPiperazines

1.5 NITROSOPIPERAZINE RISK ASSESSMENT

DNPZ and MNPZ are carcinogenic in rats (Druckery et al. 1964, 1967; Garcia et al., 1970; Thomas et al., 1965; Weisburger et al., 1966), and DNPZ has also been shown

to induce tumors in mice (Greenblatt et al., 1971; Schmehl et al., 1965; Zabezhinskii, 1969). The mutagenicity of DNPZ in *Drosophila* has been demonstrated, and DNPZ is reported to be non-mutagenic for *Escherichia coli* (Trams et al., 1965; Veleminsky and Gichner, 1968). MNPZ has not been shown to be mutagenic in any system (Love et al. 1977).

DNPZ has an acute LD50 (Lethal Dose for killing 50 % of tested species over a period of minutes to days) of 100mg/kg for mouse, and 160 mg/kg for rat. Oral administration of DNPZ (in drinking water) to rats produces epithelial tumors in the nasal cavities, upper gastrointestinal tract, liver, and lungs. DNPZ is mutagenic in the Ames test after metabolic activation. No mammalian mutagenicity or teratogenicity has been reported (Castegnaro et al., 1982).

Chapter 2: Nitrosamine Formation

Nitrosamines can be produced from the reaction between nitrites and secondary amines such as dimethylamine and PZ. Nitrosamines are a group of undesired industrial and environmental pollutants. Many of these compounds have been determined to be carcinogenic, mutagenic, or teratogenic.

Nitrosamines can cause cancers in a wide variety of animal species including humans. Since the discovery of the carcinogenicity of nitrosodimethylamine (NDMA) by Magee and Barnes (1956), much attention has been paid to the formation and characteristic carcinogenicity of several nitrosamines (Mizgireuv et al., 2004; Fukushima et al., 2005; Tanaka et al., 1988; Anderson et al., 1992). Nitrite can be formed in vivo by bacterial reduction of nitrate and by activated macrophages and endothelial cells. The mechanism of nitrite formation by mammalian cells is by enzymatic oxidation of arginine to NO followed by oxidation to N_2O_3 and N_2O_4 . Nitrosatable amines are found in many foods and some like dimethylamine are synthesized in the body. Precursors of N-nitroso compounds are almost persistently present together under favorable reaction conditions in vivo and there is, consequently, considerable interest concerning possible human health risks arising from endogenous formation of this class of compounds (Tannenbaum et al., 1991). It has been demonstrated that tertiary amines react with nitrite to form N-nitrosamines under acidic conditions (Fiddler et al., 1972; Lijinsky et al., 1972; Smith and Loepky, 1967).

Rates and kinetics of nitrosamine formation from amines and nitrous acid have been investigated. Russell et al. (1961) presented a mechanism for the reaction of diethylamine with nitric oxide. In their experiment, nitric oxide was absorbed into a methanol solution from a gas burette. They used a closed system and the volume of

observed nitric oxide was measured and then amine was added to the solution. The extinction coefficient of nitric oxide increased by adding amine. Kalatzis and Ridd (1966) studied the rate and kinetic form of the nitrosation of methylaniline with nitrous acid in aqueous perchloric acid.

Lovejoy and Vosper (1968) studied the reaction of dinitrogen trioxide with primary and secondary amines. Their experiments were conducted in an acid medium.

Mirvish et al. (1972) showed that the formation of N-nitroso compounds by the chemical reaction between nitrous acid and oxytetracycline, morpholine, piperazine, n-methylaniline, methyl urea, and dimethylamine was inhibited by ascorbic acid. They also found that urea and ammonium sulfamate were less effective inhibitors.

Keeper and Roller (1973) conducted some experiments on N-nitrosation by nitrite ion in neutral and basic media. They found that formaldehyde and chloral catalyzed the conversion of different secondary amines to nitrosamine in the pH range 6.4 to 11.

Jones et al. (1973) compared the rate of reaction with nitrous acid of four methyl substituted piperidines to form nitrosopiperidine with that of piperidine. They showed that the rate of tertiary amine nitrosation was about 10,000 times slower than that from piperidine.

Cachaza et al. (1978) studied the kinetics of dimethylnitrosamine formation in aqueous solution of perchloric acid. They showed that the initial rate of nitrosation was proportional to the square of the initial stoichiometric concentration of nitrite in the pH range of 0.8 to 4.5.

Challis and Outram (1979) investigated the formation of N-nitrosamines in solution from gaseous nitric oxide in the presence of iodine. They reported quantitative results for the N-nitrosation of piperidine, morpholine, and N-methylpiperazine by NO

(saturated solution of the gas) and iodine under anaerobic conditions in solvent ethanol, ethanol-water, and acetonitril.

Challis and Outram (1982) studied the formation of N-nitrosamines in solution from dissolved nitric oxide in the presence of hydroiodic acid (HI) or metal iodides. They reported the rapid formation of N-nitrosamines from the reaction of N-methylpiperazine, morpholine, and piperidine with nitric oxide (NO) in the presence of HI, neutral metal iodides, and acid halides plus KI in aqueous ethanol solutions at 25 °C. They noted that the formation of nitrocyll iodide and its interaction with the methylpiperazine ion are rate-limiting under neutral and mildly acidic conditions in nitrosopiperazine formation in the presence of KI and HCl.

In 2000, Masuda et al. investigated the formation of nitrosamines and nitramines by the reaction of secondary amines with nitrogen oxides, peroxyxynitrite, and nitryl chloride. They showed that peroxyxynitrite reacts with secondary amines to form both nitrosated and nitrated products and the yield of both products was higher at alkaline pH than at neutral or acidic pH.

Choi et al. (2003) investigated nitrosodimethylamine by the reaction of dimethylamine with free chlorine in the presence of ammonia and monochloramine in chlorinated water. This process did not require nitrite as nitrosation reagent. They adjusted the pH to 7.0 by using a bicarbonate buffer.

Zhao et al. (2007) presented a theoretical study on N-nitrosation of amines by NO₂ and NO. Electronic structure calculations discussed in their work suggest a free radical mechanism, in which NO₂ abstracts a hydrogen atom from the nitrogen in primary and secondary amines to form an intermediate complex of an aminyl radical and nitrous acid. The aminyl radical intermediate is then quenched by nitric oxide, leading to the formation of nitrosamine.

In 2007, Winter et al. the N-nitrosamine generation in vitro from ingested nitrate via nitric oxide with and without gastroesophageal reflux in vitro. They showed that nitric oxide generated by the reaction of salivary nitrite and acidic gastric juice may increase nitrosative stress and the generation of nitroso compounds at neutral pH.

Andrzejewski and Nawrocki (2008) investigated nitrosodimethylamine formation as a product of permanganate reaction with aqueous solutions of dimethylamine. They found that the efficiency of the reaction is lower than 0.04% and increased with increased pH. The efficiency strongly depended on the permanganate concentration and on the molar ratio of permanganate to dimethylamine.

Cooney et al. (1992) showed that nitric oxide is required for the aqueous nitrosation of amines by nitrogen dioxide. The rate of reaction is first order for both nitrogen oxide species. They also found that the formation of nitrosamines in the organic phase is also first order with respect to nitric oxide concentration, but unlike the aqueous phase reaction, extrapolation to zero NO concentration suggests that some nitrosation from N_2O_4 may occur.

Yang et al. (2009) reinvestigated the nitrosamine formation mechanism during ozonation. Their observations demonstrated the critical importance of some reactive inorganic nitrogenous intermediates, such as hydroxylamine and dinitrogen tetroxide (N_2O_4). They reported two alternative pathways that possibly explain nitrosamine. They showed the importance of reactive nitrogenous intermediates in the N-nitrosamine-formation.

Keefer and Roller (1973) conducted some experiments on N-nitrosation by nitrite ion in neutral and basic media. They found that formaldehyde and chloral catalyzed the conversion of different secondary amines to nitrosamine in the pH range 6.4 to 11. The nitrosamine formation from secondary amines and nitrites has been studied in resting

cells of *Escherichia coli*, (Kunisaki and Hayashi, 1979). They used dimethylamine and piperidine over the pH range 6 to 9. Casado et al. (1984) investigated the nitrite ion as a nitrosating reagent in the nitrosation of morpholine and diethylamine in the presence of formaldehyde. They described the kinetics of nitrosation in the presence of formaldehyde at pH values from 6.5 to 8.2 and from 6.9 to 8.7.

Mitch and Sedlak (2002) studied the formation of nitrosodimethylamine from dimethylamine during chlorination. They conducted a series of experiments in the pH range of 6 to 9 and showed that the formation of nitrosodimethylamine during chlorination may involve the slow formation of 1, 1-dimethylhydrazine from the reaction of monochloramine and dimethylamine followed by its rapid oxidation to nitrosodimethylamine and other products including dimethylcyanamide and dimethylformamide.

Lv et al. (2009) presented a theoretical investigation of nitrosodimethylamine formation from dimethylamine nitrosation catalyzed by carbonyl compounds.

2.1 NITROSAMINE CHEMISTRY

Nitrosation reactions generally have been well known in chemistry for a long time. The reactions have been much used synthetically and many features have been examined mechanistically. Literature references to N-nitrosation, include those important synthetically, industrially, and biologically, as well as mechanistically. The nitrosation (for secondary and tertiary amines) and diazotization (for primary aromatic amines) of amines have been much studied, and it has been possible to identify a variety of specific nitrosating agents as well as to describe their reactivity quantitatively for a wide collection of substances (Ridd, 1961).

Even introductory texts in organic chemistry usually discuss the chemistry of N-nitrosation in detail. Azo dyes result from the nitrosation of aromatic and heterocyclic amines. The risk regarding the formation of carcinogenic nitrosamines from secondary (and tertiary) amines is well known.

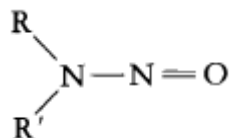
Much less is known about the S-nitrosation processes due to the relative instability of the initially formed S-nitroso species. It is to be expected that sulfur-containing compounds generally would be disposed to electrophilic nitrosation since the more polarizable sulfur atom is known (in other reactions) to be more nucleophilic than a corresponding oxygen atom. In recent years however, there has been a significant interest in the area of S-nitrosation, both from the synthetic and mechanistic viewpoints, derived from better handling techniques for the unstable compounds and the availability of fast reaction methods to measure rate constants of the rapid reactions involved (Williams, 1985).

In considering nitrosamine formation chemistry, both N-nitrosation and S-nitrosation will be considered.

2.1.1 N-Nitroso Compounds

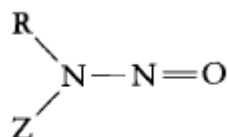
N-Nitroso compounds are formed by the interaction of a nitrogen-containing organic compound--such as an amine, amide, urea, guanidine, urethane and a nitrosating agent, such as nitrogen oxide. These compounds can be divided into two categories; nitrosamines and nitrosamides, which differ in their chemical stability, the mechanism of their carcinogenicity and their mutagenicity (Druckery et al., 1967; Druckery, 1975; Magee et al., 1976).

N-Nitrosamine



$\text{R}, \text{R}' = \text{alkyl or aryl}$

N-Nitrosamide

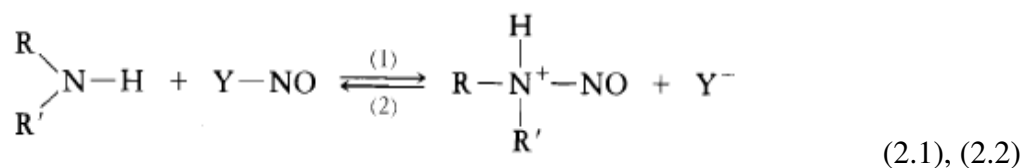


$\text{R} = \text{alkyl or aryl}$

$\text{Z} = \begin{array}{c} \text{O} \\ \parallel \\ \text{R}'\text{C}- \end{array} \text{ nitrosamide}$

Nitrosamines are very stable once they are formed. They require chemical modification in an enzyme-catalyzed action before they exhibit carcinogenic and mutagenic activity (Druckery et al., 1967; Druckery, 1975; Magee and Barnes, 1967). By comparison, the nitrosamides can be hydrolyzed, especially in neutral and alkaline solution. They exhibit carcinogenic and mutagenic activities without modification and also malignant tumors are produced at the site of their application (Druckery et al., 1967; Druckery, 1975; Magee et al., 1976; Magee and Barnes, 1967).

The chemistry of N-nitroso compounds in aqueous solution can be summarized by the following scheme.



Nitrosation of secondary amines and amides is described by Equation 2.1. The effectiveness of the nitrosating agent Y--NO depends on the nature of Y. Catalysis of nitrosation by Y' species results from its prior reaction with Y--NO, Equation 2.3 which produces the more active nitrosating agent Y'--NO. When Y is a secondary amine function, Equation 2.1 describes transnitrosation. Inhibition of nitrosation occurs by reaction of inhibitor Z with nitrosating agent Y--NO in the irreversible Equation 2.4, which is much faster than 1 and produces unreactive products.

Destruction of N-nitroso compounds by denitrosation is described by Equation 2.2. Addition of Z, in this case called a trap or scavenger, is necessary to prevent via Equation 2.4 the reversal of denitrosation, Equation 2.1 species.

Several nitrogen oxide species are nitrosating agents, but nitrous acid (HONO) and the nitrite ion (ONO-) are themselves inactive (Challis and Butler, 1968).

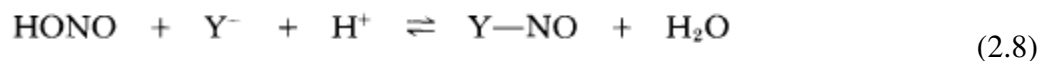
In moderately acidic aqueous nitrite solutions, the nitrosating agent is nitrous anhydride, N₂O₃ (Challis and Butler, 1968; Ridd, 1961; Mirvish, 1970, 1975), formed from nitrous acid, pK=3.138 at 25°C, after protonation of nitrite ion according to Equation 2.5 and Equation 2.6.



At lower pH, more rapid nitrosation by the nitrous acidium ion (Kalatzis and Ridd, 1966; Mirvish, 1971, 1972) becomes important, especially for weak basic aryl amines and amides.



Certain anions, Y^- , catalyze the reaction in water by forming nitrosating species Y--NO which are more reactive than N_2O_3 .



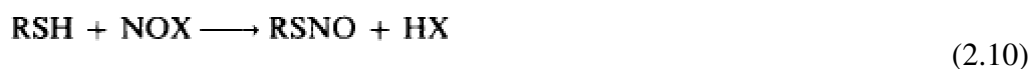
Of the anionic catalysts studied, thiocyanate has the greatest effect (Boyland, 1972; Williams, 1977; Boyland and Walker, 1974). Halide ions are also catalytic in the order SCN^- , $\text{I}^- \gg \text{Br}^- > \text{Cl}^-$ (Challis and Butler, 1968; Ridd, 1961; Mirvish, 1975; Boyland, 1971; Schweinsberg, 1974). The equilibrium concentration of Y--NO , Equation 2.8, mainly determines the order of the catalytic effect, rather than the actual reactivity of Y--NO .

As the pH is lowered below 2, rapid nitrosation by Y--NO dominates over that by N_2O_3 , lowering the pH at which the nitrosation rate is maximum compared to the uncatalyzed reaction (Mirvish, 1975; Mirvish et al., 1973; Boyland and Walker, 1974).

reactive nitrosating agents N_2O_3 and N_2O_4 . Rapid nitrosation by NO under anaerobic conditions occurs in the presence of iodine or Ag (I), Cu (I), Cu (II), Zn (II), Fe (III) or Co (II) salts (Challis and Butler, 1968; Challis et al., 1978).

2.1.2 S-Nitroso Compounds

The reaction of thiols, both aliphatic and aromatic, with nitrosating agents NOX ($NOCl$, $RONO$, NO_2 , N_2O_3 , N_2O_4 , HNO_2) to form S-nitrosothiols or thionitrites, Equation 2.10, probably represents the best-known example of an S-nitrosation process.



The reaction appears to be quite general from the point of view of the thiol and also from the range of conventional nitrosating agents, including the reaction of alkyl nitrites with thiols (Lecher and Seifken, 1926). In contrast to the corresponding reaction of alcohols (Smith, 1966), the formation of nitrosothiols is essentially irreversible. There is a recent comprehensive review of the chemistry of nitrosothiols written from the synthetic angle and in terms of the use of these compounds as synthetic reagents.

Nitrosothiols are mostly unstable (particularly when compared with alkyl nitrites), decomposing to give the disulphide and nitric oxide, Equation 2.11, presumably by a homolytic mechanism, although other non-radical pathways are possible.



Until recently it was believed that the best yields of nitrosothiols were obtained by reaction of the thiol with dinitrogen tetroxide N_2O_4 in equimolar amounts at -10°C in an

inert solvent such as hexane, ether, carbon tetrachloride, or acetonitrile (Oae et al., 1978). Dinitrogen tetroxide can act as an excellent nitrosating agent (as well as being a source of NO_2 radicals) and can be thought of as NO^+NO_3^- in a number of inorganic reactions (Addison, 1960) as well as in organic reactions where, for example, alkyl nitrites can be made from alcohols (Gray and Yoffe, 1955), nitrosamines from secondary amines (White and Feldman, 1957), nitrosamides from amides (White, 1955), and the nitroso nitrate adduct from an alkene (Parts and Miller, 1969).

A mechanism was suggested based on the formation and subsequent decomposition of S-nitrosocysteine, though it was not established whether it was formed by direct attack of the nitrosamide or whether some free nitrosating species was first formed.

It has recently been suggested (Doyle et al., 1983) that convenient syntheses of nitrosothiols can be achieved using an alkyl nitrite, specifically t-butyl nitrite, as the reagent in a solvent such as chloroform. Quantitative yields were observed from t-butyl thiol and benzyl thiol.

All the experiments so far described above on the nitrosation of amino thiols (cysteine etc.) indicate that S- rather than N-nitrosation occurs. However it does seem that under certain conditions, the product derived from N-nitrosation can be formed in reasonable yield.

Some rate measurements have been carried out on the nitrosation of thiols. Three groups of workers have independently established the rate law given in Equation 2.12 for the reactions of t-butyl thiol (in 50% aqueous dioxine), cysteine in water and a number of mercapto-carboxylic acids (in water) (Dix and Williams, 1984).

$$\text{Rate} = k[\text{Thiol}][\text{H}^+][\text{HNO}_2] \quad (2.12)$$

This is a familiar rate equation (Williams 1983) which applies under certain experimental conditions to the nitrosation of a wide variety of substrates including primary and secondary amines (aromatic and aliphatic), alcohols, hydrazine, hydrazoic acid, ureas etc., and is generally interpreted in terms of a mechanism involving rate-limiting attack by a positively charged species H_2NO_2^+ or NO^+ . At the acidities employed, the extent of protonation of the thiol is negligible, so there is no complication of speciation with respect to pH as generally found for basic substrates.

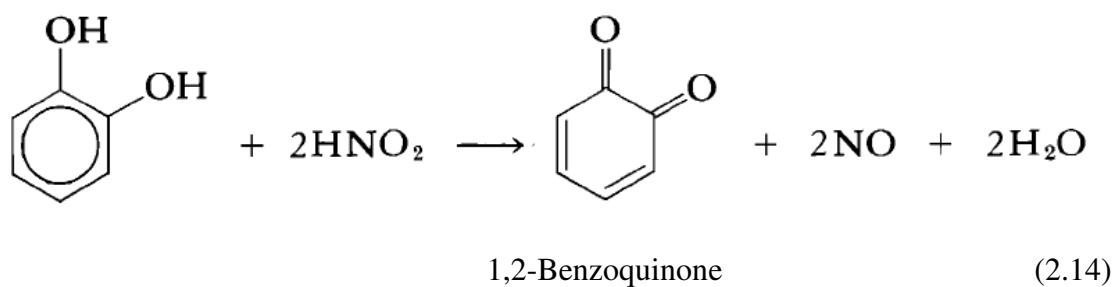
2.2 NITROSAMINE INHIBITORS

Studies of nitrosamine inhibition have consisted of the use of substances which compete with the amine for nitrosating species. Virtually all the compounds proposed for this purpose show an inhibiting influence on the reaction as a result of the inactivation of nitrosating agents, but this can be achieved in different ways. Many substances inhibiting the formation of nitrosamine react with nitrosating agents, reducing them to the relatively inactive nitric oxide. Naturally, the retardation of the reaction is achieved most simply by altering the conditions and most importantly the pH.

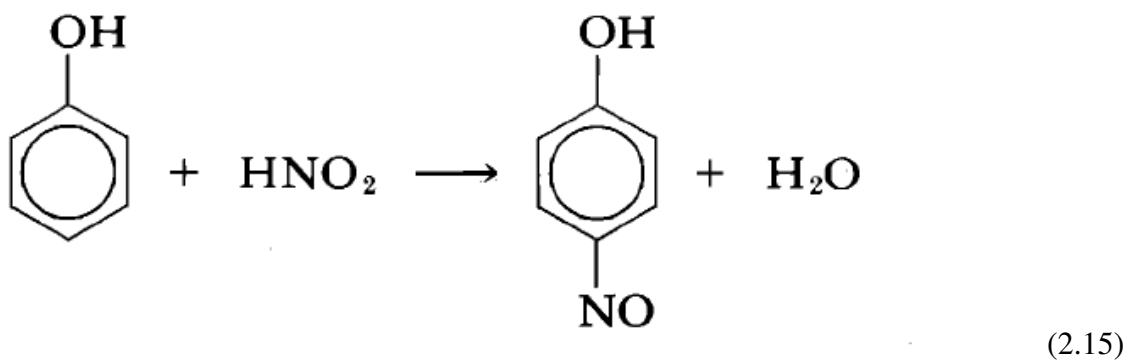
Archer et al. (1975) did a study of the nitrosation of morpholine in the presence of ascorbic acid. The amount of ascorbate required to completely inhibit the formation of nitrosomorpholine depended on whether oxygen was present. A pH dependent induction period observed during the nitrosation of morpholine in the presence of ascorbate and excess nitrite was accounted for by the kinetics of the reactions.

2.2.2 Inhibition by Phenols

Phenols inhibit nitrosamine formation; in systems containing nitrite, phenols and secondary amines several reactions compete. The inhibition of nitrosamine formation may occur by reduction of nitrite to un-reactive nitric oxide (Challis and Bartlett, 1975), and formation of quinones. The components derived from aromatic compounds by conversion of an even number of $-CH=$ groups into $-C(=O)-$ groups (Equation 2.14).



The other inhibition reaction is removing the nitrite by C-nitrosation, Equation 2.15.

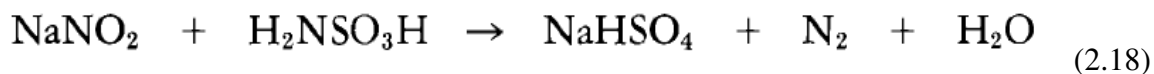


2.2.3 Inhibition by Sulfur Compounds

Bisulfite reduces nitrite in two steps (Hisatune, 1961), first to nitric oxide, Equation 2.16 and then to nitrous oxide, Equation 2.17.

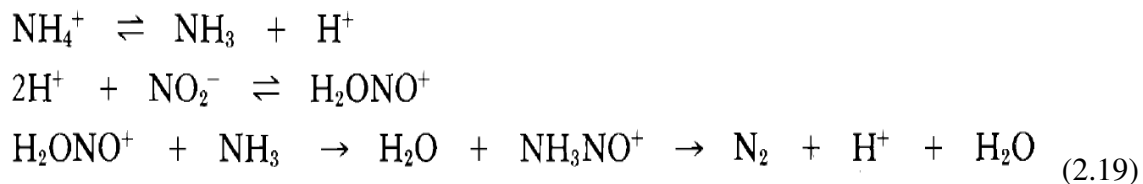


Sulfamate is the other sulfur compound which reduces nitrite, in this case to molecular nitrogen, Equation 2.18.



2.2.4 Inhibition by some other components

Ammonium ion is one of the components which react with nitrite to form molecular nitrogen (Jones et al., 1973) by the following chain reactions:

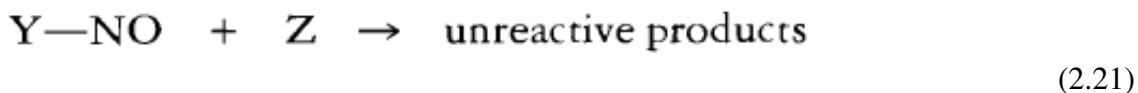
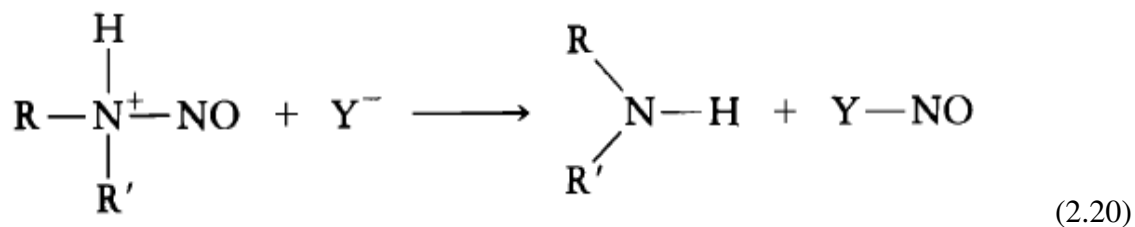


Hydroxylamine, urea, caffeine, vitamin A, and ethanol are also nitrosamine formation inhibitors (Mirvish et al., 1972; Gray and Dugan, 1975).

2.3 N-NITROSO COMPOUND DESTRUCTION

Nitrosamines are usually stable and hard to destroy. Most of them are stable in neutral and strong alkaline solutions, but they can be destroyed slowly in acid solution at concentration of 1-5 M acid (Magee and Barnes, 1967).

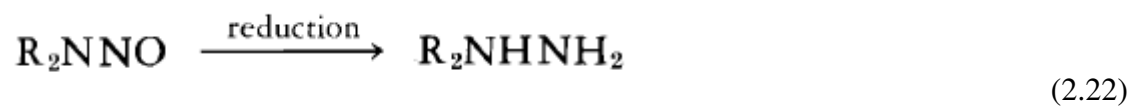
Some anions (Y^-) such as I^- , $SC(NH_2)_2$, SCN^- , Br^- , and Cl^- can catalyze the denitrosation reaction, Equation 2.20 (Williams, 1977; Biggs and Williams, 1975). To prevent a reverse reaction and producing nitrosamine, a substance (Z) should be added which can react with $Y-NO$ faster than the amine. Hydrazoic acid, hydrazine, sulfamic acid, aniline, hydroxylamine, and urea (Williams, 1975) are such substances, Equation 2.21.



Exposure to UV light can decompose nitrosamine to aldehydes, nitrogen, and nitrous oxide or even to amine and nitrous acid depending on the used wavelength used (Polo et al., 1976; Polo and Chow, 1976).

Nitrosamines can be reduced by zinc in acetic acid, sodium amalgam, tin in hydrochloric acid, and lithium aluminum hydride (Friedman et al., 1971). This nitrosamine reduction will form hydrazines, as in Equation 2.22, with other products

depending on reducing agent and reaction condition (Crosby and Sawyer, 1976). Hydrazines are carcinogenic but their carcinogenicity is about 100 times less than the corresponding nitrosamines.



Chapter 3: Nitrosopiperazine Formation and Detection

This research developed a method to quantify Mononitrosopiperazine (MNPZ) and N, N Dinitrosopiperazine (DNPZ) using a combination of mass spectrometry and/or HPLC in non-biological conditions. The kinetics of nitrosamine formation and decomposition was measured at conditions of CO₂ capture using aqueous piperazine (PZ).

A standard sample of MNPZ was purchased. DNPZ was synthesized by USP method 24 (2000). In the production of DNPZ from piperazine citrate and from PZ, a quantitative comparison has been made on the DNPZ production efficiency. The USP 24 procedure uses nitrosation under acidic conditions. Attempts were also made to prepare DNPZ in the presence of formaldehyde, because studies showed that formaldehyde can catalyze the nitrosation under alkaline conditions (Keefer and Roller, 1973; Kunisaiki and Hayashi, 1978). Experiments were conducted over the range of CO₂ capture absorber temperature.

3.1 STANDARD SAMPLE OF DINITROSOPIPERAZINE

The fundamental procedure is the same for experiments in both acidic and alkaline conditions and follows USP 24.

3.1.1 Nitrosation in presence of hydrochloric acid

The following steps are included in the USP 24 method.

- 1- Make a solution of 2 g PZ citrate and 50 mL hydrochloric acid 3N and filter it.
- 2- Add 10 mL of sodium nitrite solution (1 part sodium nitrite and 2 parts water).
- 3- Chill the solution in an ice bath for 15 minutes while stirring.

- 4- Filter solution to separate precipitate.
- 5- Wash filtrate with cold water.
- 6- Dry the product (N, N-dinitrosopiperazine).

The above steps were followed and after drying the filtrate, yellow pale crystals of DNPZ were obtained. During the reaction a significant amount of brown gas was released, which is nitrogen dioxide.

DNPZ was synthesized over a range of pH. Results are shown in Tables 3.1 and 3.2 and Figure 3.1.

To see the difference between nitrosation yield of PZ citrate and PZ, the experiments were done with PZ as well.

Table 3.1 shows the conditions of reaction between PZ citrate and sodium nitrite (NaNO_2) in the presence of HCl. At low pH, amine will be protonated and NO^+ , which is a nitrosating reagent, will be released. The nitrite ion reacts with the PZ ion and makes MNPZ and DNPZ. Experiments show a greater yield of DNPZ at pH 2 and 3 than at other pH values. This pH range is almost the same for reactions which use PZ instead of PZ citrate (2.11–3.11).

The general reaction equation for the producing DNPZ from piperazine citrate is as follows:

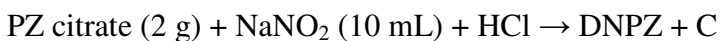


Table 3.1: The effect of HCl on dinitrosopiperazine yield by USP 24 method

Piperazine citrate (g)	Sodium nitrite (1 to 2) (mL)	Hydrochloric acid (3N) (mL)	pH of the Solution	N,N-Dinitrosopiperazine (g)
2	10	0	8.20	0
2	10	10	4.00	1.06
2	10	20	2.98	1.72
2	10	30	2.40	1.10
2	10	40	2.00	1.21
2	10	50	1.76	0.90
2	10	60	1.57	0.88
2	10	70	1.40	0.60

Table 3.2: The effect of HCl on dinitrosopiperazine production using piperazine in USP 24 method

Piperazine (g)	Sodium nitrite (1 to 2) (mL)	Hydrochloric acid (3N) (mL)	pH of the Solution	N,N-Dinitrosopiperazine (g)
2	10	0	6.90	0
2	10	10	4.21	1.09
2	10	20	3.11	3.73
2	10	30	2.50	2.77
2	10	40	2.11	3.3
2	10	50	1.83	3.1
2	10	60	1.62	3.00
2	10	70	1.45	2.49

Figure 3.1 shows a comparison between DNPZ formation when PZ citrate and PZ have been used in the presence of different quantities of HCl, at different pH values. These observations have been demonstrated before for some secondary amines and amino acids, (Mirvish, 1972, 1975; Zeibarth, 1975; Lijinsky and Keefer, 1970; Bonnett and Nicolaidou, 1977), and this research shows the same behavior for both PZ and PZ

citrate nitrosation. DNPZ that has been synthesized at a pH of 1.76 will be used as a standard to develop a preferred method for DNPZ detection in LC-MS

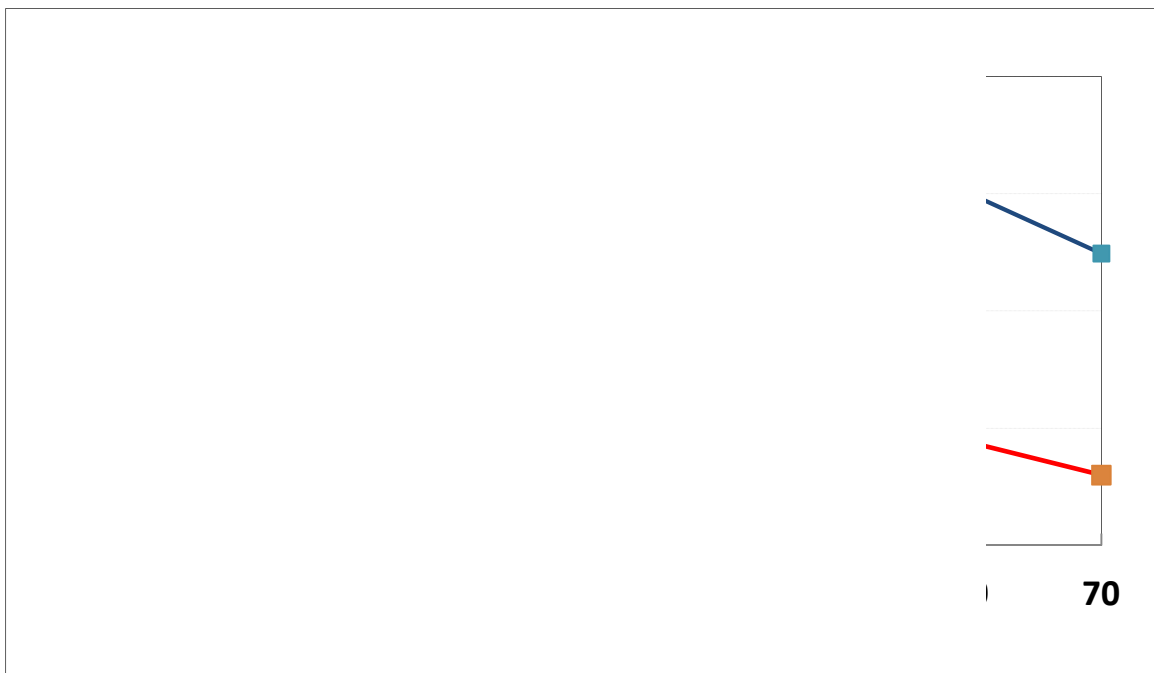


Figure 3.1: N, N-dinitrosopiperazine production respect to the amount of hydrochloric acid in the reaction between piperazine citrate and piperazine with sodium nitrite.

3.1.2 Nitrosation of piperazine citrate in presence of formaldehyde

In an alkaline solution, there is no nitrosation reaction. Thus when experiments were performed with a mixture of PZ citrate and sodium nitrite with at pH of 8.2, there was no evidence for the production of DNPZ. When formaldehyde was added to the process, however, DNPZ precipitation was observed. Experiments have been performed using different concentrations of formaldehyde, and under the range of temperature conditions found in the absorber. Results are shown in Table 3.3 and Figure 3.2.

Table 3.3: The effect of formaldehyde on dinitrosopiperazine production by the reaction between PZ citrate and sodium nitrite in the range of absorber temperatures

Piperazine citrate (g)	Sodium nitrite (1 to 2) (mL)	Formaldehyde (37%) (mL)	pH of the Solution	N,N-Dinitrosopiperazine (<i>mole DNPZ/mole PZ</i>)			
				20°C	40°C	50°C	60°C
2	10	0	8.20	0	0	0	0
2	10	1	6.18	0.56	0.59	0.45	0.4
2	10	2	5.91	0.76	0.77	0.62	0.52
2	10	3	5.69	0.57	0.53	0.44	0.42
2	10	5	5.33	0.93	0.66	0.52	0.49
2	10	10	4.75	0	0	0	0
2	10	15	4.40	0.56	0.59	0.45	0.4
2	10	20	4.0	0.0	0.0	0.47	0.0

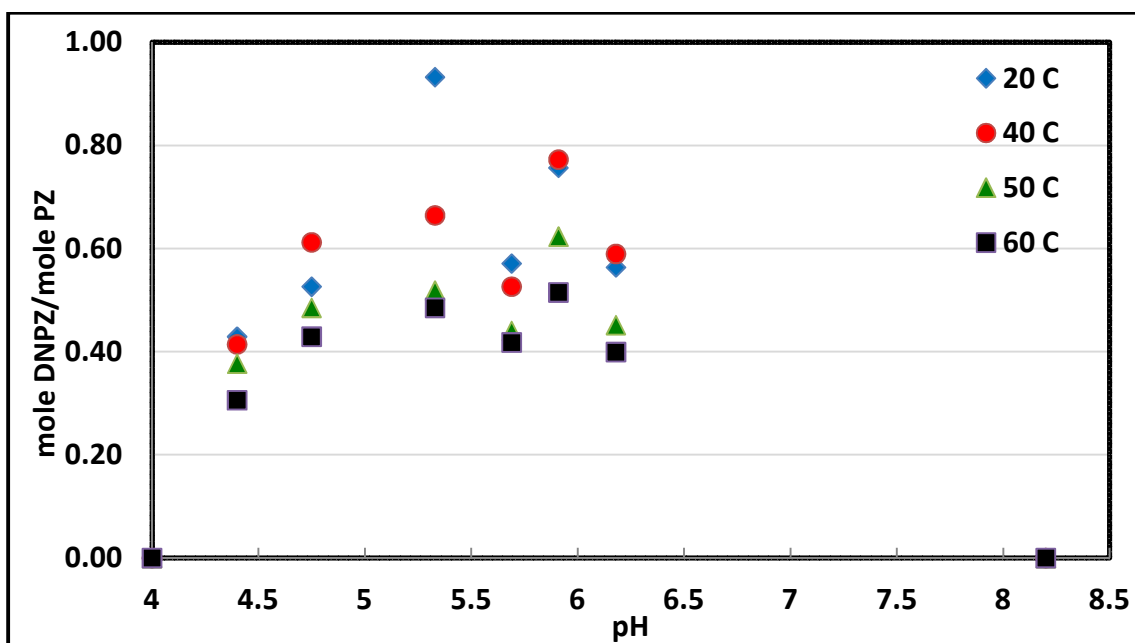


Figure 3.2: Nitrosation PZ citrate with formaldehyde present in absorber temperature range

Previous research shows that there is no evidence of PZ citrate nitrosation at a pH greater than 4. This new result shows that formaldehyde has a catalytic effect on the reaction and nitrosation does occur at a pH greater than 4.

Figure 3.2 shows a comparison between nitrosation reaction products when PZ citrate has been used in the presence of different quantities of formaldehyde (different pH).

The temperature effect on nitrosation reaction has been investigated and the results are given in Figure 3.2. At low temperature (20 °C) the reaction efficiency is greater than at other temperatures, and when the temperature increases, the efficiency of nitrosation decreases. At higher temperature, more time is required for starting the reaction.

3.1.3 Nitrosation of piperazine in the presence of formaldehyde

A solution of 2 g PZ and 10 mL sodium nitrite (1/2 V) was prepared with a measured pH of 10.45. Under the defined conditions there was no evidence of any reaction between these reagents, but adding formaldehyde and changing the pH initiated a nitrosation reaction. Experiments have been conducted with different concentrations of formaldehyde and at various pH levels in the temperature range of 20–98 °C; results are shown in Table 3.4 and Figure 3.3. These reactions have been investigated because there is some evidence of aldehydes in amine degradation products, and an aldehyde can be formed as an intermediate product of the reaction between CO₂ and monoethanolamine (MEA).

Table 3.4 shows conditions of reaction between PZ and sodium nitrite (NaNO₂) in the presence of formaldehyde. As noted in the introduction, nitrosation at alkaline

conditions is unlikely, but catalysts such as formaldehyde can accelerate the nitrosating reaction.

Reactions at high pH have been started by PZ citrate and sodium nitrite and, as expected, there is no evidence of DNPZ. Adding formaldehyde and maintaining a high pH, however, causes the largest amounts of DNPZ to form (precipitation). Figure 3 shows the effect of increasing the formaldehyde value in reactions at different temperatures in the range of absorber temperature.



Nitrosation of PZ did not occur at a pH greater than 8, an alkaline environment without formaldehyde, but the new results show that in very strong basic medium (high pH), formaldehyde can catalyze a nitrosation reaction of PZ.

Figure 3.3 shows a comparison between nitrosation reaction products when PZ has been used in the presence of different quantities of formaldehyde (different pH). These observations have been demonstrated before for some secondary amines and amino acids (Mirvish, 1970, 1975; Lijinsky and Keefer, 1970), and this research shows the same behavior for PZ nitrosation.

The temperature effect on nitrosation reaction has been investigated and the results are shown in Figure 3.2. At low temperature (20 °C) the reaction efficiency is greater than at other temperatures and increasing the temperature decreases the efficiency of nitrosation reaction. It is also observed that at a higher temperature it takes longer for the reaction to start.

Table 3.4: The effect of formaldehyde concentration on nitrosation reaction between PZ and sodium nitrite at different temperatures

Piperazine (g)	Sodium nitrite (1 to 2) (mL)	Formaldehyde (37%) (mL)	pH of the Solution	Nitrosation reaction products (g)				
				20 °C	40 °C	60 °C	80 °C	98 °C
2	10	0	10.45	0	0	0	0	0
2	10	1	10.21	0.6	0.81	0.64	0.6	0.62
2	10	2	10.17	0.9	0.94	0.94	0.94	0.94
2	10	3	10.06	0.7	0.68	0.81	0.62	0.77
2	10	4	9.98	0.7	0.62	0.56	0.43	0.85
2	10	5	9.65	0.8	0.72	0.62	0.31	0.53
2	10	6	9.51	0.7	0.6	0.36	0.34	0.25
2	10	7	9.33	0.5	0.58	0.47	0.24	0.28
2	10	8	9.12	0.6	0.36	0.45	0.39	0.25
2	10	10	8.96	0.6	0.31	0.23	0.26	0.21
2	10	12	8.8	0.5	0.35	0.25	0.17	0.12
2	10	15	8.71	0.4	0.21	0.13	0.13	0.12
2	10	20	8.55	0.3	0.21	0.11	0.08	0.05
2	10	30	8.00	0.0	0.0	0.0	0.0	0.0

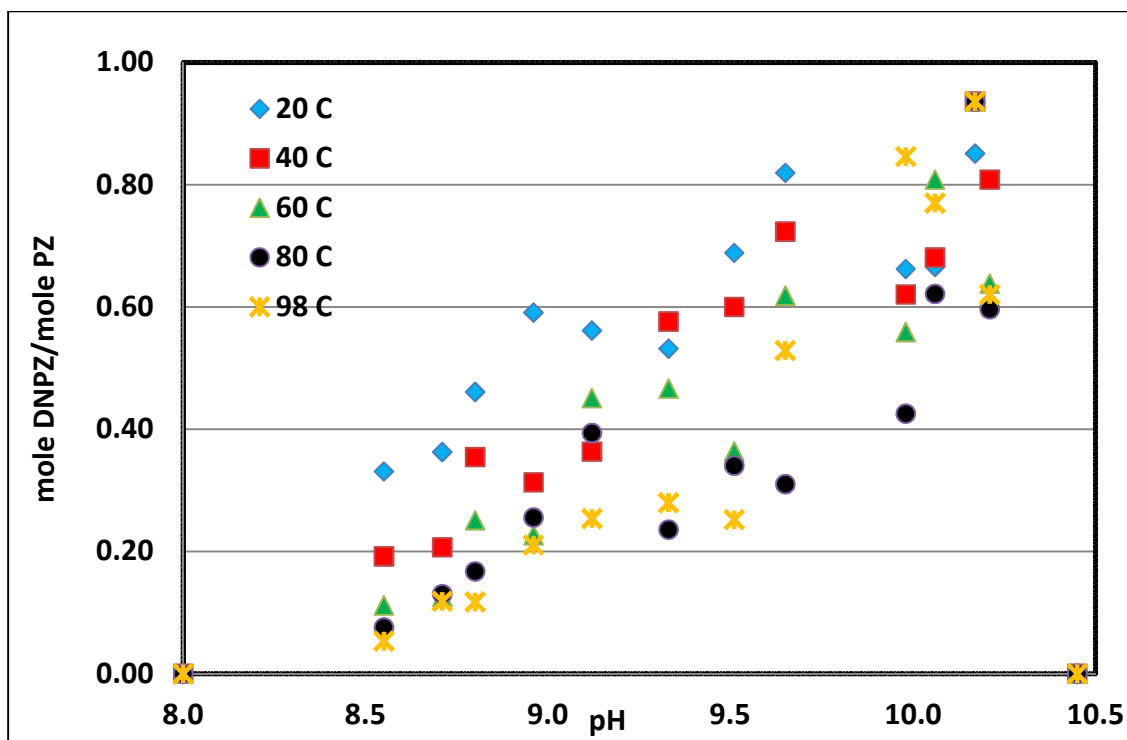


Figure 3.3: Nitrosation reaction of PZ in different concentrations of formaldehyde as indicated by pH

3.2 QUANTIFYING MONONITROSOPIPERAZINE BY HPLC

An analytical method has been applied to standard solutions of MNPZ using HPLC. A calibration curve for measuring MNPZ was prepared using a standard reverse phase of 0.01 M acetonitrile in water buffered with ammonium carbonate to analyze a standard MNPZ solution of methanol with a dilution factor of 20. Figure 3.4 shows the calibration curve of MNPZ.

The HPLC used is a Dionex UltiMate 3000 LC with Chromeleon interface and an Acclaim[®] Polar Advantage column. The device uses a 2100 UV detector and scanning wavelength for detecting MNPZ is 240 nm.

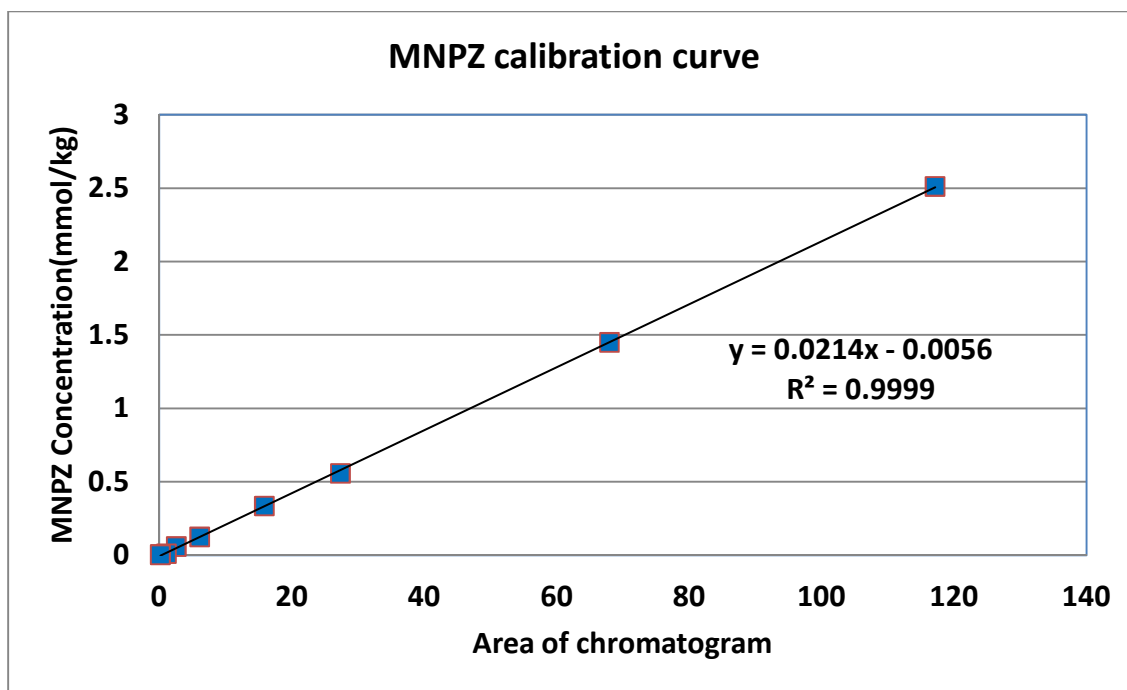


Figure 3.4: Calibration curve for standard MNPZ, with a detection limit of 4×10^{-4} mmol/kg

Chapter 4: Reaction of Piperazine (PZ) and Nitrite

This section presents results on the kinetic study of the reaction between PZ and nitrite.

Two different methods have been used in this section for low temperature experiments and high temperature experiments. At low temperature, the reactor was a mL clear glass volumetric flask with glass top, the heating source was a water bath, and samples were collected in clear glass sampling bottles. Therefore the reactants and samples were exposed to the UV from the light in the fume hood and room. At high temperature, the reaction was done in closed 10 mL cylinder and samples were collected in amber glass bottles which reduced the exposure to the UV. Later studies show that exposure to the UV causes nitrosamine decomposition.

4.1 EFFECT OF NITRITE CONCENTRATION

The experiments started with 8 molal (8 m) loaded PZ at 60 °C, which is the absorber temperature. Three different concentrations of NaNO₂, 5, 20, and 50 mmolal, were reacted with PZ solution to measure the loss of nitrite. Eight samples were taken over 7 days and analyzed by IC to monitor the concentration of nitrite. Results show that lower concentrations of nitrite react more slowly with 8 m loaded PZ (Figure 4.1), and nitrite loss is pseudo linear. Therefore the concentration of 50 mmolal of nitrite was chosen for later experiments.

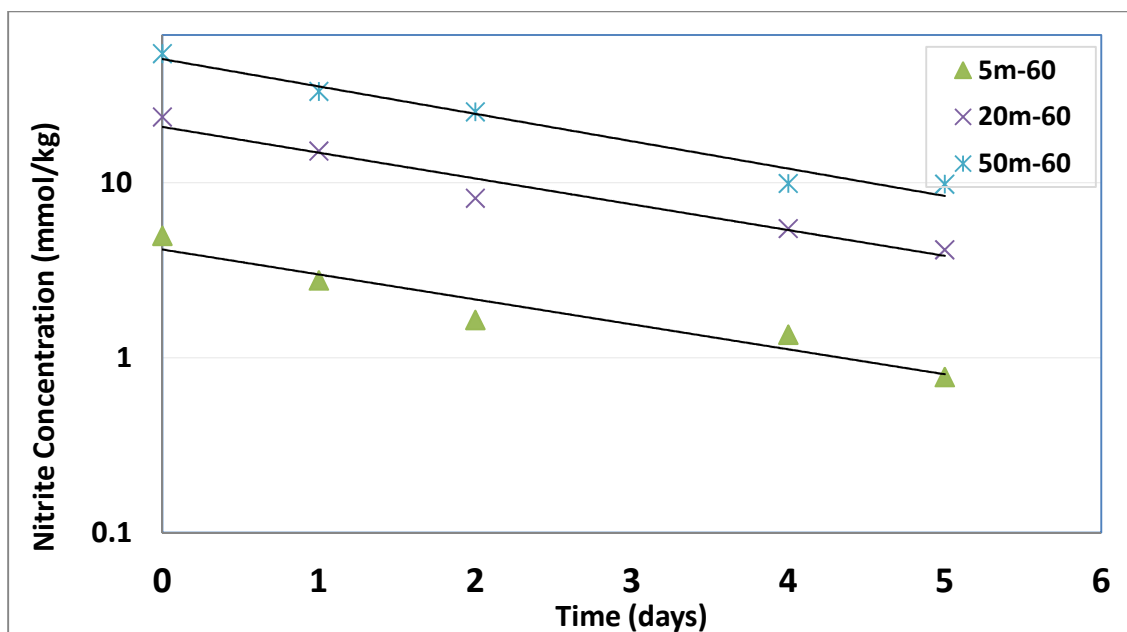


Figure 4.1: Nitrite concentration change in the reaction at 60°C and different initial nitrite concentration, (5 mmol/kg, 20 mmol/kg, and 50 mmol/kg)

4.2 EFFECT OF TEMPERATURE

Additional experiments were carried out to determine the activation energy of reaction, using 8 m loaded PZ and 50 mmolal of NaNO_2 at three different temperatures, 21, 60, and 75 °C for 6 days. Results show that at 75 °C, nitrite concentration decreases faster than at the other two temperatures (Figure 4.2).

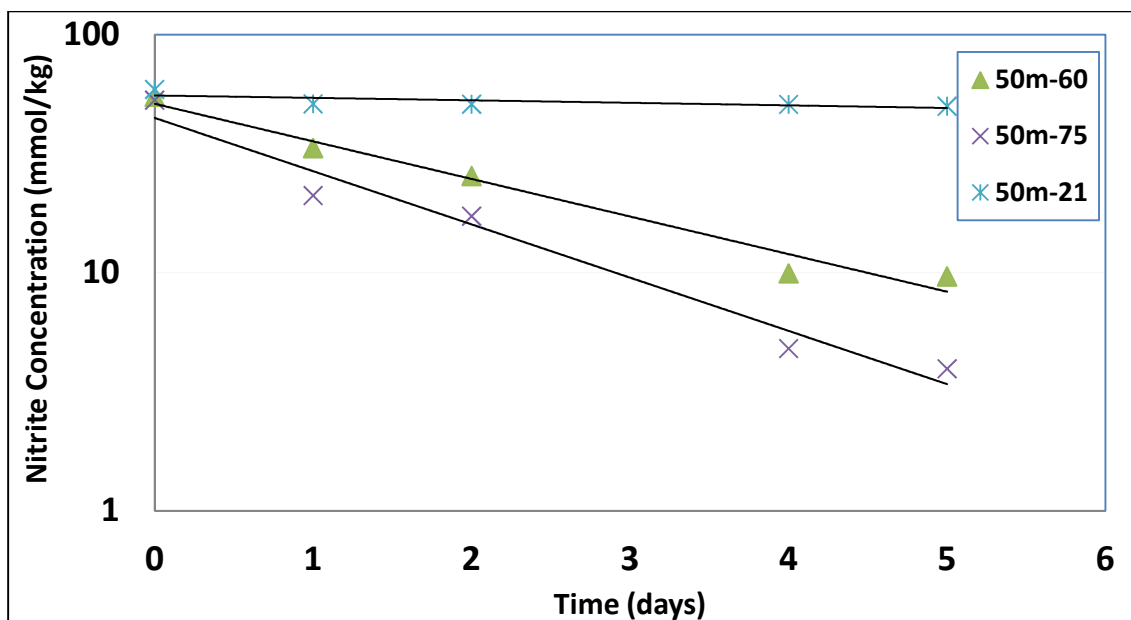


Figure 4.2: Nitrite concentration changes in different temperature (21, 60, and 75°C) over a 5 days reaction time

4.3 EFFECT OF PZ CONCENTRATION

To assess the effect of PZ concentration on nitrite loss, instead of 8 m loaded PZ, the nitrite reaction of 2 m loaded PZ and 50 mmolal of nitrite at 60 °C was examined. Results show that a lower concentration of PZ causes lower nitrite consumption (Figure 4.3), but reaction to the PZ concentration is first order (Figure 4.3).

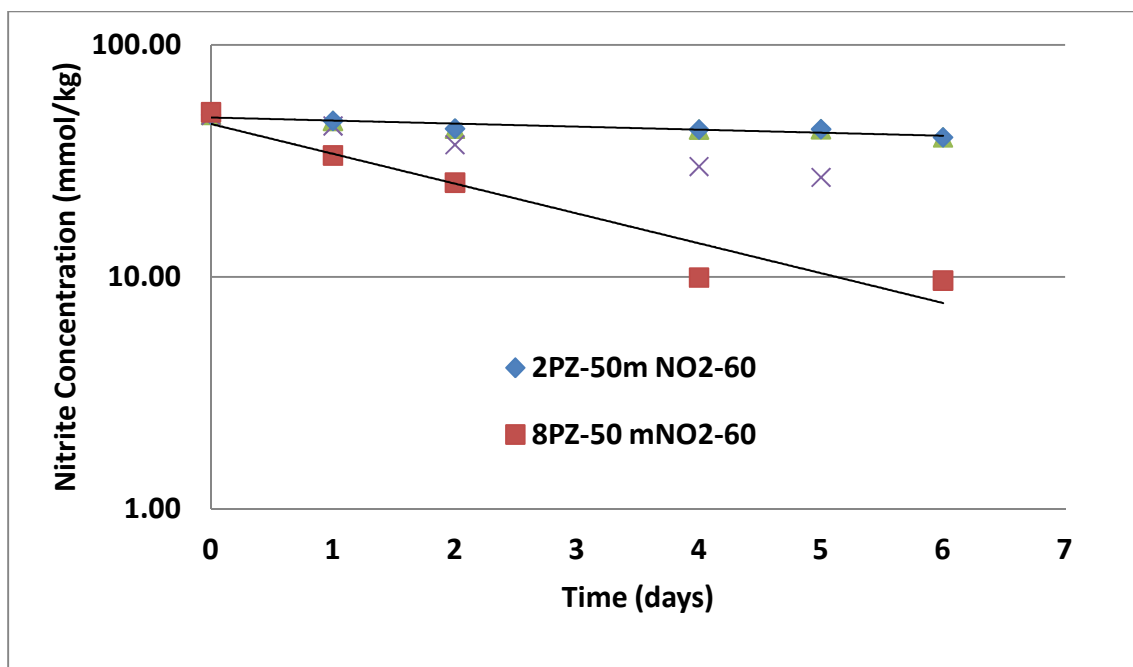


Figure 4.3: Nitrite concentration changes in different PZ concentrations (2 and 8 molal) over a 6 days reaction time and 60°C.

4.4 THE EFFECT OF pH

Unloaded PZ reacts very slowly with nitrite compared to loaded PZ. H_2SO_4 was used to adjust the pH of the solution in order to confirm the effect of loading. Sulfuric acid was shown to catalyze the reaction but to a lesser degree than CO_2 in loaded PZ (Figure 4.4).

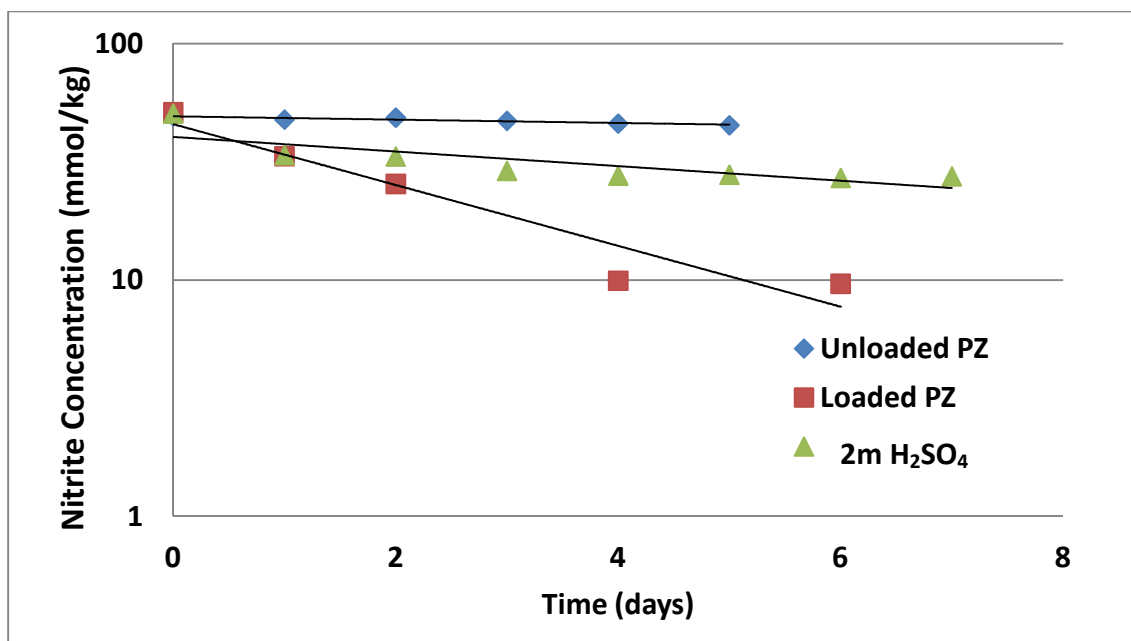


Figure 4.4: Effect of acidity (pH) on nitrite consumption during the reaction with 8 m PZ at 60°C.

4.5 EFFECT OF FORMALDEHYDE

Since formaldehyde is known as a catalyst for nitrosation in alkaline solution, nitrite loss in 8 m loaded PZ in the presence of 50 mmol/kg formaldehyde has been studied. Formaldehyde increases the rate of reaction slightly, with more nitrite consumption after the same period compared to the reaction without formaldehyde (Figure 4.5).

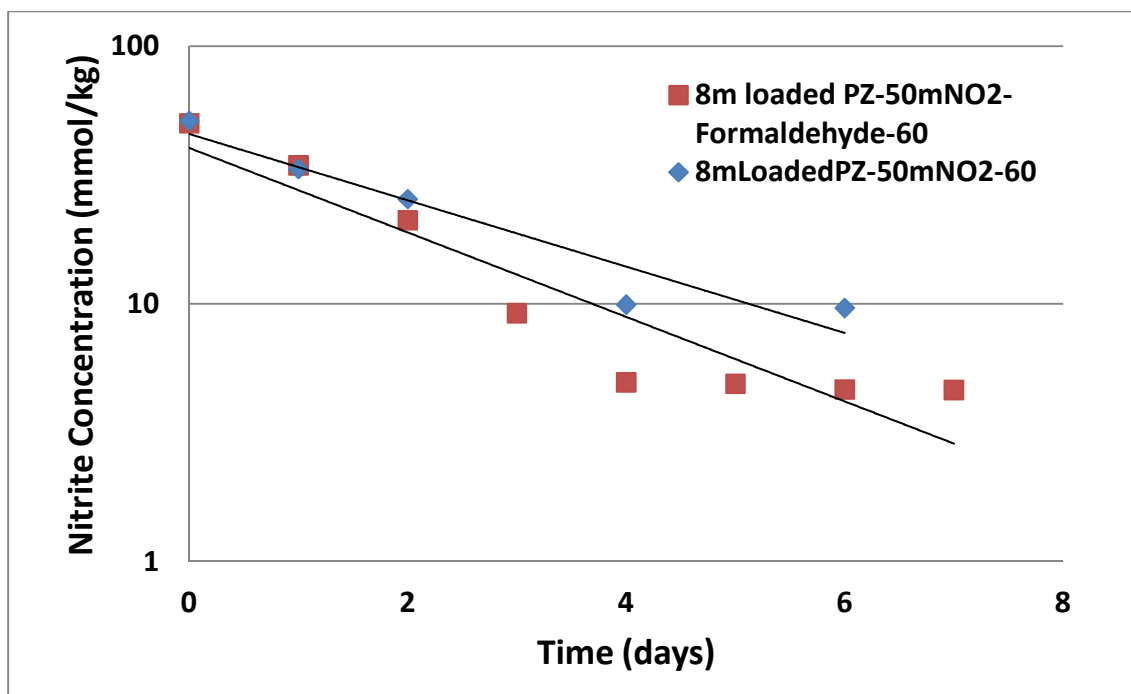


Figure 4.5: Effect of 50 mM formaldehyde on nitrite consumption during the reaction with 8 m PZ at 60°C.

4.6 KINETICS OF THE REACTION BETWEEN NITRITE AND LOADED PIPERAZINE

The results for the disappearance of nitrite suggest that nitrite reacts with PZ by a first order reaction in both total PZ and total nitrite:

$$\text{Rate (mol/day-kg solution)} = k_2 [\text{PZ}]_T [\text{NO}_2^-]$$

where the concentrations are given in mol/kg solution

In a given experiment the total piperazine $[\text{PZ}]_T$ is assumed to be constant and the loss of nitrite follows first order behavior, so the rate constant, k_2 , is determined from the fit of data given by:

$$\ln[\text{NO}_2^-] = \ln [\text{NO}_2^-]_0 - k_2 t$$

or

$$\ln[\text{NO}_2^-] = \ln [\text{NO}_2^-]_0 - k_2[\text{PZ}]_T t$$

Where $k_2 = b/[\text{PZ}]_T$

The rate constant, k_2 , is further correlated as a function of temperature using the Arrhenius expression:

$$k_2 = (k_2)_{\text{ref}} e^{(-E/RT)}$$

$$\ln(k_2) = \ln(k_2)_{60^\circ\text{C}} + (E/R)(1/T - 1/333)$$

Figure 4.6 shows that all three reactions (at 21, 60, and 75 °C) follow a linear path on a log/linear plot so the slope of each line is the first order reaction rate constant at each temperature (K_r). The reaction activation energy is obtained from the slope of $\ln(k_2)$ versus reciprocal temperature as in Figure 4.6.

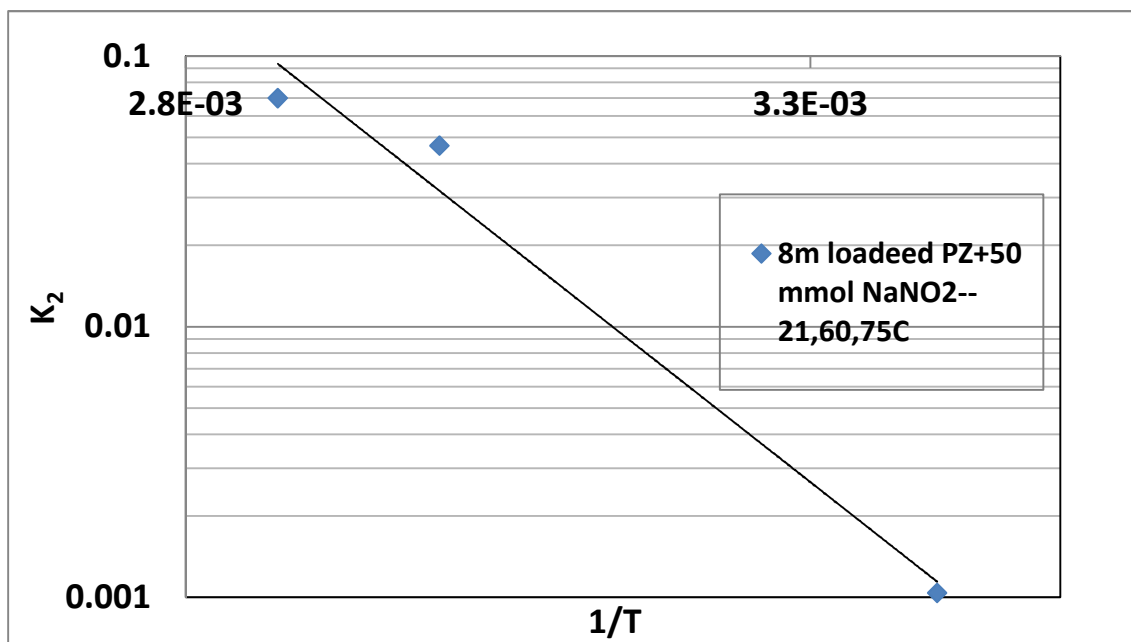


Figure 4.6: Natural log of reaction rate constant in terms of $1/T$ to calculate the activation energy of reaction

Reaction activation energy has been calculated as follow;

$$k_{2(60^{\circ}\text{C})} = 0.0463$$

$$R = 8.314 \text{ J/K.mole}$$

$$E_a/R = 8346$$

$$E_a = 69.4 \text{ KJ/mole}$$

Based on previous results and calculations, the following equation represents a general reaction rate of loaded PZ and nitrite:

$$R = k_2[\text{PZ}]_T[\text{NO}_2^-]$$

From this, the equation for calculating the reaction rate constant for PZ and nitrite is as follows:

$$\ln(k_2) = 0.0463 + (8346)(1/T - 1/333)$$

Formaldehyde is a well-known catalyst in nitrosation reactions, but results show that the reaction rate of 8 m loaded PZ and 50 mmol/kg nitrite in the presence of formaldehyde is slightly higher than without catalyst. Loaded PZ is more reactive with nitrite, which might be related to the acidic behavior of CO_2 and water in solution, but results of the reaction of unloaded 8 m PZ and 50 mmol NaNO_2 when the pH of reaction is adjusted using H_2SO_4 to the pH of loaded solution show that pH is not the acceleration factor for loaded PZ reaction. This might be because of producing piperazine carbamate which reacts more rapidly with nitrite.

Figure 4.7 summarizes all the reactions by presenting the reaction rate versus inverse absolute temperature ($1/T$), reaction between PZ and nitrite when the CO_2 loading is zero, is very low and at the low temperature of 21°C , as well. H_2SO_4 accelerates the reaction slightly between unloaded PZ and nitrite, loaded PZ has more reactivity with nitrite, and formaldehyde can increase the reaction rate but not significantly.

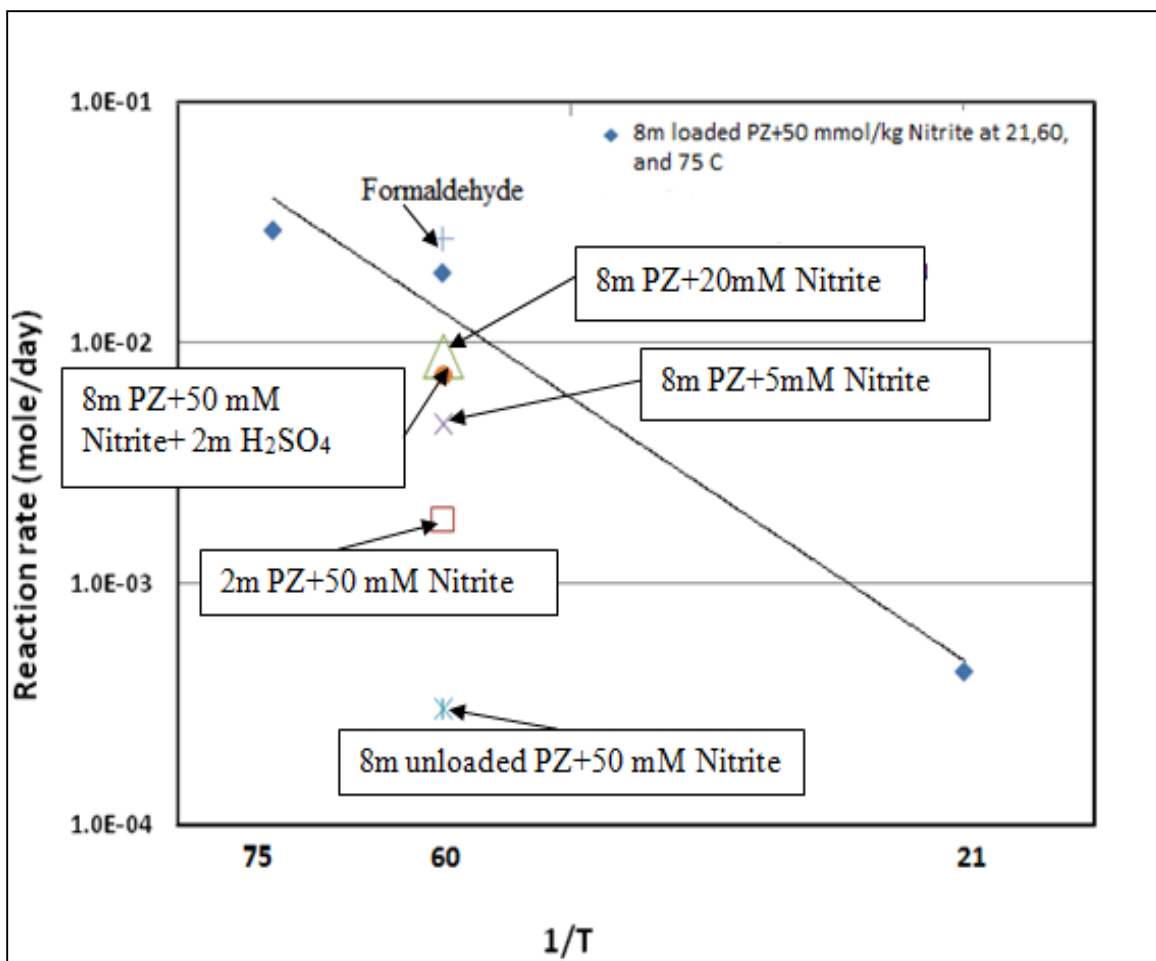


Figure 4.7: Reaction rate of PZ and nitrite under different conditions with respect to temperature (1/T)

Table 4.1 shows the data for reaction conditions and rate constants of above figures in detail.

Table 4.1: Reaction conditions and rate constant of reaction between PZ and nitrite for the experiments performed in glass reactor.

T (°C)	[PZ] _T (mole/kg)	CO ₂ loading	NaNO ₂ (mmole/kg)	Formaldehyde (mmole/kg)	H ₂ SO ₄ (m)	k ₂ (mole/Kg. day)
60	8	0.3	5	-	-	0.0462
60	8	0.3	20	-	-	0.0462
60	8	0.3	50	-	-	0.0467
60	2	0.3	50	-	-	0.0461
60	8	0.3	50	50	-	0.0675
60	8	0.3	50	-	2	0.018
21	8	0.3	50	-	-	0.00104
75	8	0.3	50	-	-	0.07
60	8	0.0	50	-	-	0.0042

4.5 REACTION OF NO₂ AND NITRITE WITH LOADED PIPERAZINE

In the process of absorbing CO₂ by amine solution, flue gas, which contains mainly air and CO₂ with small amounts of NO₂ and other gases, contacts the amine solution. Three experiments were conducted to simulate this process using about 350 mL 8 m loaded PZ in contact with:

1. Low gas flow (100 mL/min) containing 98% O₂, 2% CO₂, and 50 ppm_v NO₂ for 2 weeks;
2. High gas flow (7.7 L/min) containing 98% O₂, 2% CO₂, and 50 ppm NO₂ for 5 days;
3. Low gas flow (100 mL/min) containing 98% O₂, 2% CO₂, and 50 mmol NaNO₂ for 7 days.

In these continuous experiments the rate of nitrite loss is slightly slower than when the process is done at batch conditions (Figure 4.8).

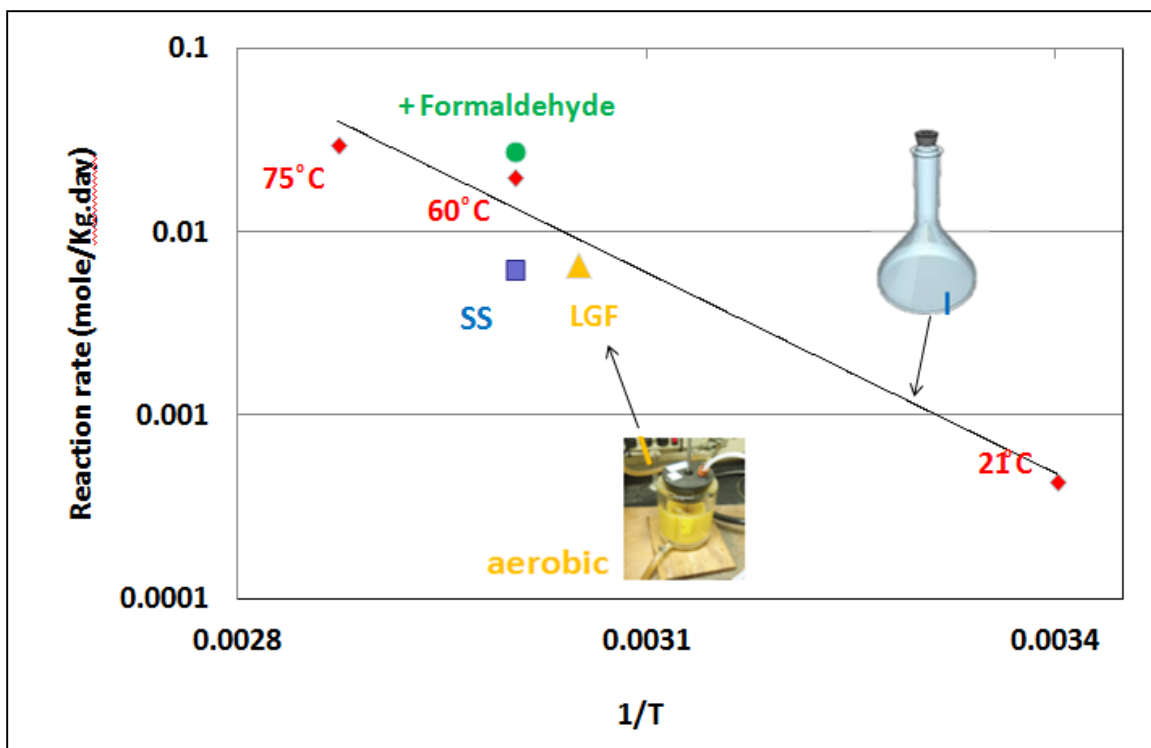


Figure 4.8: Nitrite disappearance rate in an aerated reactor from the reaction of 8 m PZ and 50 mmolal/kg nitrite at 55 °C during 7 days

The line in Figure 4.8 shows the results from previous experiments without oxygen. In the low gas flow experiment, the flow rate was 100 mL/min of gas containing 98% O₂, 2% CO₂, and 50 ppm NO₂. 4.8 mmole of nitrite entered the reactor during the experiment and 3.2 mmole of total nitrite ion remained in the reactor at the end, which means that 1.6 mmole (33%) was lost either by reaction or by exiting with the gas.

The reaction of both low and high flow rate gas containing NO₂ shows an accumulation of nitrite in solution, but analysis shows that some of the entering nitrite reacted with the amine solution or exited the system in the low flow rate experiment (Figure 4.9).

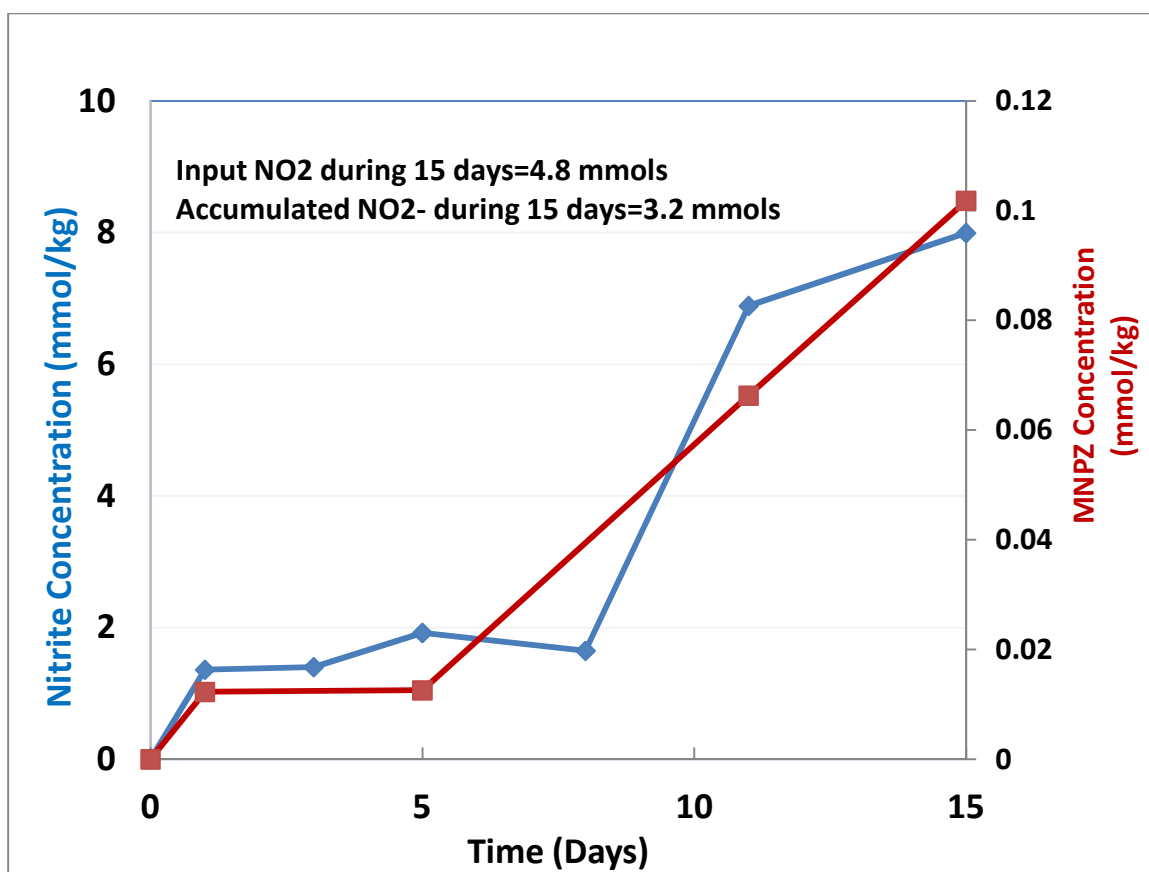


Figure 4.9: Nitrite accumulation and MNPZ production from the reaction of 8 m loaded PZ and 50 ppm NO₂ in a low gas flow experiment with 98% O₂, 2% CO₂, and 50 ppm NO₂ at 55 °C.

In the high gas flow experiment, the gas flow rate was 7.7 L/min with 98% O₂, 2% CO₂, and 50 ppm NO₂. 148.5 mmole of NO₂ entered the reactor during the experiment and 29.9 mmole of total nitrite ion remained at the end of experiment, which means that 119 mmol (80%) was lost either by reaction or leaving the reactor with exiting gas.

The rate of nitrite accumulation in the high gas flow experiment is considerably greater than with low gas flow. 20% of inlet NO₂ is absorbed as nitrite, there is a greater

rate of nitrite accumulation in the system, and the yield of MNPZ is higher than with low gas flow (Figure 4.10).

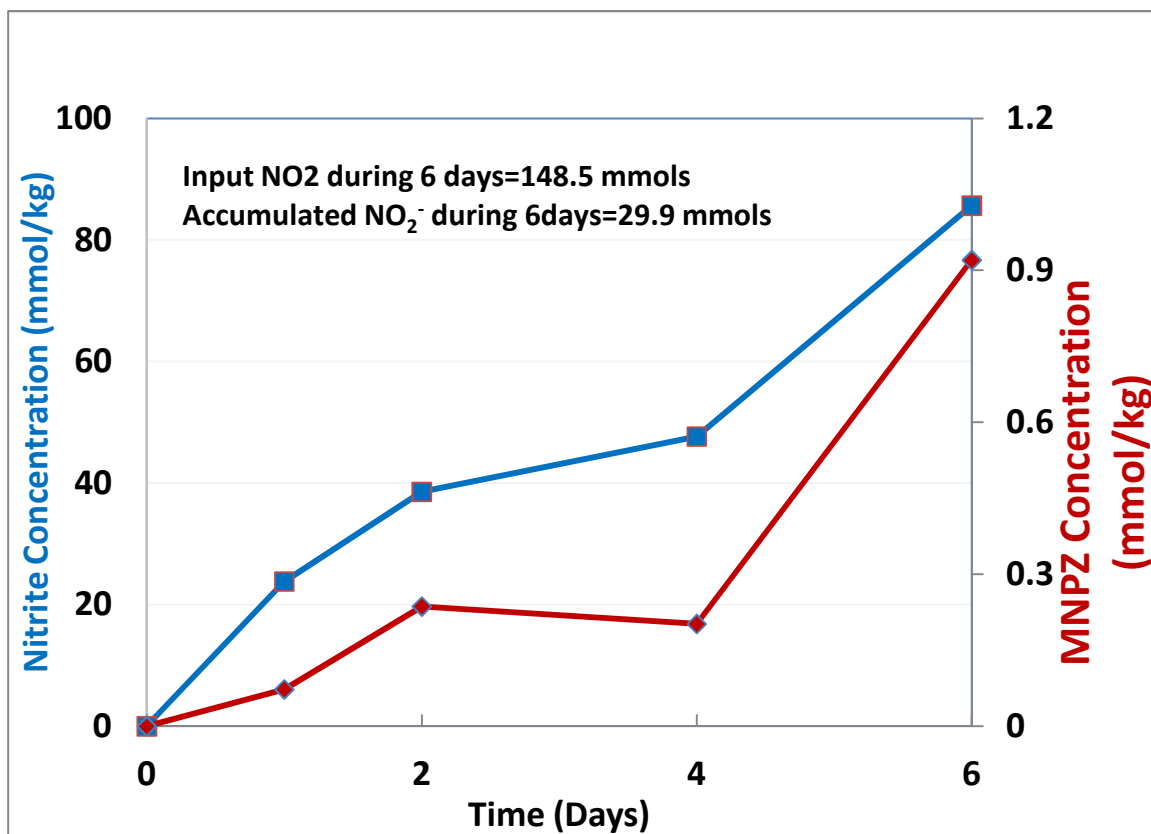


Figure 4.10: The reaction of 8 m loaded PZ and 50 ppm NO₂ in high gas flow experiment with 98% O₂, 2% CO₂, and 50 ppm NO₂ at 55 °C.

In a semi-batch experiment with low gas flow rate of CO₂ and O₂, using 5 mmol/kg nitrite instead of NO₂, at 55 °C, as expected the rate of nitrite consumption follows first order reaction rate and the yield of MNPZ production is greater, at 6% (Figure 4.11).

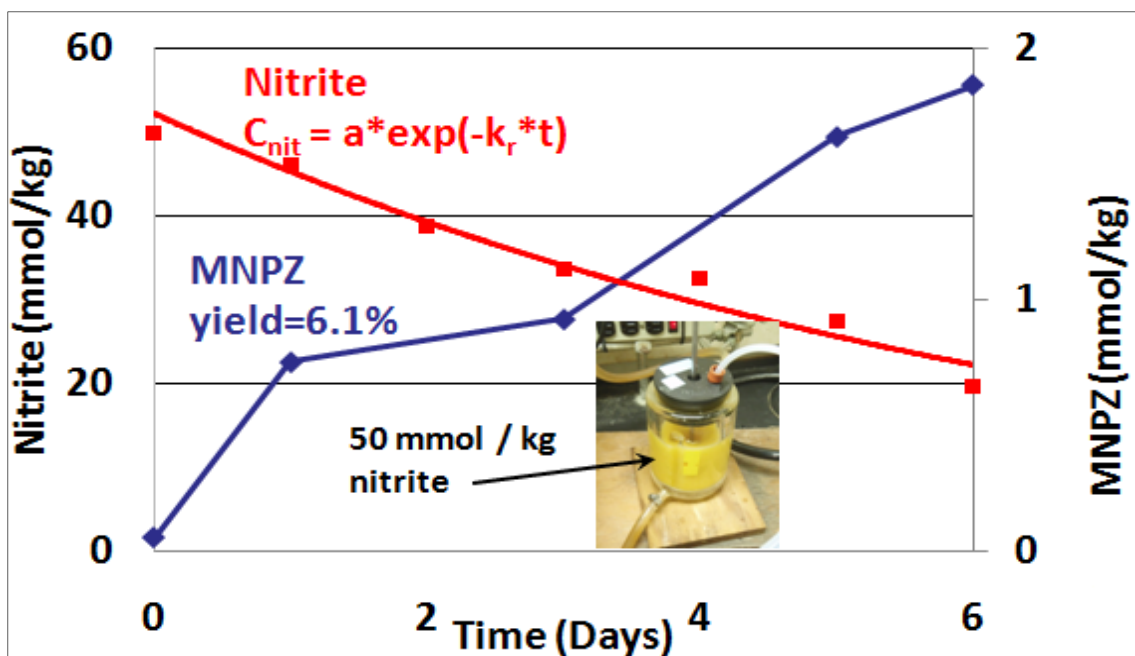


Figure 4.11: Nitrite consumption and MNPZ production from the reaction of 8 m loaded PZ and 50 mmol/kg nitrite in a low gas flow experiment , 100 mL/min of 98% O₂, 2% CO₂. 55°C.

4.6 REACTION OF NITRITE WITH LOADED PIPERAZINE AT HIGH TEMPERATURE

High temperature experiments using 8 m loaded PZ and 50 mmol/kg nitrite were performed using thermal cylinders at 100, 135, and 150 °C. At 100 °C nitrite concentration decreases following first order reaction rate as observed at lower T. At 135 and 150 °C, the nitrite disappears in less than 3 hours, and it is not possible to extract a reaction order (Figure 4.12).

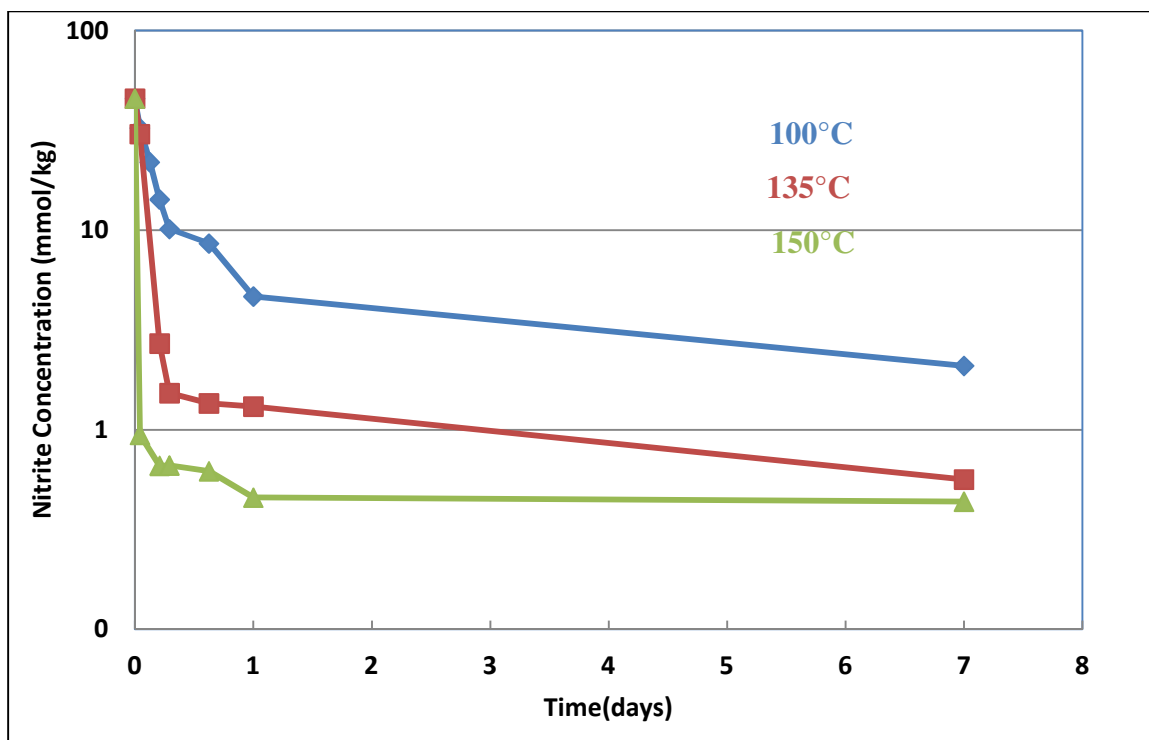


Figure 4.12: Nitrite consumption from the reaction of 8 m PZ, 0.3 mol CO₂/equiv N, and 50 mmol/kg of nitrite at high temperature

Appendix B contains all detailed data of high temperature experiments.

The results of high temperature experiments examined through HPLC show that at 100°C, MNPZ increases during first 15 hrs but after that decreases gradually. The same happens at 135°C, but the maximum concentration of MNPZ occurs in the first 7 hours, after which it seems MNPZ decomposes and disappears rapidly. At 150 °C, MNPZ is produced in just 1 hour and then it disappears rapidly. After 24 hrs no trace of MNPZ remains (Figure 4.13).

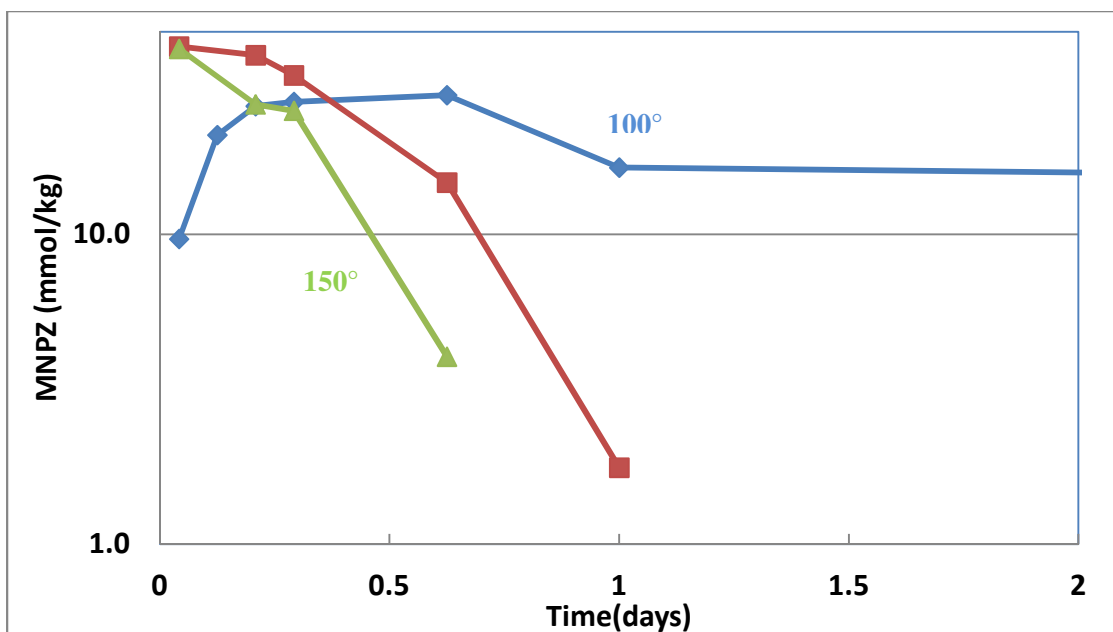


Figure 4.13: MNPZ production from the reaction of 8 mPZ, 0.3 mol CO₂/equiv N, and 50 mmol/kg nitrite at high temperature

Experiments have also been conducted using 2 m loaded PZ and 50 mmol/kg of nitrite at the above temperatures. The trends of nitrite consumption and MNPZ production are given in Figures 4.14 and 4.15, respectively. Figures 4.12 and 4.14 show that the rate of nitrite disappearance in nitrosation of 8 m PZ is faster than in 2 m PZ.

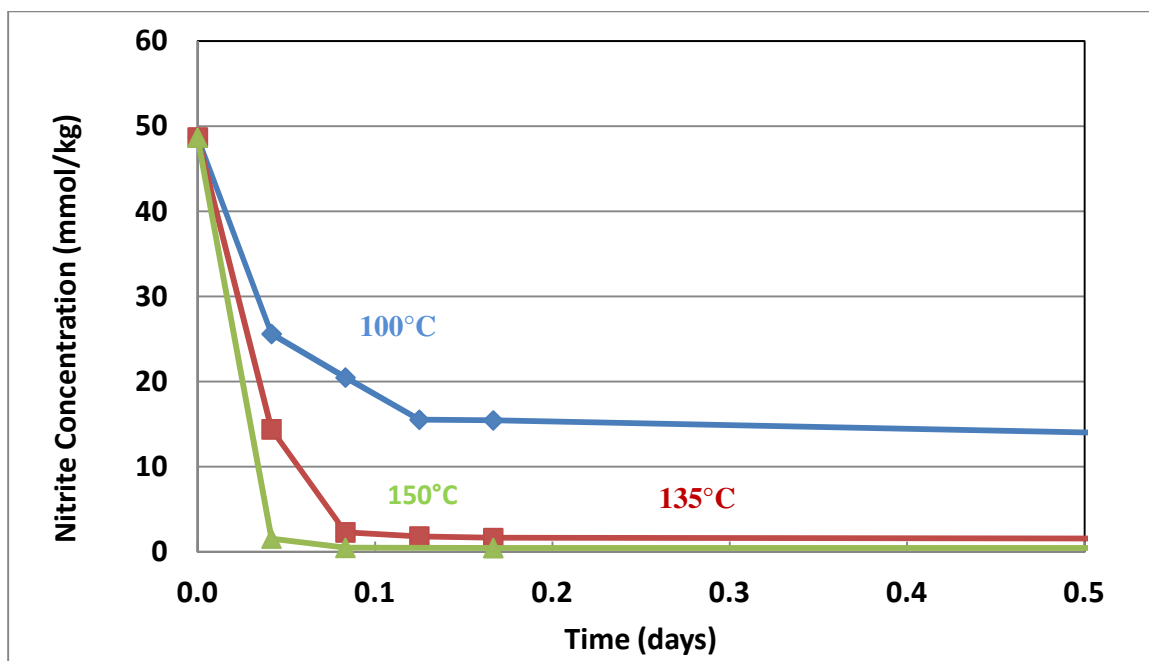


Figure 4.14: Nitrite consumption from the reaction of 2 m PZ, 0.3 mol CO₂/equiv N and 50 mmol/kg nitrite at high temperature.

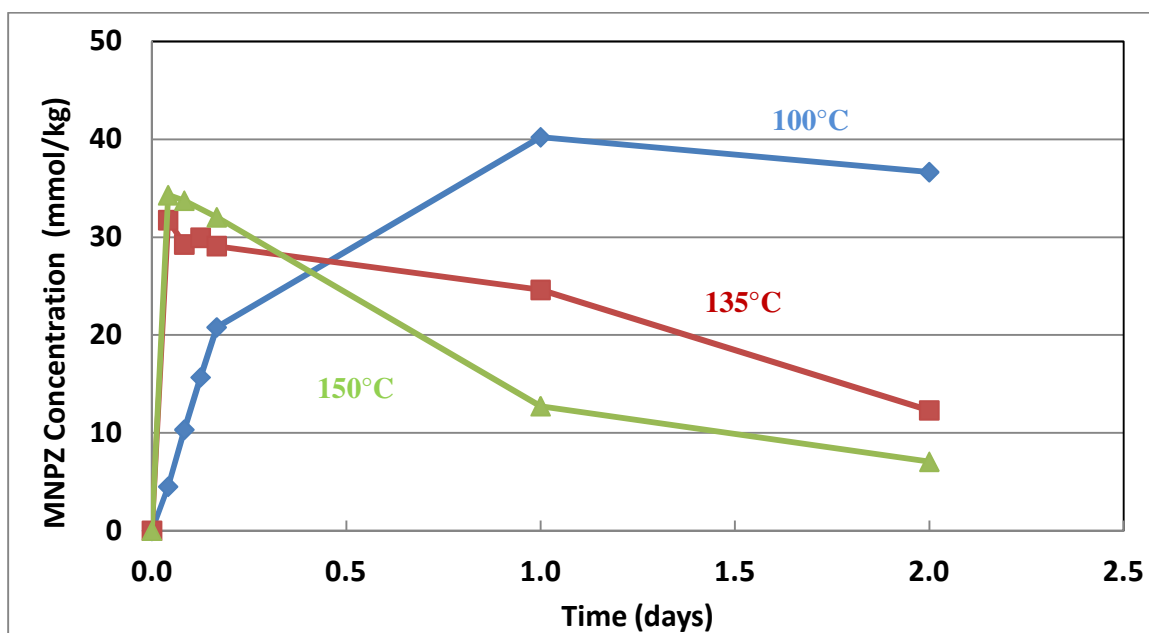


Figure 4.15: MNPZ from the reaction of 2 mPZ, 0.3 mol CO₂/equiv N and 50 mmol/kg of nitrite at high temperature.

For a better understanding of the process of MNPZ production and decomposition at high temperature and stripper conditions, loading has been selected as one factor in modeling the behavior of MNPZ. Figures 4.16 and 4.17 present the nitrite consumption and MNPZ production at a loading of 0.1.

Figures 4.18 and 4.19 show the same results but for a loading 0.2.

Nitrite consumption rate is not a strong function of loading. The rate of MNPZ production increases at higher loading while the rate of MNPZ decomposition at lower loading is more rapid than that at higher loading.

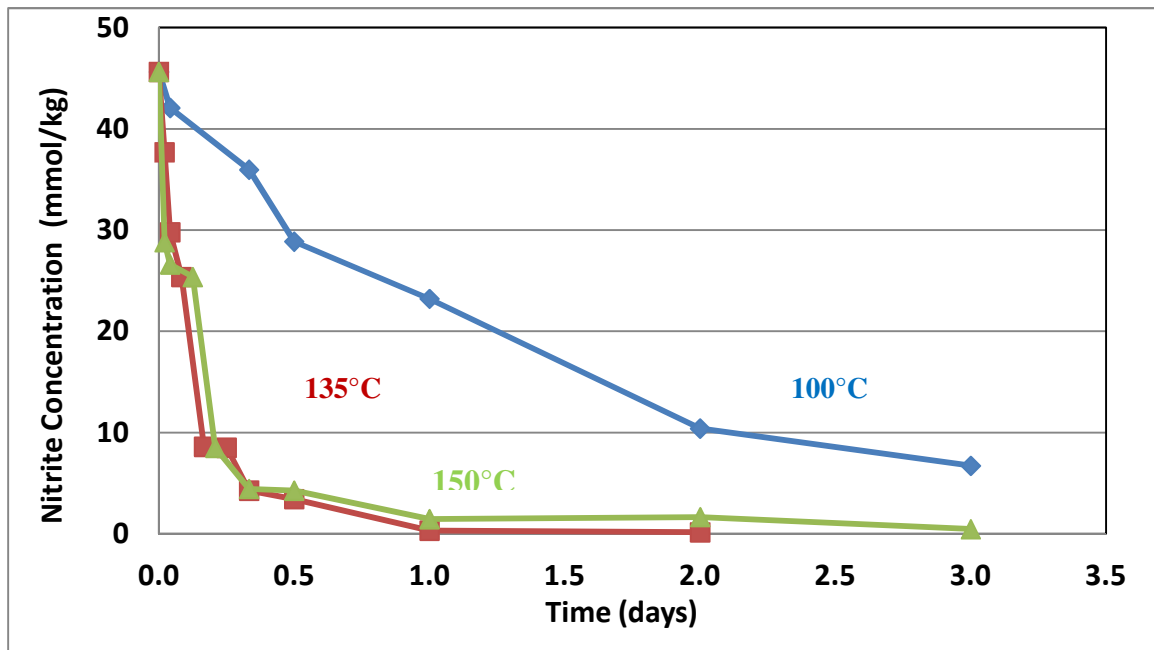


Figure 4.16: Nitrite consumption from the reaction of 8 m loaded PZ, 0.1 mol CO₂/equiv N , and 50 mmol/kg nitrite at high temperature.

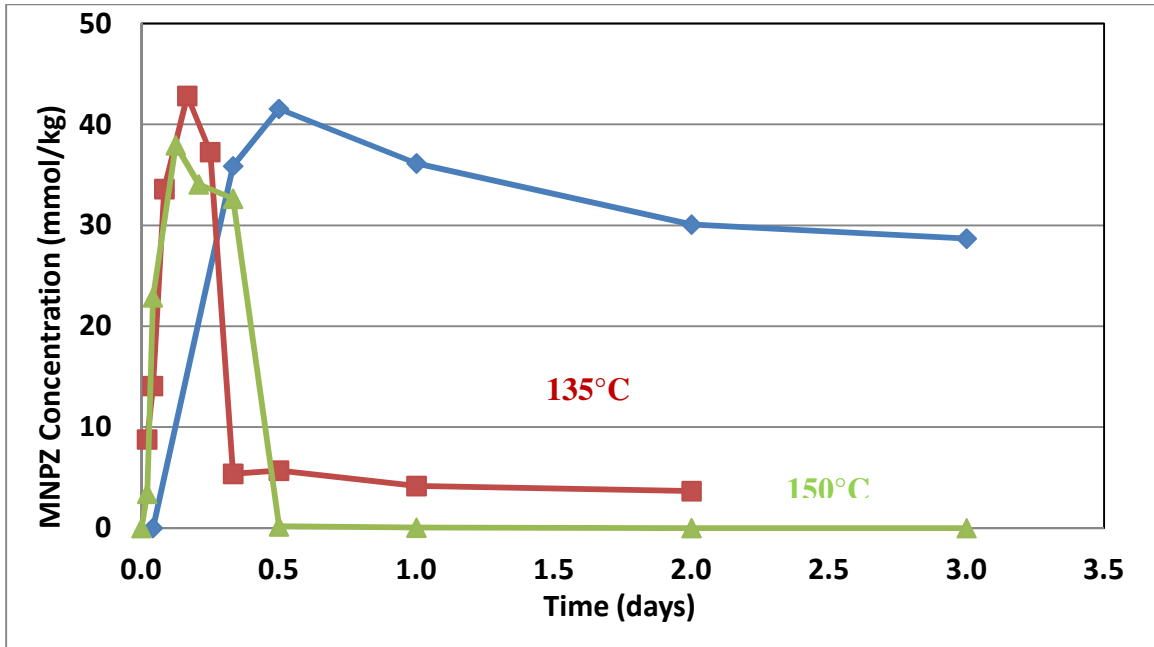


Figure 4.17: MNPZ production from the reaction of 8 mPZ, 0.1 mol CO₂/equiv N and 50 mmol/kg of nitrite at high temperature.

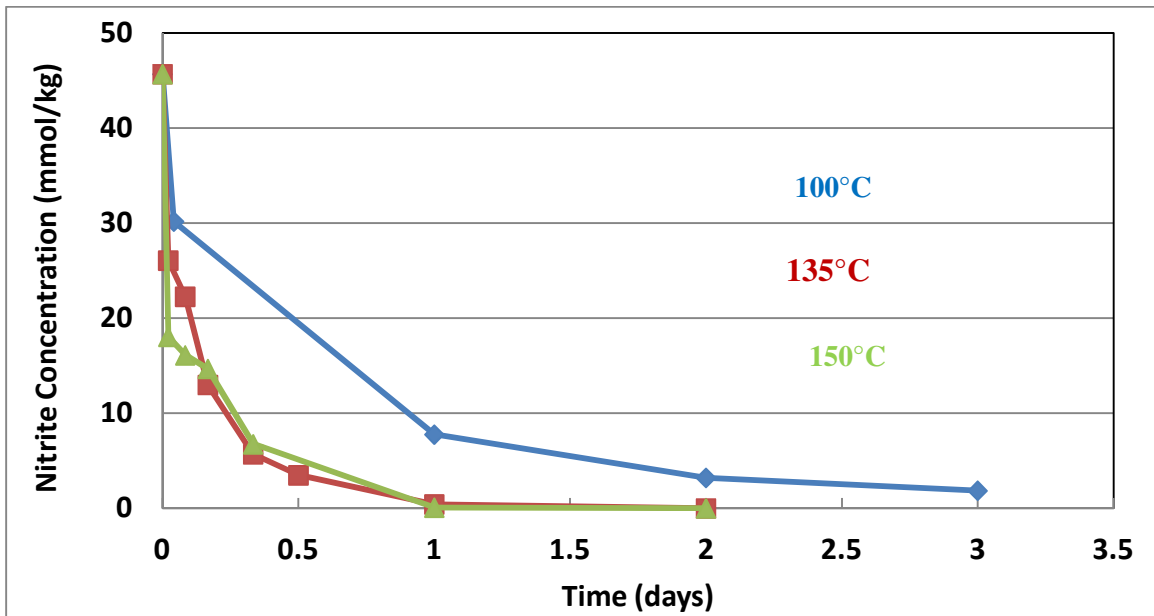


Figure 4.18: Nitrite consumption from the reaction of 8 m loaded PZ, 0.2 mol CO₂/equiv N, and 50 mmol/kg nitrite at high temperature.

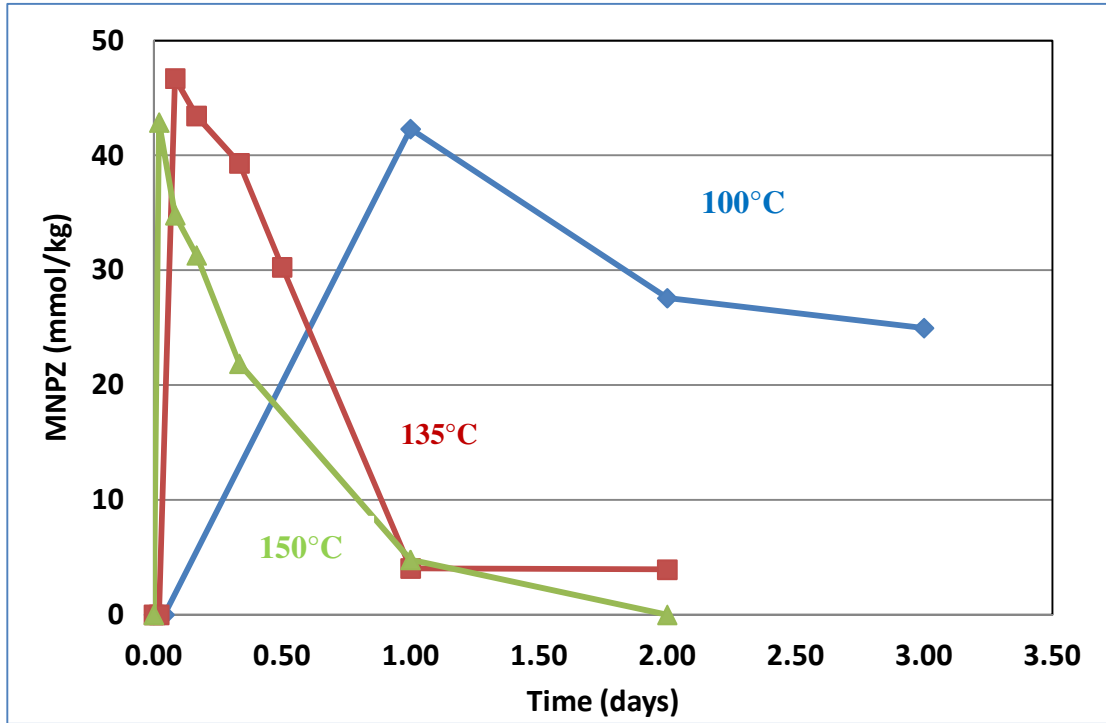


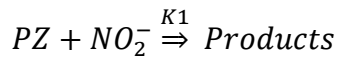
Figure 4.19: MNPZ production from the reaction of 8 m loaded PZ, 0.2 mol CO₂/equiv N, and 50 mmol/kg nitrite at high temperature

Chapter 5: Nitrosopiperazine Formation and Decomposition Modeling

Different reaction conditions have been investigated for the reaction of PZ and nitrite. Results show that the temperature is the most important factor affecting this reaction. Therefore a temperature dependent model has been established to define the reaction behavior in term of consuming nitrite and producing MNPZ, followed by MNPZ decomposition.

There are three temperature ranges; absorber temperature range which is less than 75°C, a transition temperature range between 90°C and 100°C, and finally stripper temperature range which is higher than 135°C. For each of these categories there is a reaction rate model.

In low temperature experiments, there is no detectable MNPZ and nitrite consumption is a first degree reaction by nitrite concentration and total PZ concentration, (Equation 5.1 and Figure 5.1).



$$d[NO_2^-]/dt = -K1[NO_2^-][PZ][loading] \quad (5.1)$$

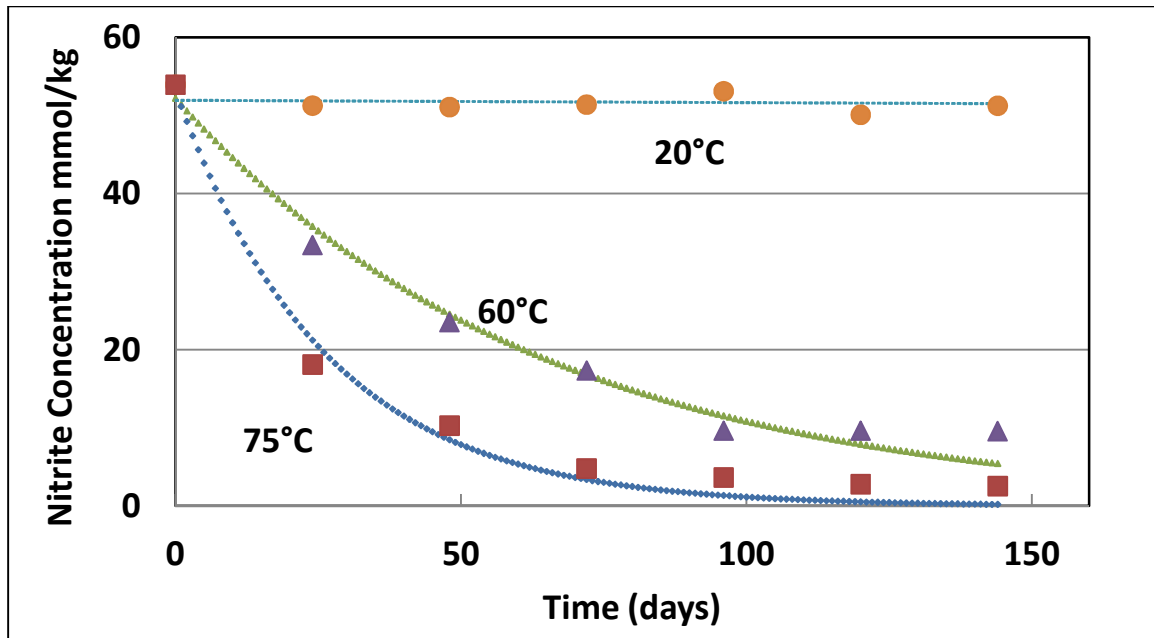


Figure 5.1: Nitrite consumption data point and best fit curves from the reaction of 8 m loaded PZ, 0.2 mol CO₂/equiv N, and 50 mmol/kg nitrite at the absorber temperature range.

Equation 5.2 expresses the relation between the reaction rate constant and temperature based on Figure 5.2. The activation energy for this reaction has been calculated as well.

$$K1 = \text{Exp} \left[-15365 \left(\frac{1}{T} \right) + 41.669 \right] \quad 20^\circ\text{C} < T < 75^\circ\text{C} \quad (5.2)$$

$$E1 = 127.75 \text{ KJ/mole}$$

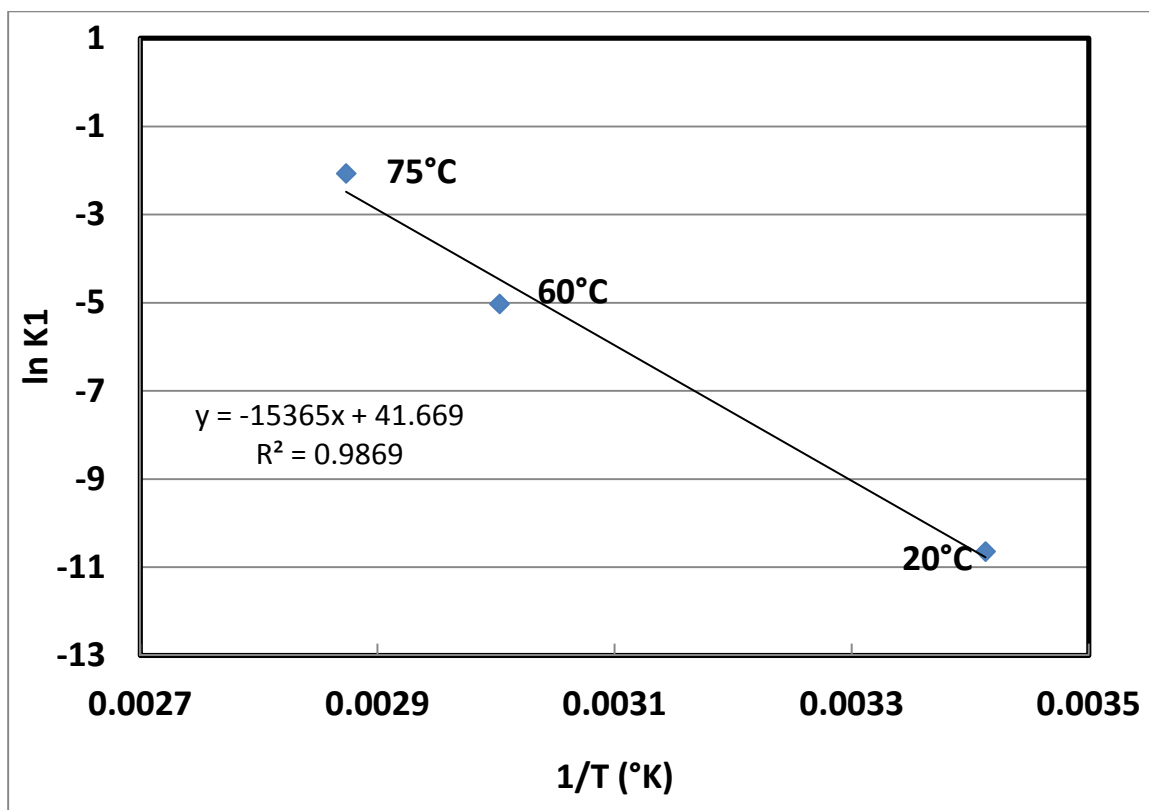


Figure 5.2: Reaction rate constant for nitrite consumption during the reaction of 8 m loaded PZ, 0.2 mol CO₂/equiv N, and 50 mmol/kg nitrite at the absorber temperature range.

At the transition temperature, nitrite disappears, MNPZ is produced, and MNPZ begins to decompose. There is a reversible equilibrium reaction between the rate of producing MNPZ and decomposing MNPZ to nitrite as well as a slower decomposition of MNPZ to other products, Equation 5.3.



Figure 5.3 shows the fitted points regarding to the following reaction rate equations.

$$\frac{d[NO_2^-]}{dt} = -K_1[NO_2^-][PZ][loading] + K_2[MNPZ][loading]$$

$$\frac{d[MNPZ]}{dt} = K_1[NO_2^-][PZ][loading] - K_2[MNPZ][loading] - K_3[PZ][MNPZ][loading]$$

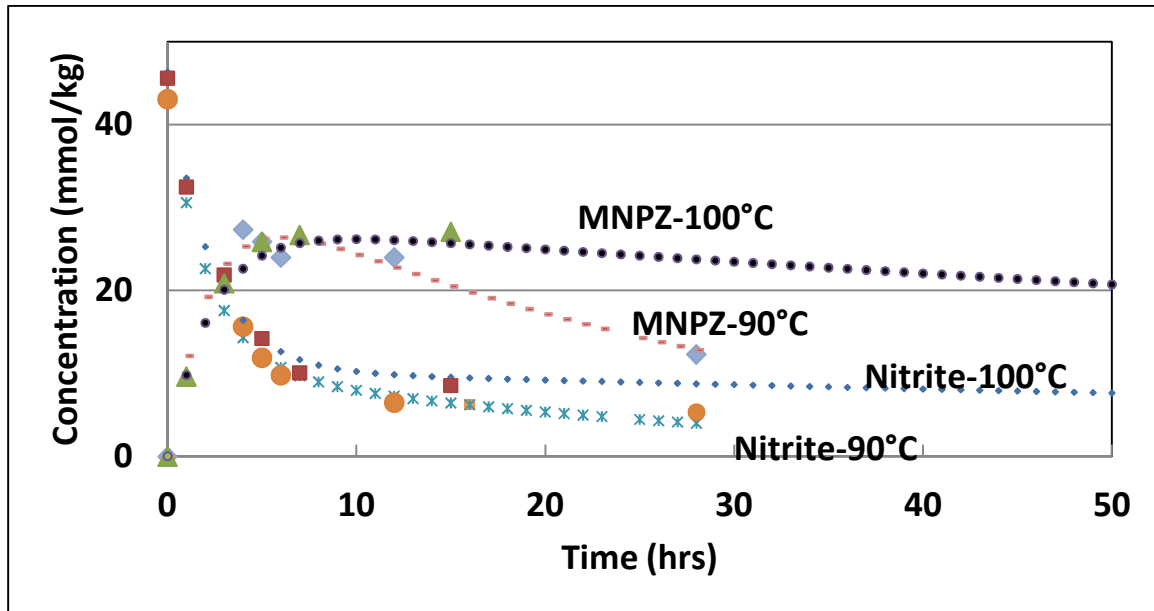


Figure 5.3: Nitrite consumption data point and fitted equation from the reaction of 8 m loaded PZ, 0.2 mol CO₂/equiv N, and 50 mmol/kg nitrite at the transition temperature range.

Figure 5.4 shows the reaction rate constant for nitrite consumption in the transition temperature range followed by the equation 5.4. The activation energy for this reaction has been calculated as well.

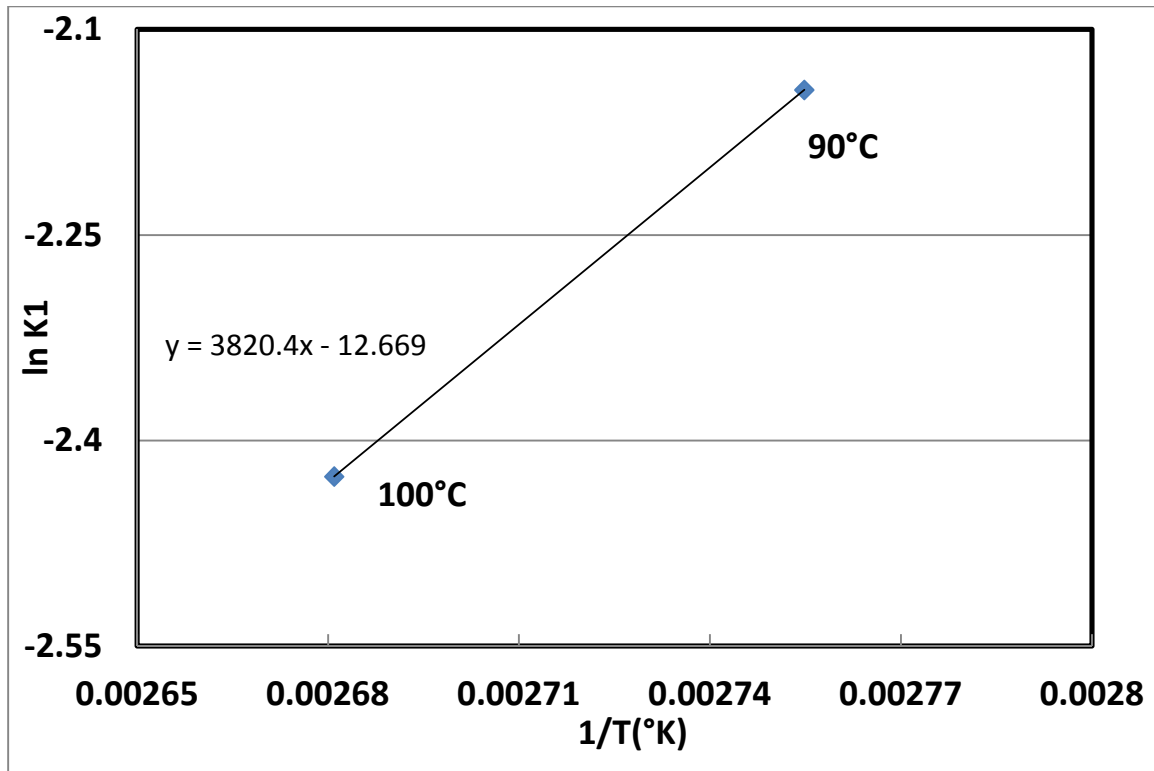


Figure 5.4: Reaction rate constant for nitrite consumption during the reaction of 8 m loaded PZ, 0.2 mol CO₂/equiv N, and 50 mmol/kg nitrite at the absorber temperature range.

$$K1 = \text{Exp} \left[3820.4 \left(\frac{1}{T} \right) - 12.669 \right] \quad (5.4)$$

$$E1 = 31.8 \text{ KJ/mole}$$

Figure 5.5 shows the reaction rate constant for reverse reaction of MNPZ decomposition to the nitrite and PZ in the transition temperature range followed by the equation 5.5.

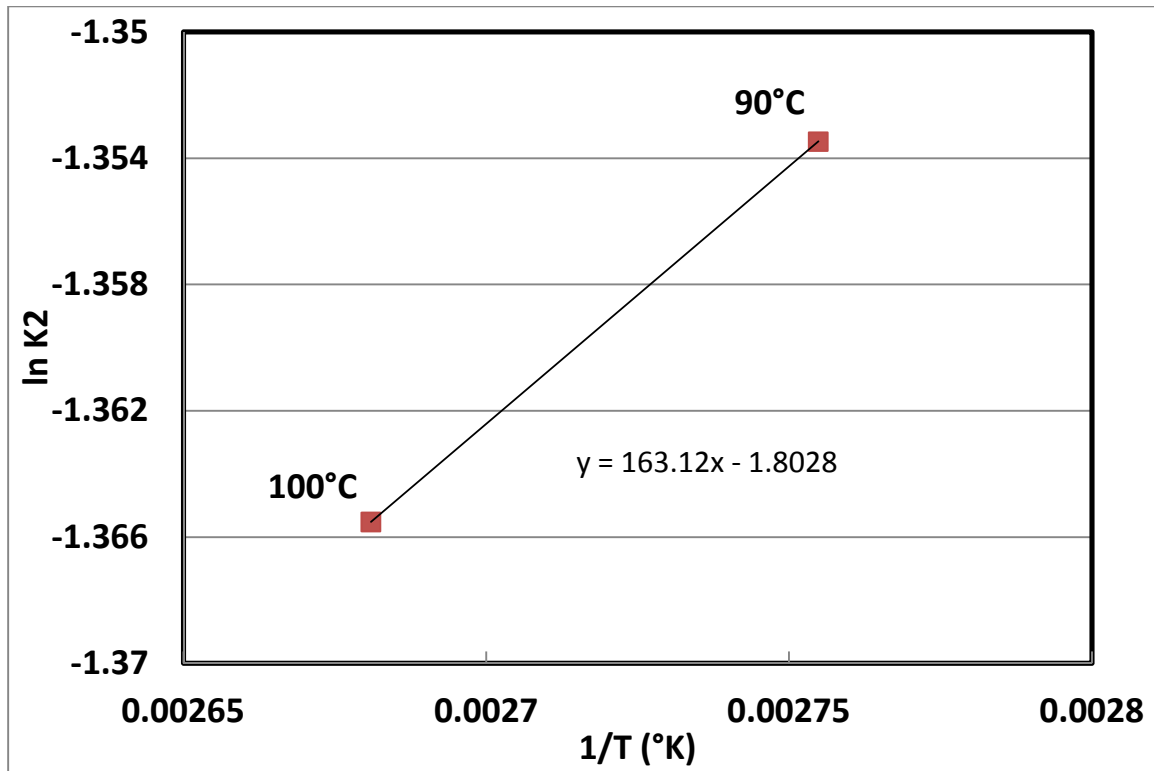


Figure 5.5: Reaction rate constant for reverse reaction during the reaction of 8 m loaded PZ, 0.2 mol CO₂/equiv N, and 50 mmol/kg nitrite at the transition temperature range.

$$K2 = \text{Exp} \left[163.12 \left(\frac{1}{T} \right) - 1.8028 \right] \quad (5.5)$$

$$E2 = 1.36 \text{ KJ/mole}$$

Figure 5.6 shows the reaction rate constant for the reaction of MNPZ decomposition to the other products in the transition temperature range followed by the equation 5.6.

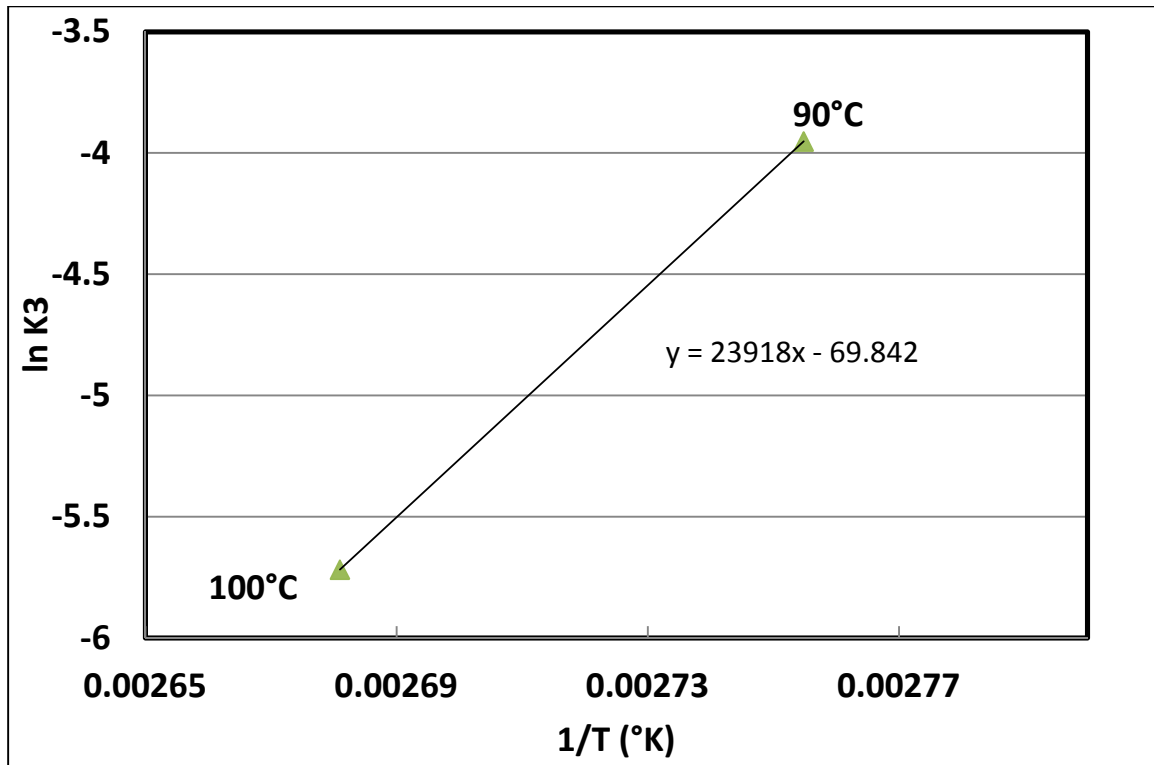


Figure 5.6: Reaction rate constant for MNPZ decomposition during the reaction of 8 m loaded PZ, 0.2 mol CO₂/equiv N, and 50 mmol/kg nitrite at the transition temperature range.

$$K3 = \text{Exp} \left[23918 \left(\frac{1}{T} \right) - 69.842 \right] \quad (5.6)$$

$$E3 = 198.85 \text{ KJ/mole}$$

At the stripper temperature range, nitrite disappears very quickly and produces MNPZ but the produced MNPZ also decomposes fairly quickly, Equation 5.7.



Figure 5.3 shows the fitted points regarding to the following reaction rate equations.

$$\frac{d[NO_2^-]}{dt} = -K1[NO_2^-][PZ][loading]$$

$$\frac{d[MNPZ]}{dt} = K1[NO_2^-][PZ][loading] - K3[PZ][MNPZ][loading]$$

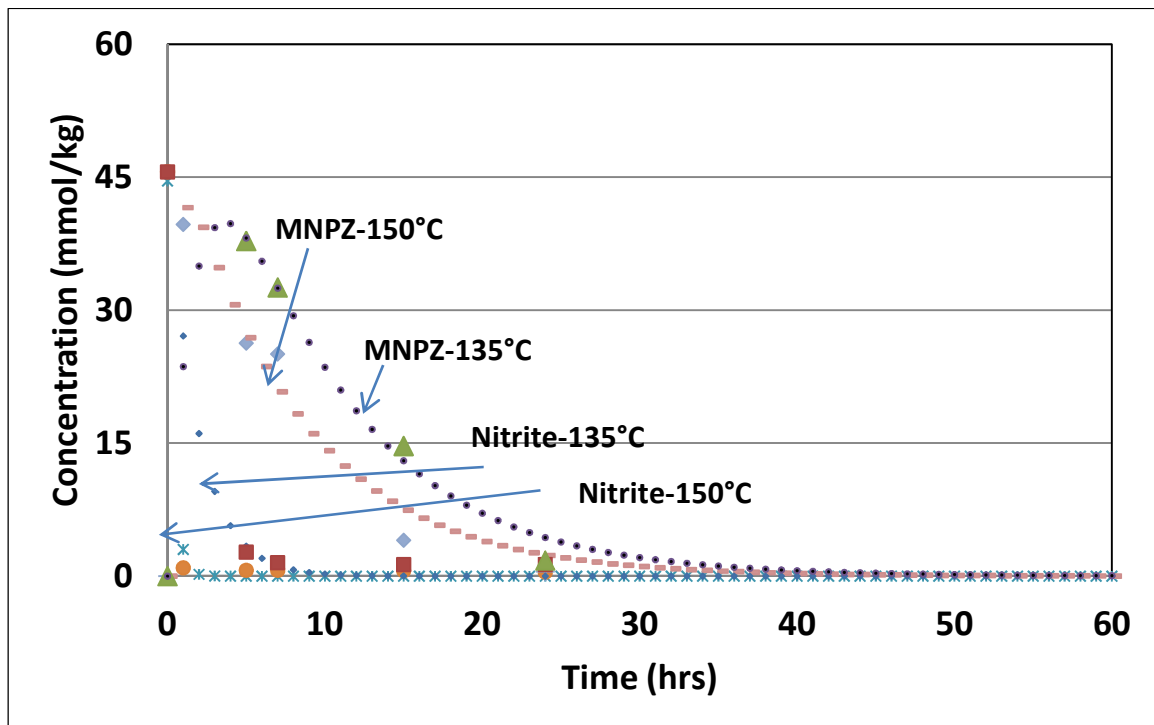


Figure 5.7: Nitrite and MNPZ concentration change data point and fitted equation from the reaction of 8 m loaded PZ, 0.2 mol CO₂/equiv N, and 50 mmol/kg nitrite at the stripper temperature range.

Figure 5.8 shows the reaction rate constant for nitrite consumption at the stripper temperature range followed by the equation 5.8. The activation energy for this reaction has been calculated as well.

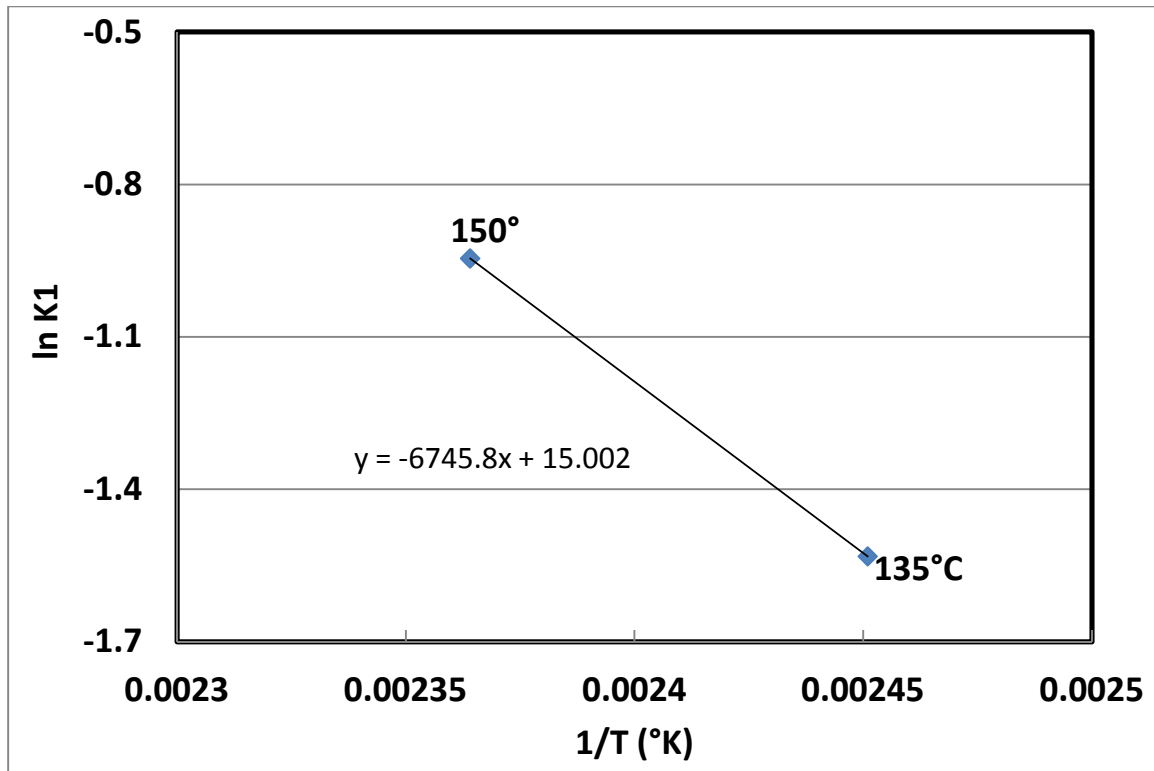


Figure 5.8: Reaction rate constant for nitrite consumption during the reaction of 8 m loaded PZ, 0.2 mol CO₂/equiv N, and 50 mmol/kg nitrite at the stripper temperature range.

$$K1 = \text{Exp} \left[-6745.8 \left(\frac{1}{T} \right) + 15.002 \right] \quad (5.8)$$

E1=56.1KJ/mole

Figure 5.9 shows the reaction rate constant for nitrite consumption at the stripper temperature range followed by the equation 5.9.

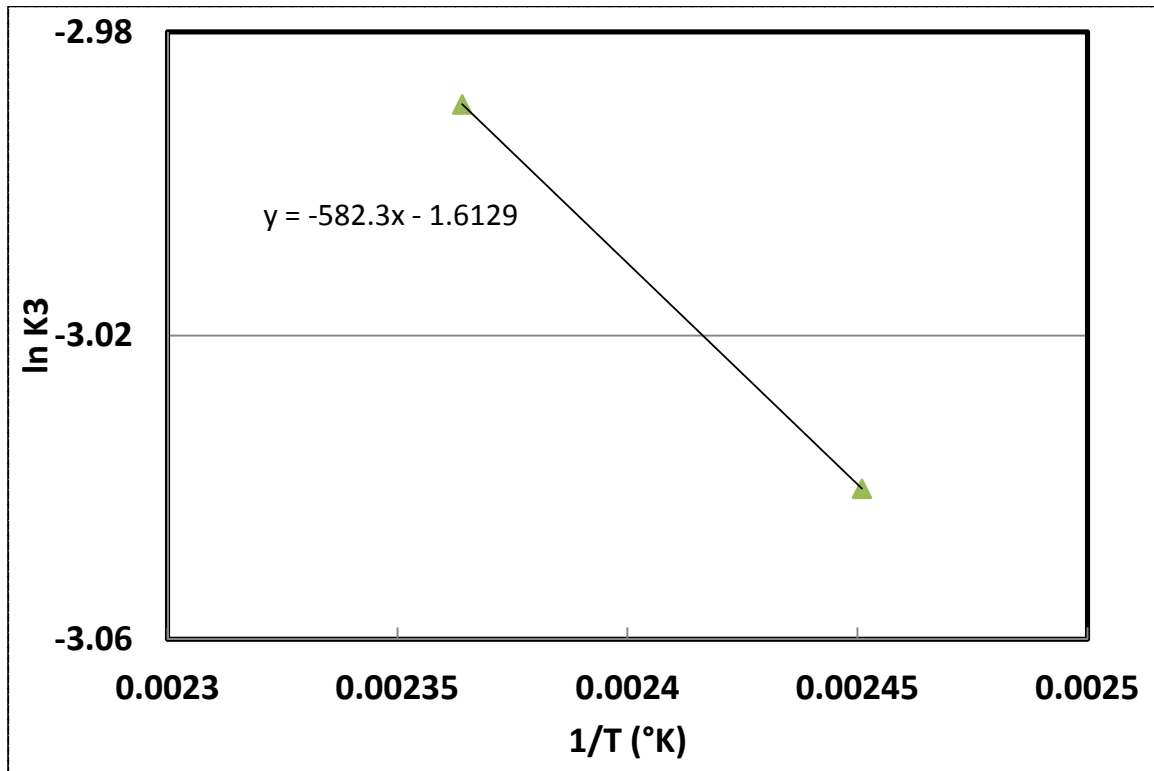


Figure 5.9: Reaction rate constant for MNPZ decomposition during the reaction of 8 m loaded PZ, 0.2 mol CO₂/equiv N, and 50 mmol/kg nitrite at the stripper temperature range.

$$K3 = \text{Exp}\left[-582.3\left(\frac{1}{T} - 1.6129\right)\right] \quad (5.9)$$

$$E3=4.84 \text{ KJ/mole}$$

Table 5.1: Reaction rate constants for different temperatures

Temperature (°C)	K1(kg/mmol.hr)	K2(kg/mmol.hr)	K3(kg/mmol.hr)
20	2.39E-5	0.00	0.00
60	0.00658	0.00	0.00
75	0.1238	0.00	0.00
90	0.1171	0.258	0.0192
100	0.0883	0.255	0.00328
135	0.216	0.00	0.0478
150	0.388	0.00	0.0503

Chapter 6: Conclusions and Recommendations

6.1 TEMPERATURE EFFECT

Nitrosamine can be produced in CO₂ capture process using PZ, but there are mechanisms which encourage the decomposition of produced MNPZ. At absorber temperature (less than 60°C), the possibility of MNPZ formation from the reaction of 2 to 8 m PZ and NO₂⁻ in the CO₂ loading range of 0.1-0.3 is low. The reaction rate constant of nitrite disappearance increases during the time with a base reaction rate of 0.00658 kg/mmol.hr and the activation energy of 128 KJ/mole. At the transition temperature, the reverse reaction rate constant is more than the nitrite disappearance and MNPZ decomposition reaction the activation energy for this reverse reaction is calculated as 1.36 KJ/mole. However nitrosamine is produced quickly in the stripper at 150°C, where it also decomposes very quickly as well and MNPZ decomposing reaction activation energy is 4.84 KJ/mole.

6.2 THE EFFECT OF UV LIGHT

Since the low temperature nitrosamine formation reaction were done in a clear glass reactor, reactants were exposed to the UV radiation from environment (inside the fume hood and room) light. The UV radiation found in fluorescent lighting is present in three forms: UVA (320 to 400 nm), UVB (280-320 nm), and UVC (100-280 nm). UVA radiation easily transmits through air and glass. UVB and UVC radiation transmit through air and quartz, but are absorbed by regular glass. MNPZ absorbs UV wavelength at 240 nm (UVC) and 330 nm (UVA). Therefore destructive effect of UV on nitrosamines formed is possible under the experimental conditions, and the exposure to

UV might be another factor for lower yield of MNPZ at low temperature. Further investigation on this issue is recommended.

Appendix A

METHOD DEVELOPMENT FOR DETECTING AND MEASURING DNPZ AND MNPZ

A.1 DIRECT INJECTION OF DINITROSOPIPERAZINE (DNPZ) TO MASS SPECTROMETRY

Mass Spectrometry (MS) is an analytical technique used to determine the elemental composition of a sample or molecule. The instrument consists of three main sections:

- 1- Ion source, which converts gas phase sample molecules into ions;
- 2- Mass analyzer, which sorts the ions by their mass to charge ratios by applying electromagnetic fields;
- 3- Detector, which measures the ion intensity and provides data for calculating the quantities of each ion present.

Here is a short explanation of the keywords that appear later in this section:

Direct Injection: Using the syringe pump that can be connected directly to the ion source to provide a steady state introduction of sample or tuning and calibrating solution.

Fragmentation: Breaking molecules into specific ions. Fragmentation pattern has led to mass spectra being used as “fingerprints” for identifying compounds.

According to the suggested method (Atalla et al., 2010) for detection, samples of 0.00007–0.7 mmol of DNPZ per mL of methanol have been injected directly to MS to see if MS can detect it. The mass spectrum diagram is shown in Figure A.1.

When the process outlined above showed no evidence of DNPZ, water was added to the solution and in this case DNPZ could be detected by MS. To obtain more accurate results, the fragmentation method has been run with results shown in Figures A.2– A.5.

For quantifying DNPZ, an LC-MS system has been used; the method of measurement was developed by employing a reverse phase column.

Solutions of 500 ppm PZ, DNPZ, and DNPZ + PZ in 80% methanol (MeOH) and 20% water have been injected to the LC-MS, and primary results are shown in Figures A.6–A.14.

Mass spectrometry shows the mass per charge of molecules and their relative abundance. For DNPZ we are looking for $m/z = 145$ because the molecular weight of DNPZ is 144 and by protonating with one hydrogen atom, the mass of ion will be 145.

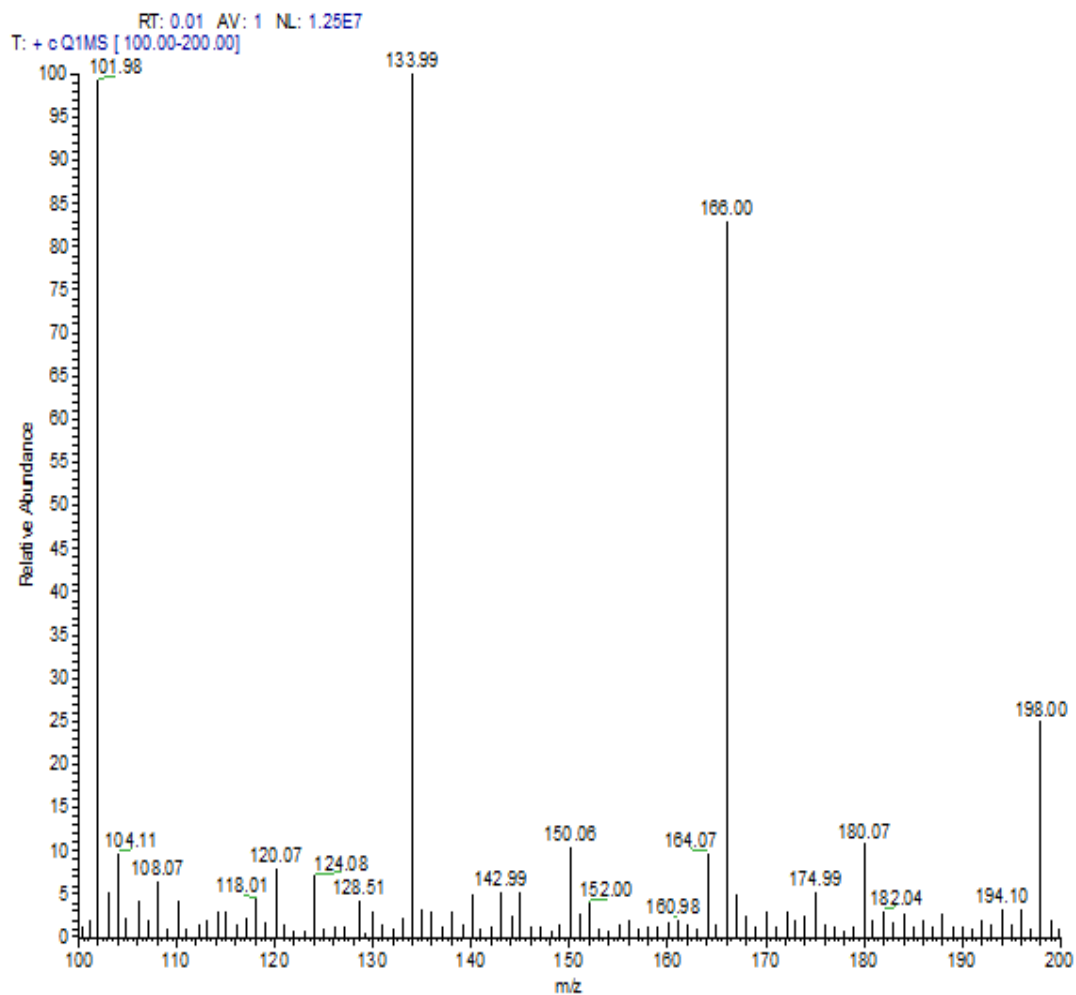


Figure A.1: Mass spectrum of a sample of DNPZ and methanol (relative abundance in terms of m/z)

Figure A.1 shows the typical mass spectrum of samples that have been injected into the MS. All sample results were almost the same, and in this report, just one common spectrum has been described. There is no evidence of $m/z = 145$.

By adding water to the solutions (2 parts methanol and 1 part water) and then injecting new samples to the MS, surprisingly, mass spectrum showed a peak at m/z of 145 which is DNPZ (Figure A.2).

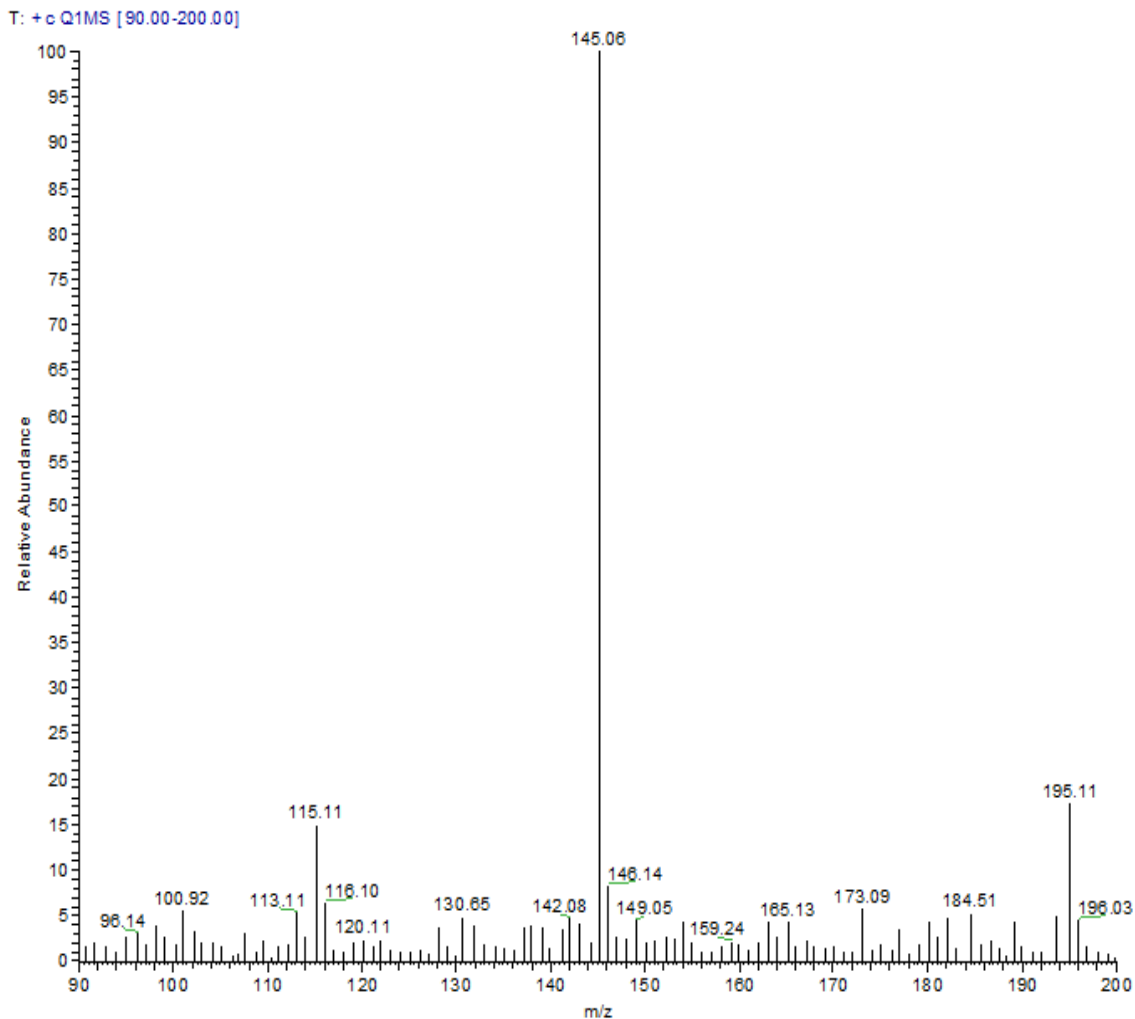


Figure A.2: Mass spectrum of a sample of DNPZ in methanol and water (Relative abundance in terms of m/z)

Rather than a big peak of DNPZ, there is a small amount of MNPZ in the injected sample as shown in Figure A.2. The m/z of 116.1 represents the molecular weight of MNPZ which is 115.

When there is a very small amount of a molecule in a sample or when more than one molecule with the same molecular weight may exist, the fragmentation method has

been used to confirm the detection of a specific molecule. By using fragmentation, an extremely small quantity of a component is recognizable.

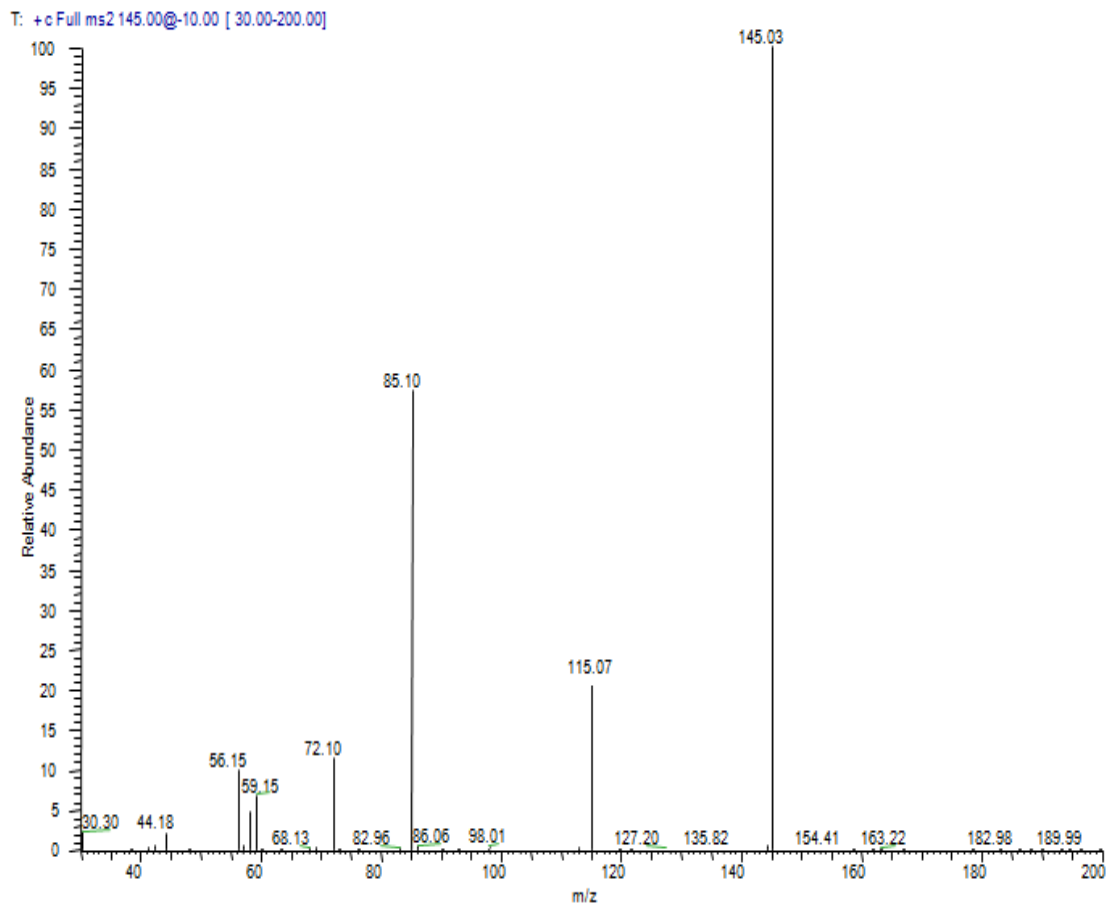


Figure A.3: Mass spectrum of fragmentation of a sample of DNPZ in methanol and water by collision energy of 10. (Relative abundance in terms of m/z)

Figures A.3– A.5 show the fragmentation steps of DNPZ to 2 ions with m/z of 85.1 and 56.15.

Figure A.3 indicates that collision energy of 10 does not break DNPZ very well and just one ion with m/z of 85.1 appears. By increasing collision energy to 20, DNPZ

breaks and rather than decreasing in its relative abundance ions, with m/z of 85.1 and 56.15 it showed up very well, as seen in Figure A.4.

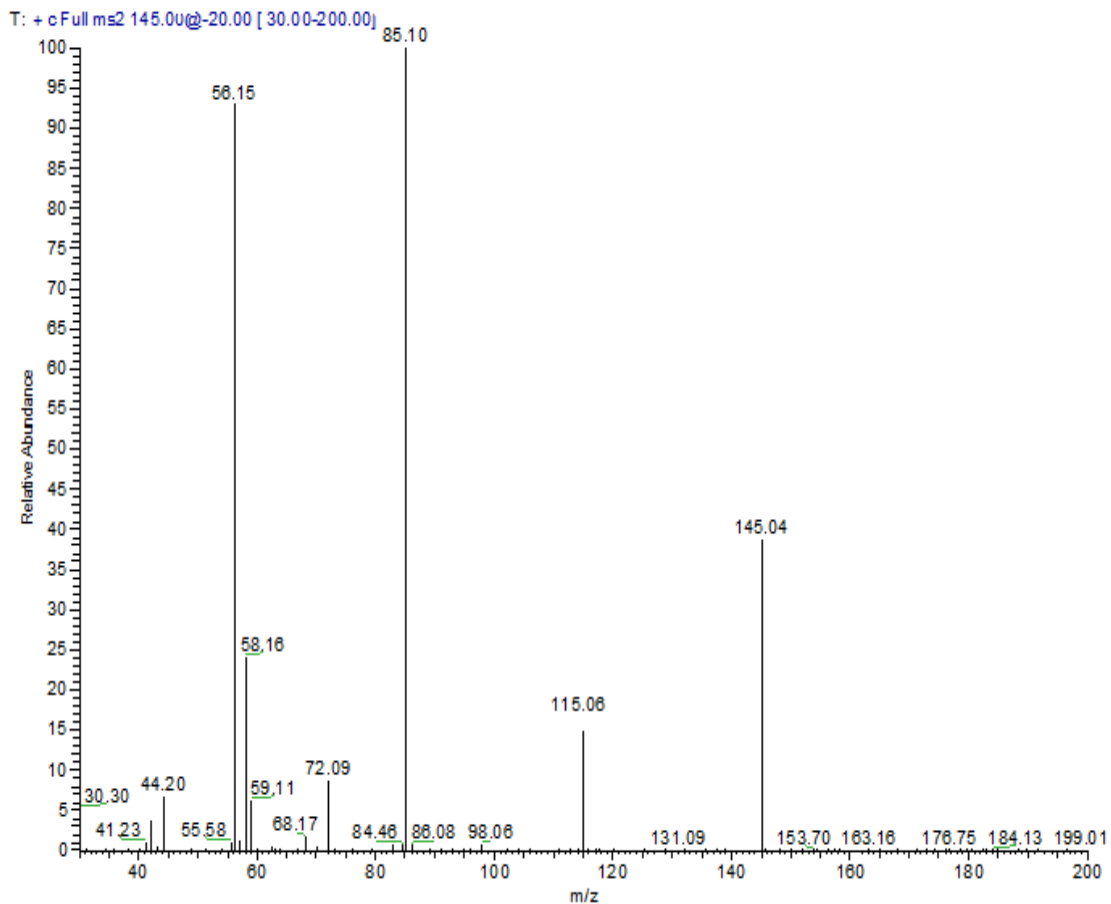


Figure A.4: Mass spectrum of fragmentation of a sample of DNPZ in methanol and water by collision energy of 20. (Relative abundance in terms of m/z)

Collision energy of 20 breaks almost 40% of the DNPZ, so the collision energy has been increased one more step to 30. Figure A.5 shows that with collision energy of 30 almost all DNPZ is broken into ions with m/z of 85.1 and 58.15.

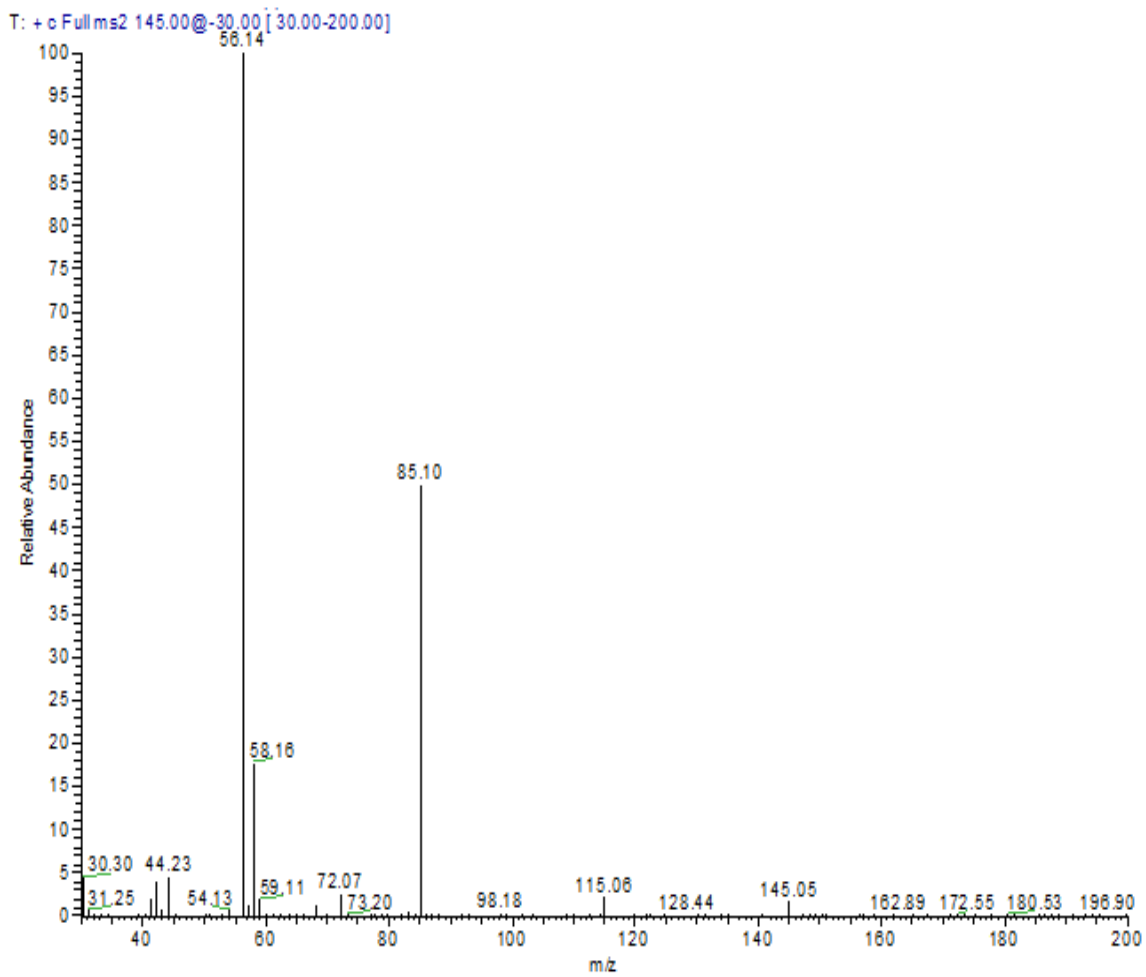


Figure A.5: Mass spectrum of fragmentation of a sample of DNPZ in methanol and water by collision energy of 30. (Relative abundance in terms of m/z)

A.2 QUANTIFYING DNPZ BY LIQUID CHROMATOGRAPHY AND MASS SPECTROMETRY (LC-MS)

After DNPZ has been detected by MS, its concentration in different solutions was quantified using a LC-MS system. Samples of DNPZ, PZ, and DNPZ+PZ in 80% methanol and 20% were separated with LC-MS using a reverse phase column.

The chromatograms were divided in three parts of mass ranges, 145–145.2 for DNPZ, 116–116.2 for MNPZ, and 87–87.2 for PZ. Figures A.6–A.14 show the respective results.

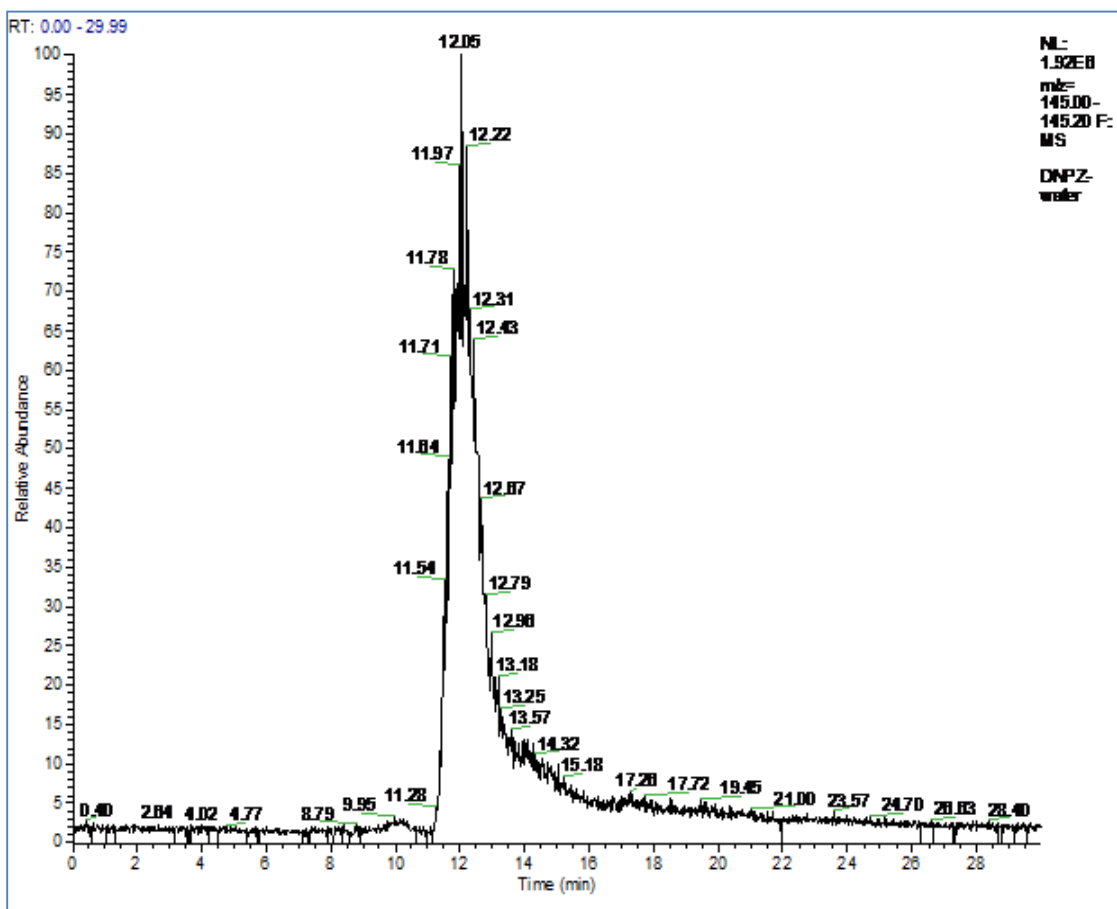


Figure A.6: Chromatogram of a sample of DNPZ in methanol and water analyzed by LC-MS

Figure A.6 shows the chromatogram of DNPZ analysis by LC-MS when the mass range of detection is between 145 and 145.2. The vertical axis presents relative abundance and the horizontal axis shows retention time.

DNPZ comes out at 12.05 minutes with a high relative abundance while there are other components with mass close to DNPZ, and considerably lower relative abundance, around it.

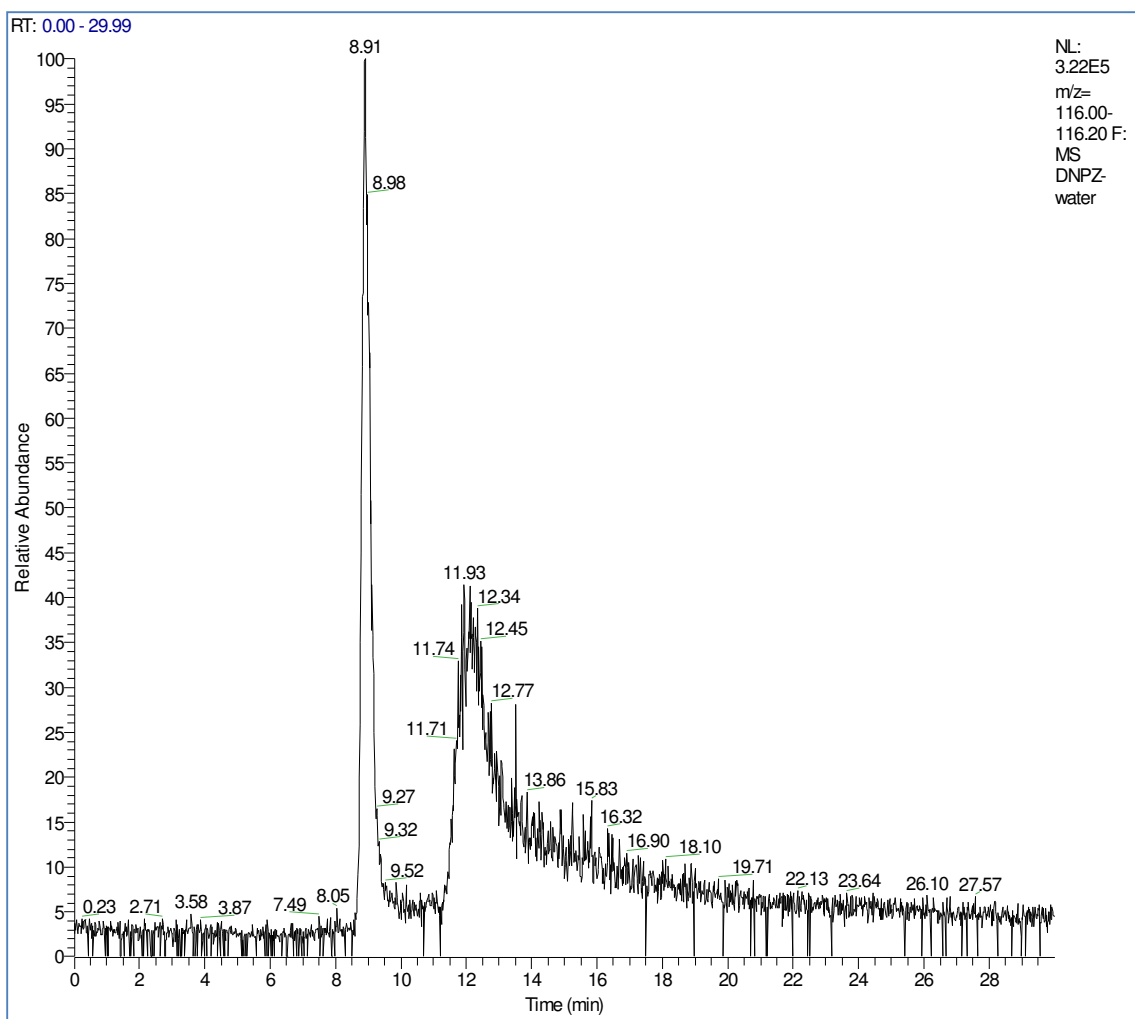


Figure A.7: Chromatogram of a sample of DNPZ in methanol and water analyzed by LC-MS in mass range of MNPZ (116)

Figure A.7 shows that MNPZ can be produced when DNPZ is dissolved in methanol and water. Its retention time is 8.9 minutes.

Figure A.8 shows that there is very little PZ in a DNPZ sample, showing that LC-MS is a good method to quantify DNPZ, although more work must be done to obtain calibration curves and measurement sensitivity.

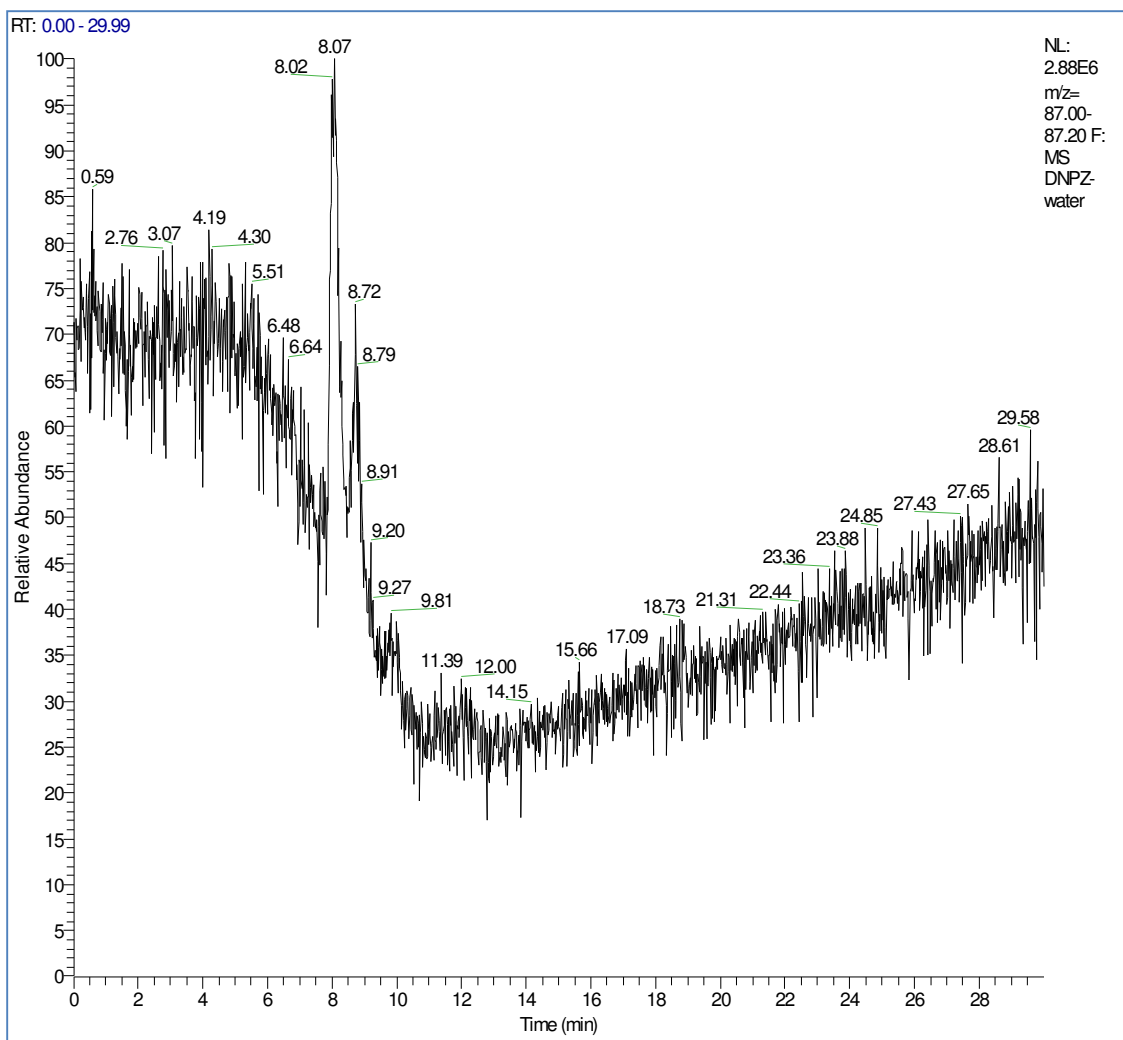


Figure A.8: Chromatogram of a sample of DNPZ in methanol and water analyzed by LC-MS in mass range of PZ (87)

The following two chromatograms show the response of LC-MS to a solution of PZ in methanol and water.

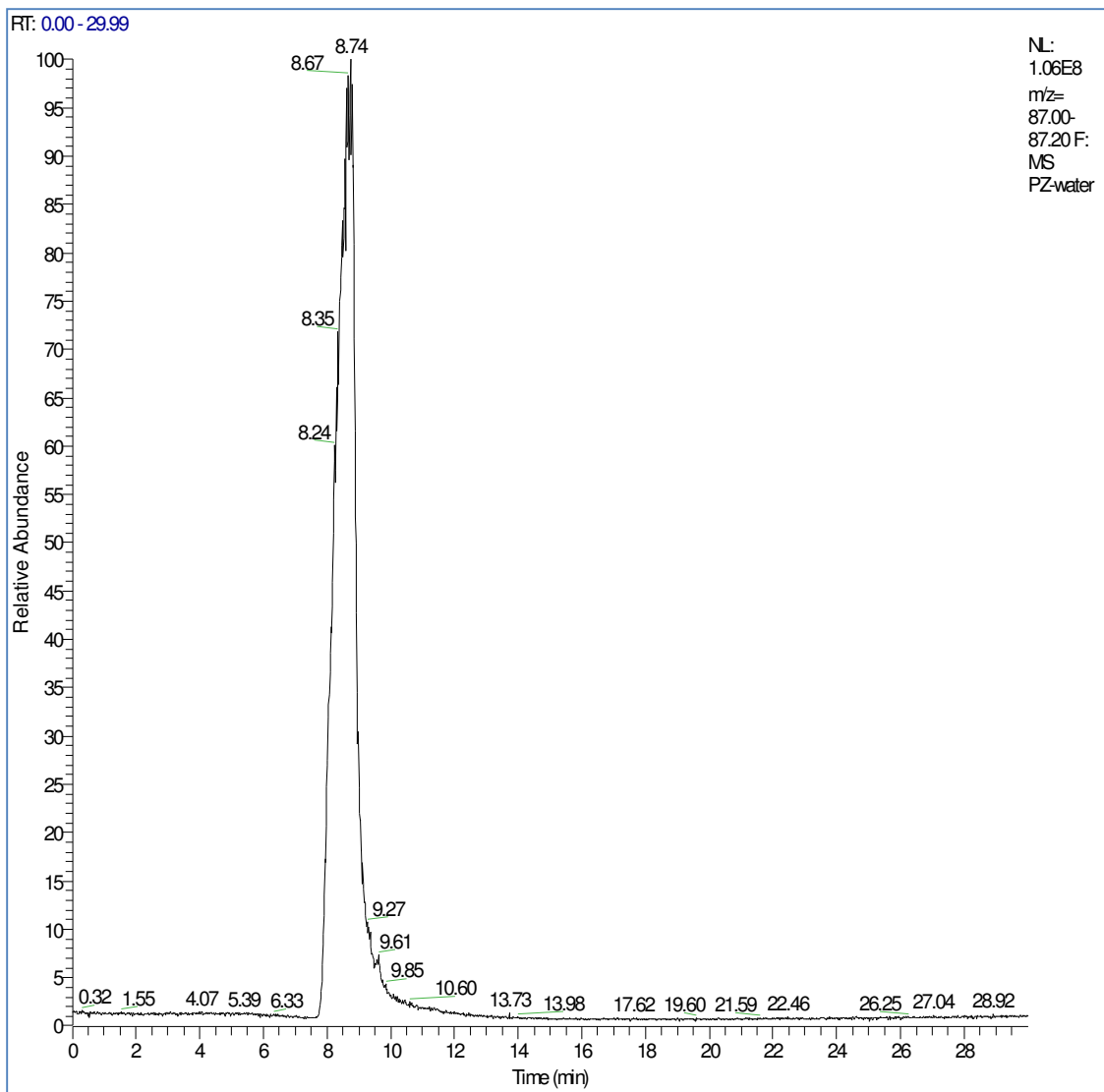


Figure A.9: Chromatogram of a sample of PZ in methanol and water analyzed by LC-MS in mass range of PZ (87)

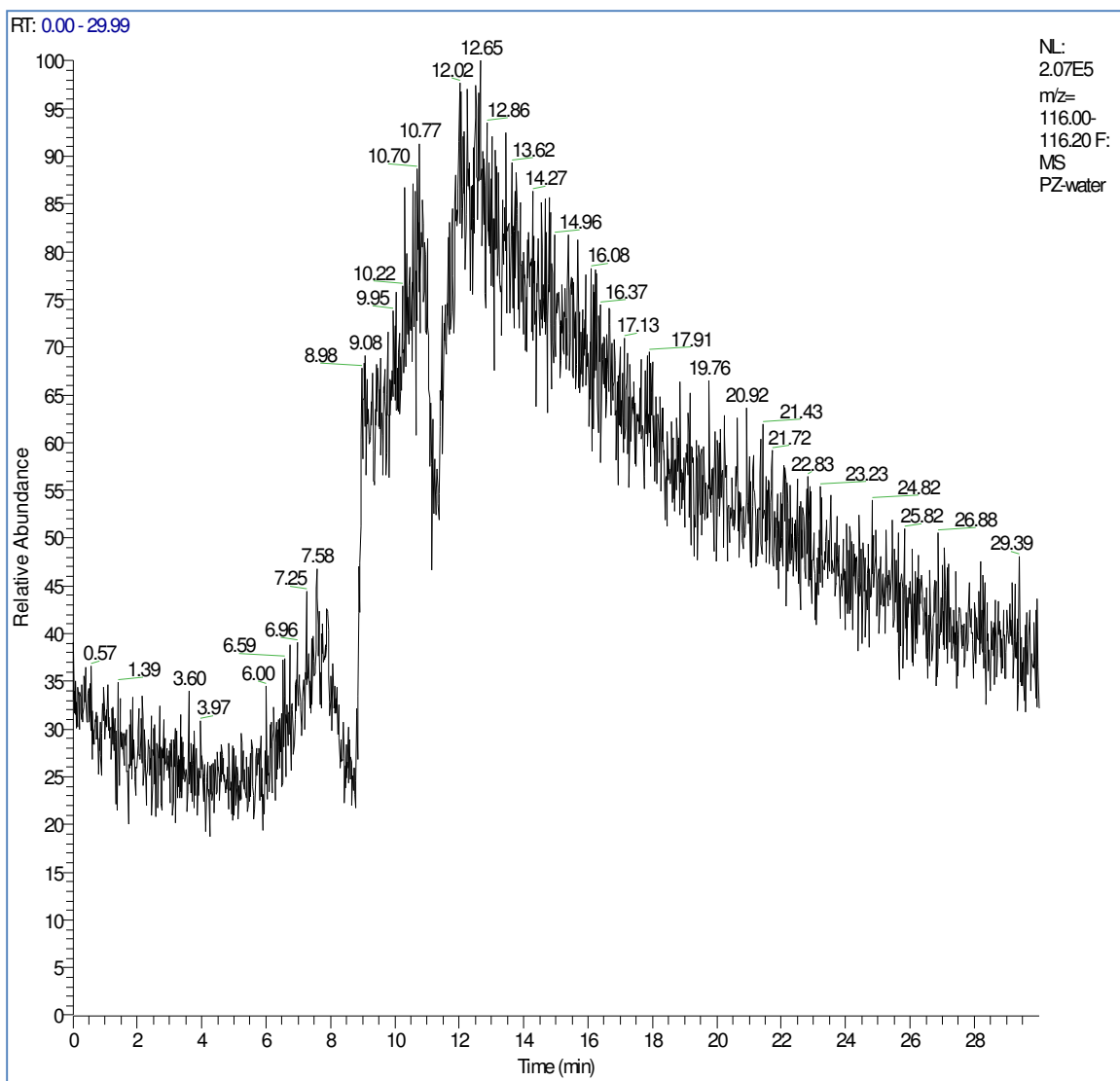


Figure A.10: Chromatogram of a sample of PZ in methanol and water analyzed by LC-MS in mass range of MNPZ (116)

The following three chromatograms show the analysis of equal concentrations of DNPZ and PZ in methanol and water by LC-MS. As noted, there is some MNPZ rather than PZ and DNPZ in LC-MS analysis.

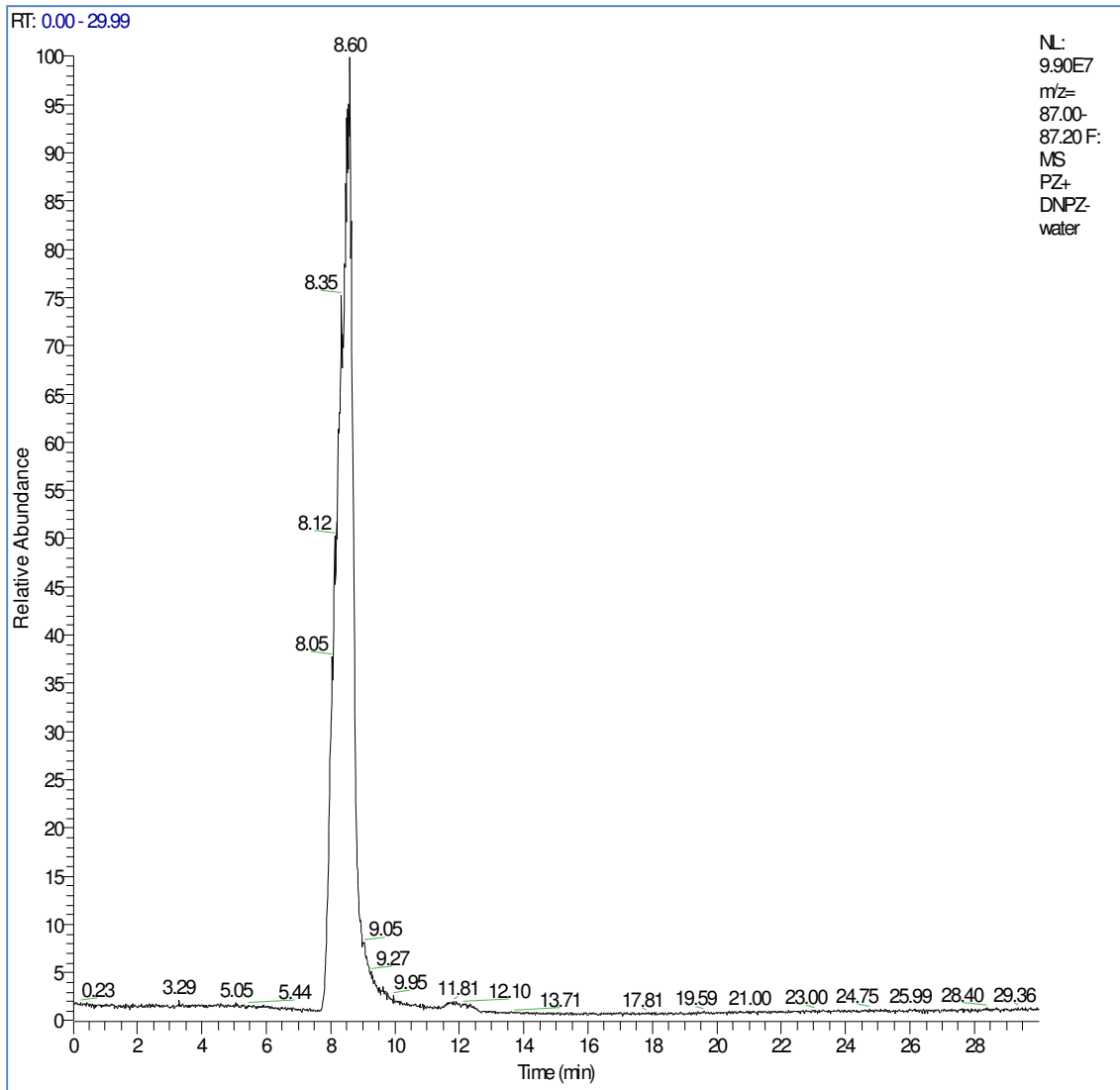


Figure A.11: Chromatogram of a sample of PZ and DNPZ in methanol and water analyzed by LC-MS in mass range of PZ (87)

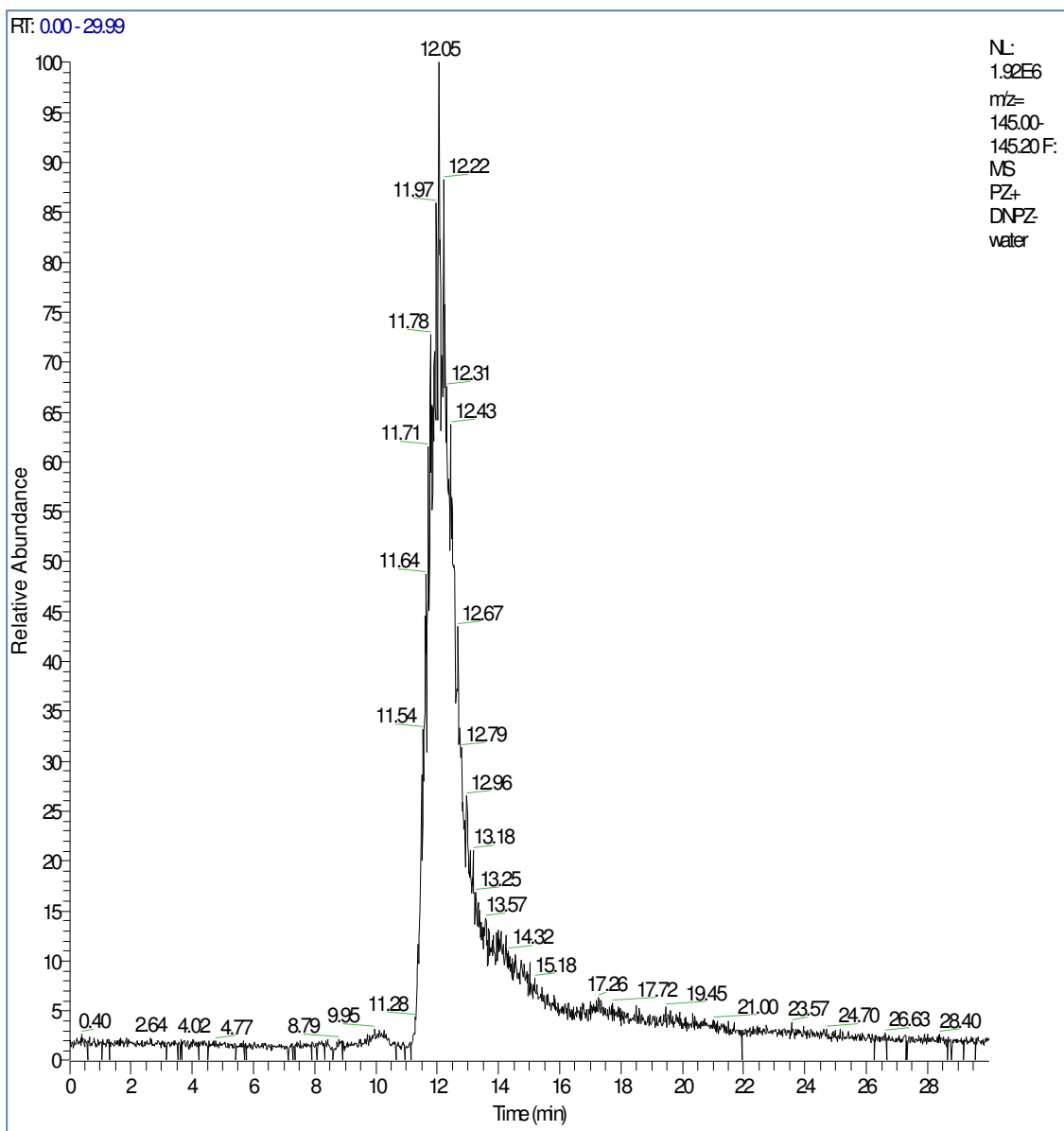


Figure A.12: Chromatogram of a sample of PZ in methanol and water analyzed by LC-MS in mass range of DNPZ (145)

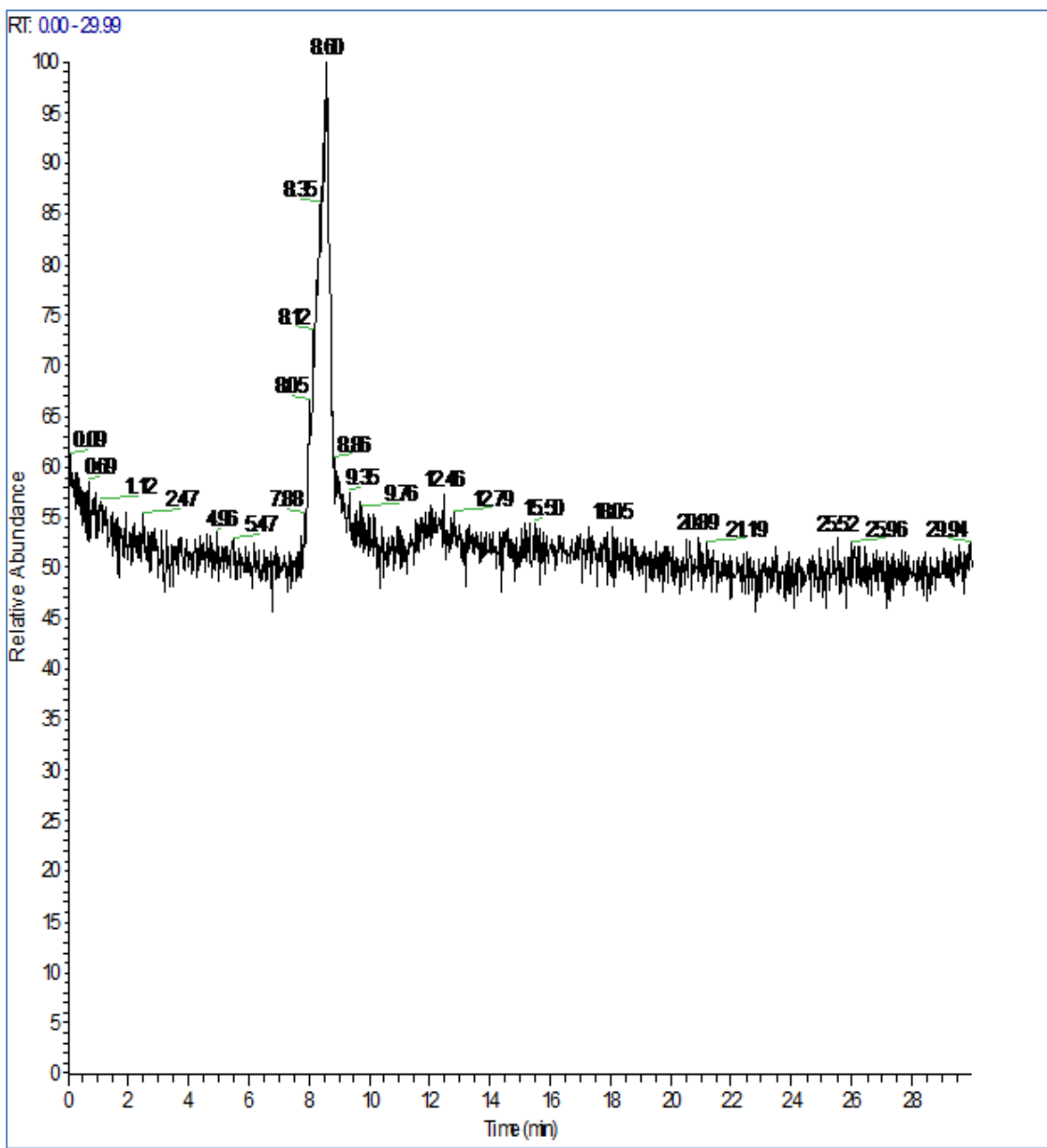


Figure A.13: Chromatogram of a sample of PZ in methanol and water analyzed by LC-MS in mass range of MNPZ (116)

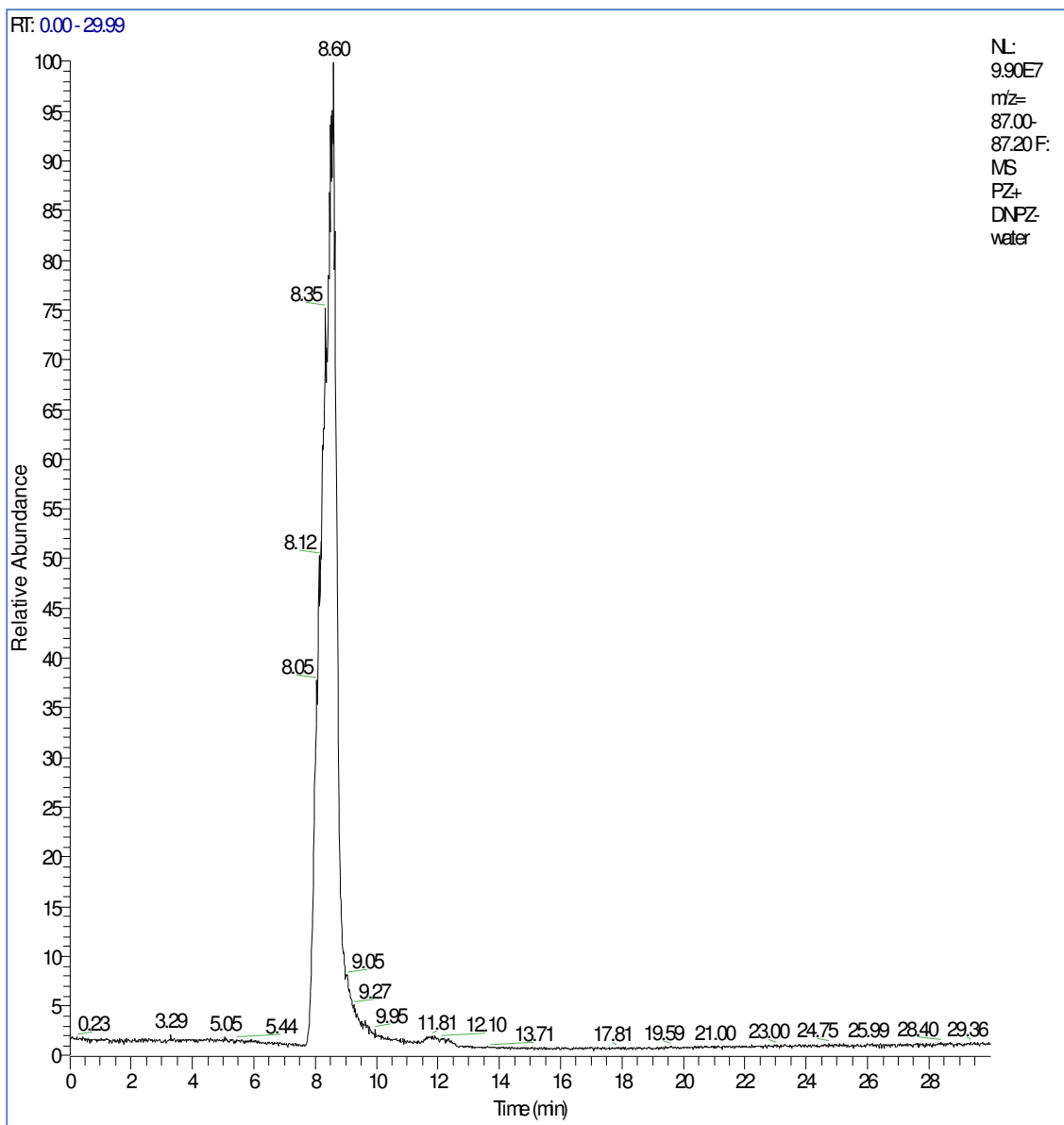


Figure A.14: Chromatogram of a sample of piperazine in methanol and water analyzed by LC-MS in mass range of PZ (87)

After detection of DNPZ by MS, for quantifying the concentration of DNPZ in different solutions, a LC-MS system was used. Different concentrations of standard DNPZ in 80% methanol and 20% water have been applied to LC-MS using a reverse phase column. The areas under the peaks in the chromatograms are related to the concentration of each standard, so a calibration curve has been established with a sensitivity of 5×10^{-5} (Figure A.15).

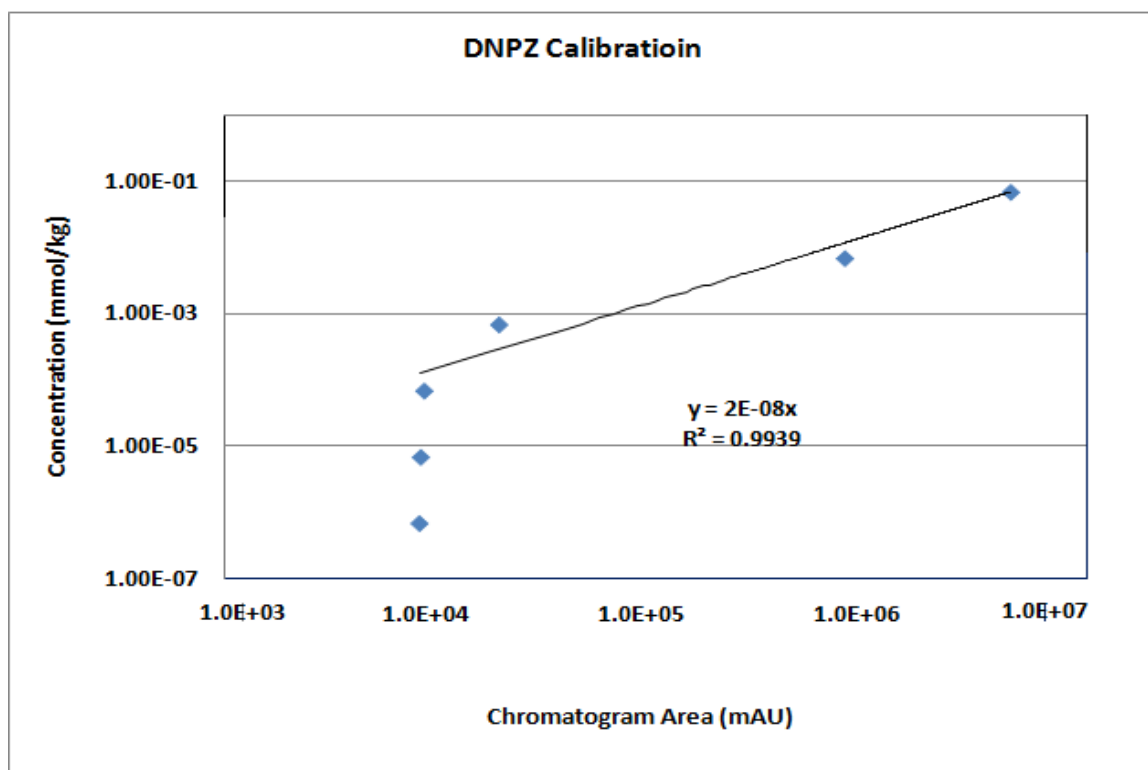


Figure A.15: Calibration curve for standard DNPZ, with a detection limit of 9×10^{-5} mmol/kg

Figure A.15 designates the chromatogram area by the mass spec detector related to the different concentrations of DNPZ, and the relevant calibration curve. This will be

used when a sample with an unknown concentration of DNPZ is injected into the LC-MS.

A.3 DETECTING MNPZ AND DNPZ IN A SOLUTION OF PZ

The DNPZ detection method has been used for purchased standard MNPZ, but results show that the method should be refined. Therefore a new method was established in which the mobile phase contains 10% methanol and 90% water with the rate of 200 $\mu\text{L}/\text{min}$ over 30 minutes. This method gives better separation of PZ, MNPZ, and DNPZ.

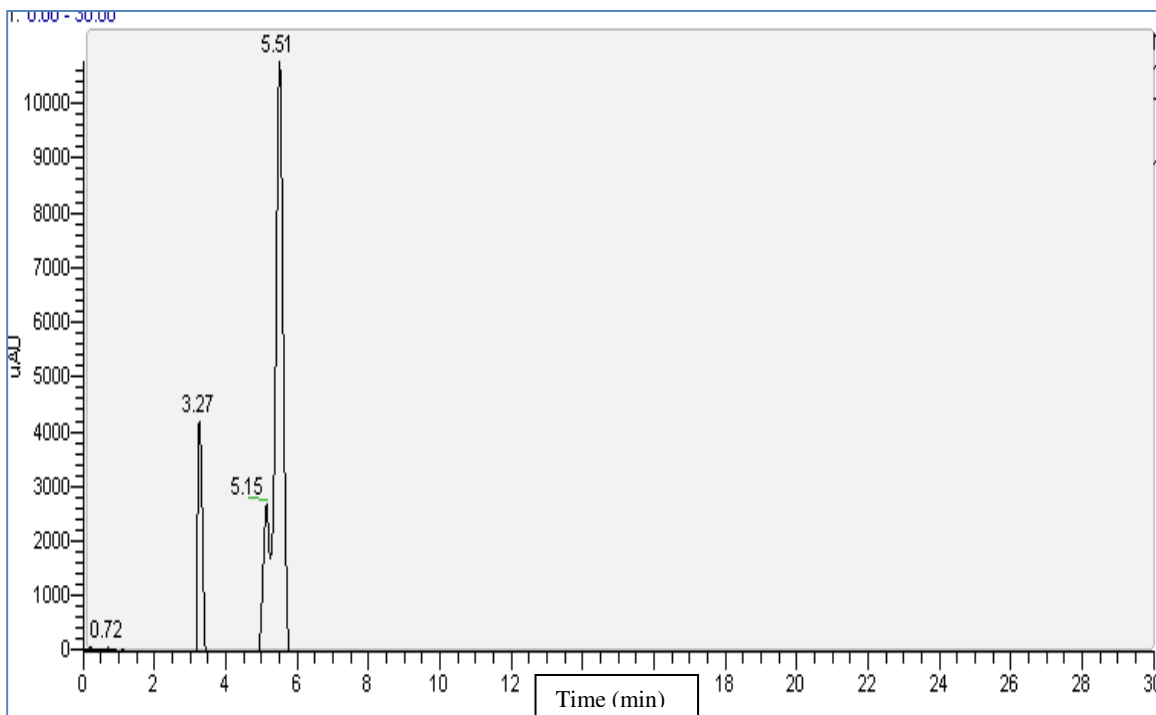


Figure A.16: Chromatogram of MNPZ, DNPZ, and PZ when the mobile phase contains 50% methanol and 50% water

Figure A.16 presents the response of LC-MS to a sample which contains 8 m loaded PZ, MNPZ, and DNPZ, where the mobile phase contains 50% methanol and 50%

water at a rate of 350 $\mu\text{L}/\text{min}$. As seen in the figure, there is not a good separation between component peaks, so the mobile phase composition has been changed. When the rate of methanol was increased, peaks were combined and there was no specific peak for each species in solution. The method has been developed by decreasing the portion of methanol in the mobile phase and the results are shown in the following figures. Decreasing the flow rate of the mobile phase to 200 $\mu\text{L}/\text{min}$ improves results.

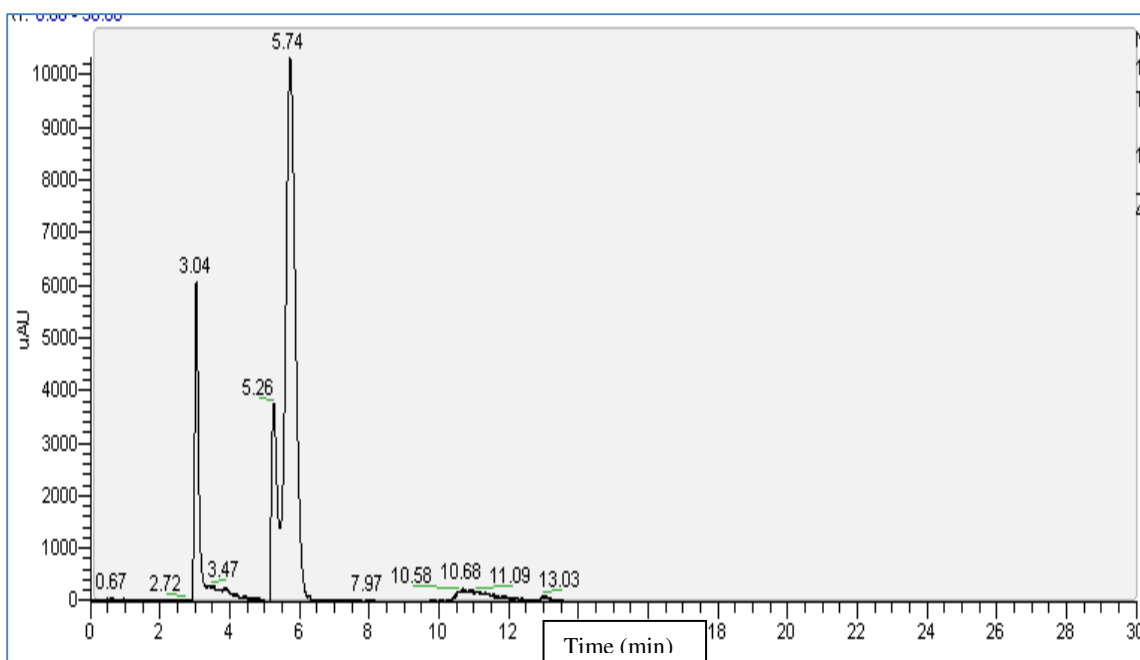


Figure A.17: Chromatogram of MNPZ, DNPZ, and PZ when the mobile phase contains 40% methanol and 60% water

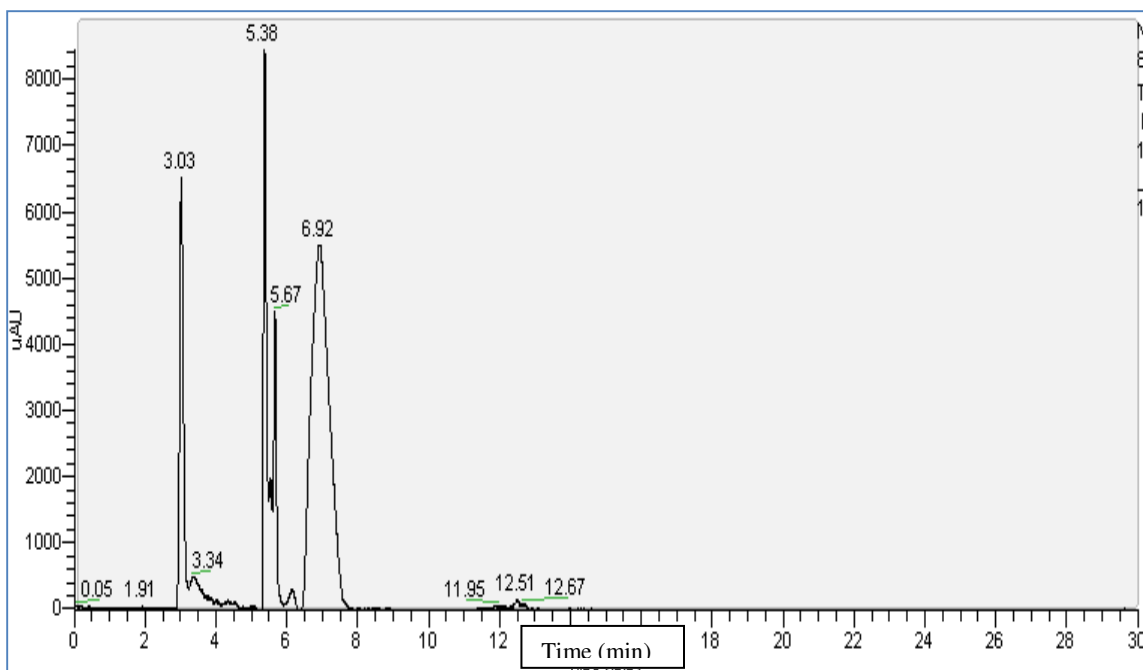


Figure A.18: Chromatogram of MNPZ, DNPZ, and PZ when the mobile phase contains 20% methanol and 80% water

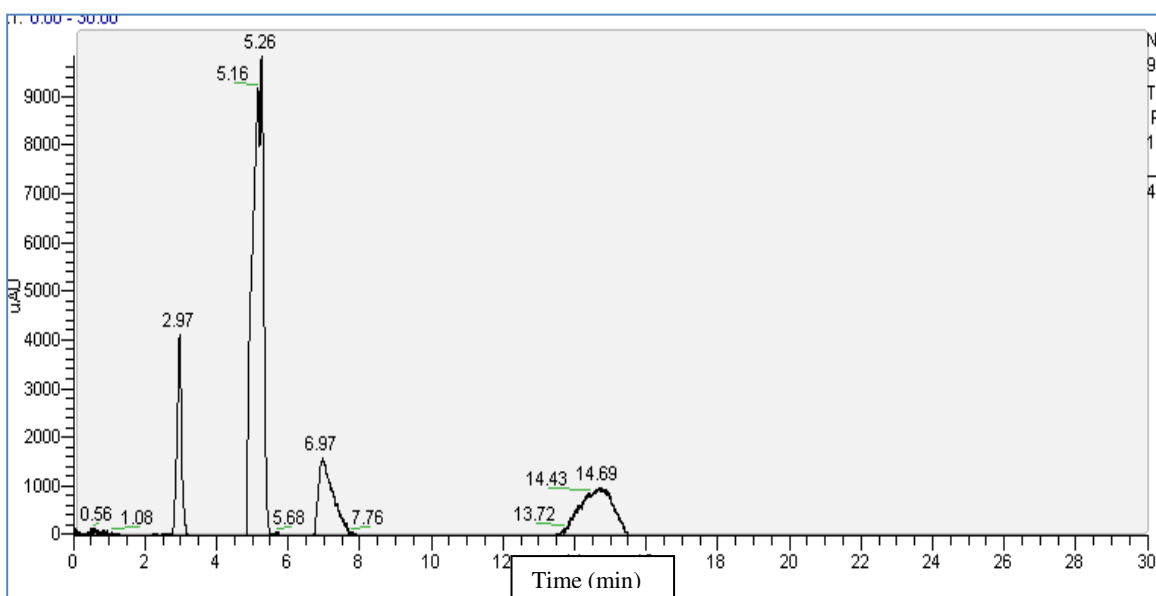


Figure A.19: Chromatogram of MNPZ, DNPZ, and PZ when the mobile phase contains 10% methanol and 90% water

When experimental samples from the kinetic study of nitrosation were analyzed, many components other than MNPZ and DNPZ were found in the reaction products. For example, m/z of 87.19 represents PZ and m/z of 65 indicates methanol, but m/z of 74.17, 97.21, 106.21, and 128.19 are unidentified (Figure A.20). However MS analysis shows that MNPZ and DNPZ are the least common products from nitrosation of 8 m loaded PZ (Figure A.20).

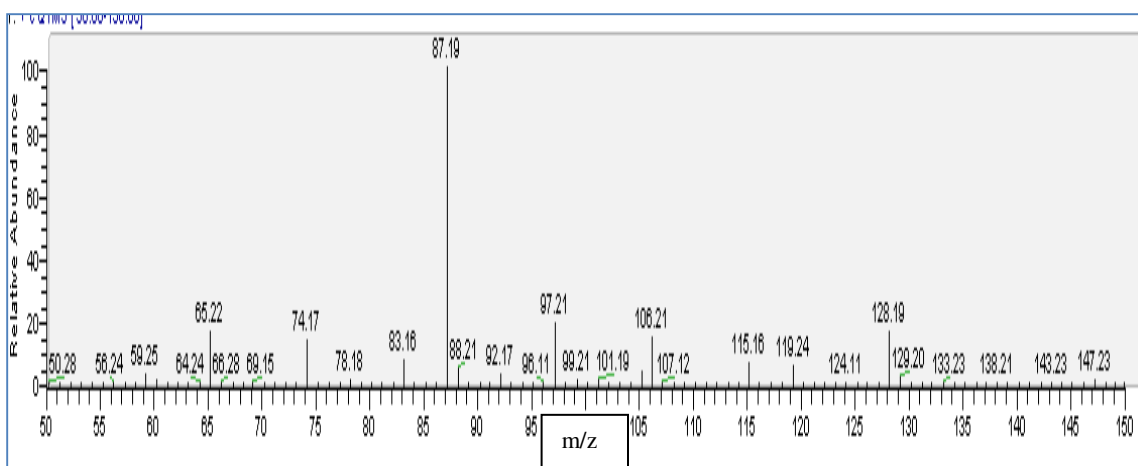


Figure A.20: Chromatogram of the reaction product of 8 m loaded PZ and 50 mmol/kg NaNO_2 at 60 °C.

Analysis of the MS chromatogram of specific samples shows that the concentration of MNPZ and DNPZ is very low (Figure A.21).

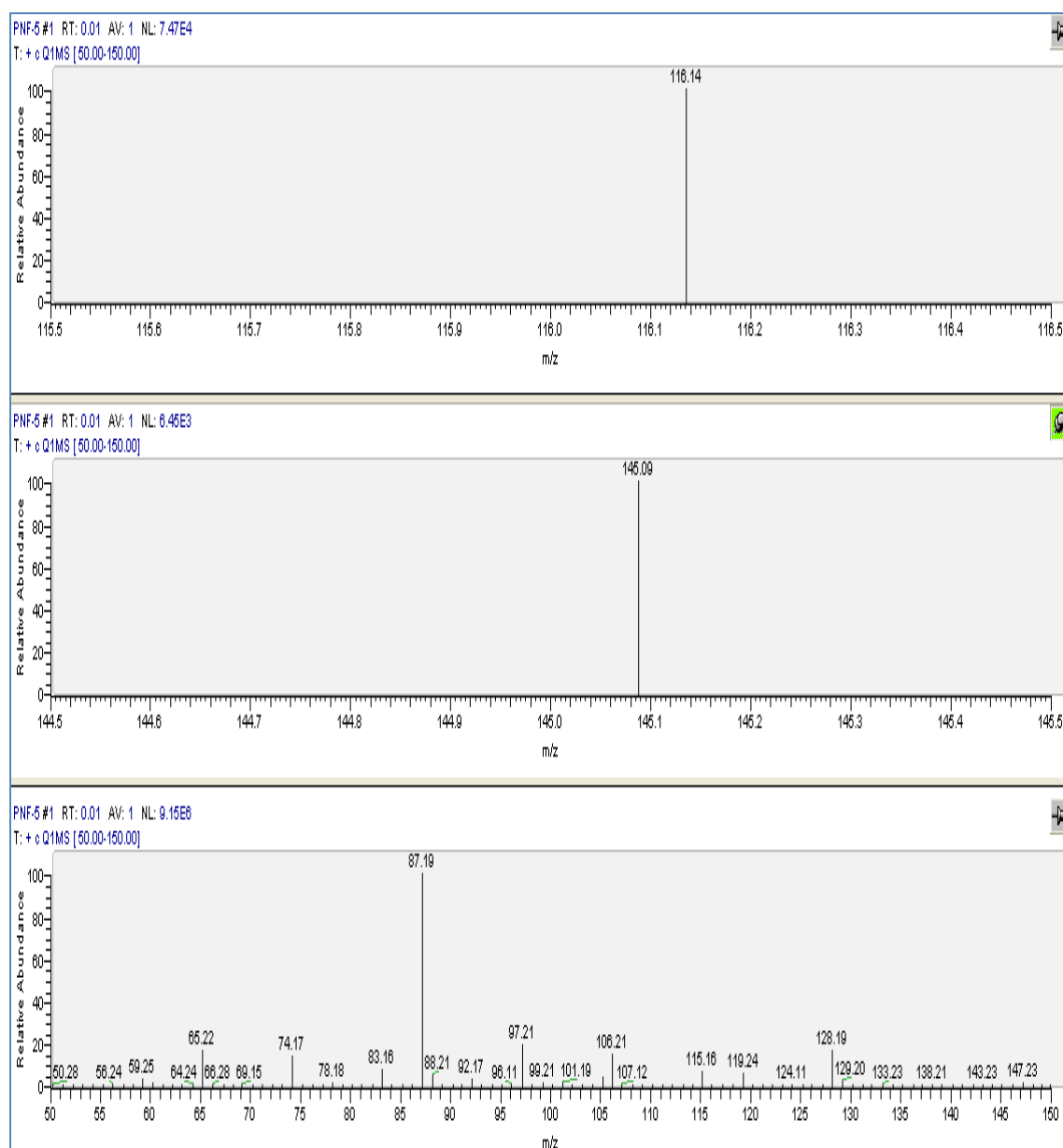


Figure A.21: Concentrations of MNPZ and DNPZ in reaction products of 8 m loaded PZ and 50 mmol/kg nitrite at 60 °C.

The total ion content of the original sample is 9.15E6. By calculating the ratio of MNPZ and DNPZ ion content to the total ion content of the sample, the concentration of

MNPZ and DNPZ can be obtained, which for this sample, is 0.05 ppm ($4.35\text{E-}4$ mM) MNPZ and 0.004 ppm ($2.77\text{E-}5$ mM) DNPZ.

Further studies are being done to obtain a calibration curve that will show the concentration of different species in an unknown sample using the MS data.

Note that the amount of MNPZ and DNPZ in the sample of the reaction products of 8 m loaded PZ and 50 mmol/kg NaNO_2 is related to the reaction between PZ and a high concentration of nitrite.

A.4 DETECTING MNPZ AND DNPZ IN AQUEOUS PZ USING HPLC WITH UV DETECTION

A new detection method has been applied to standard solutions of MNPZ, DNPZ, and a solution of PZ containing MNPZ and DNPZ using HPLC. This detection method has been applied to standard solutions of MNPZ using HPLC. To perform a calibration curve for measuring MNPZ, the best method is to use standard reverse phase of 0.01 M acetonitrile in water buffered with ammonium carbonate to detect a standard MNPZ solution of methanol with a dilution factor of 20. Figure 3.4 shows the calibration curve of MNPZ.

The HPLC used is a Dionex UltiMate 3000 LC with Chimeleon interface and an Acclaim[®] Polar Advantage column. The device uses a 2100 UV detector and scanning wavelength for detecting MNPZ is 240 nm.

Primary results show that MNPZ and DNPZ are detectable with this HPLC method but PZ is not. Figure A.22 shows a chromatogram of a sample containing MNPZ, DNPZ, and PZ. MNPZ gives a better detection peak while DNPZ has a wider peak, which might be because of some impurities in DNPZ standards.

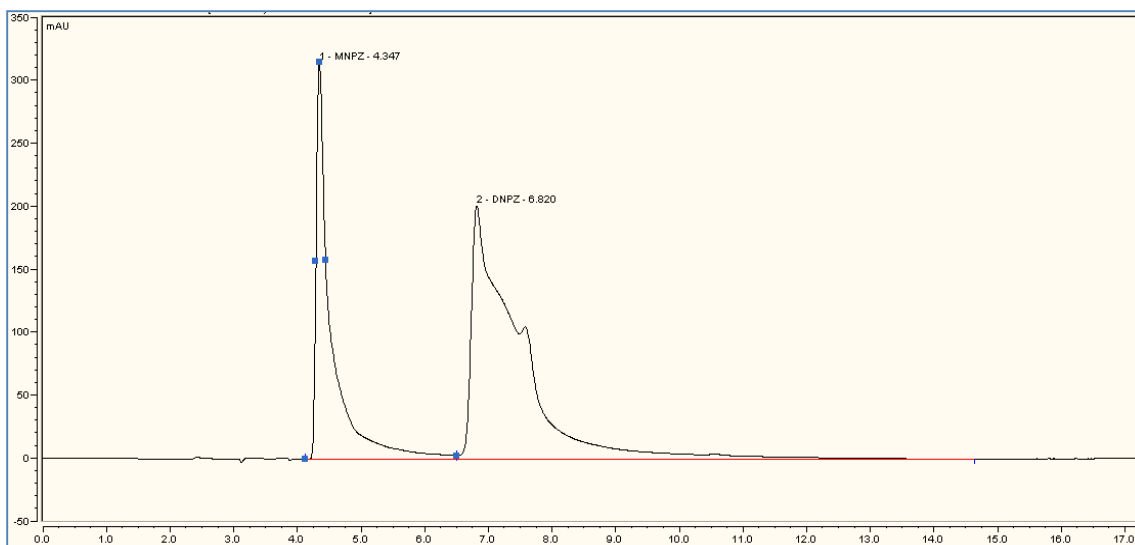


Figure A.22: Chromatogram of 500 ppm of MNPZ, DNPZ, and PZ, using HPLC

A.5 COMPARING THE RESULTS OF LC-MS AND HPLC FOR UNKNOWN SAMPLES

Samples were injected into both LC-MS and HPLC to compare the analysis and select the more accurate way to detect and measure nitrosopiperazines.

Figure A.23 shows the results of samples from high gas flow experiments at the beginning, middle, and end of the course of experiments. There are three clear peaks that show PZ, MNPZ, and DNPZ. Chromatograms show evidence of MNPZ and DNPZ, but by developing the reaction, MNPZ and DNPZ disappear. Applying the peak area of these results and the calibration curves show that the concentration of MNPZ and DNPZ is very low and less than 6×10^{-5} mmol/kg at the beginning.

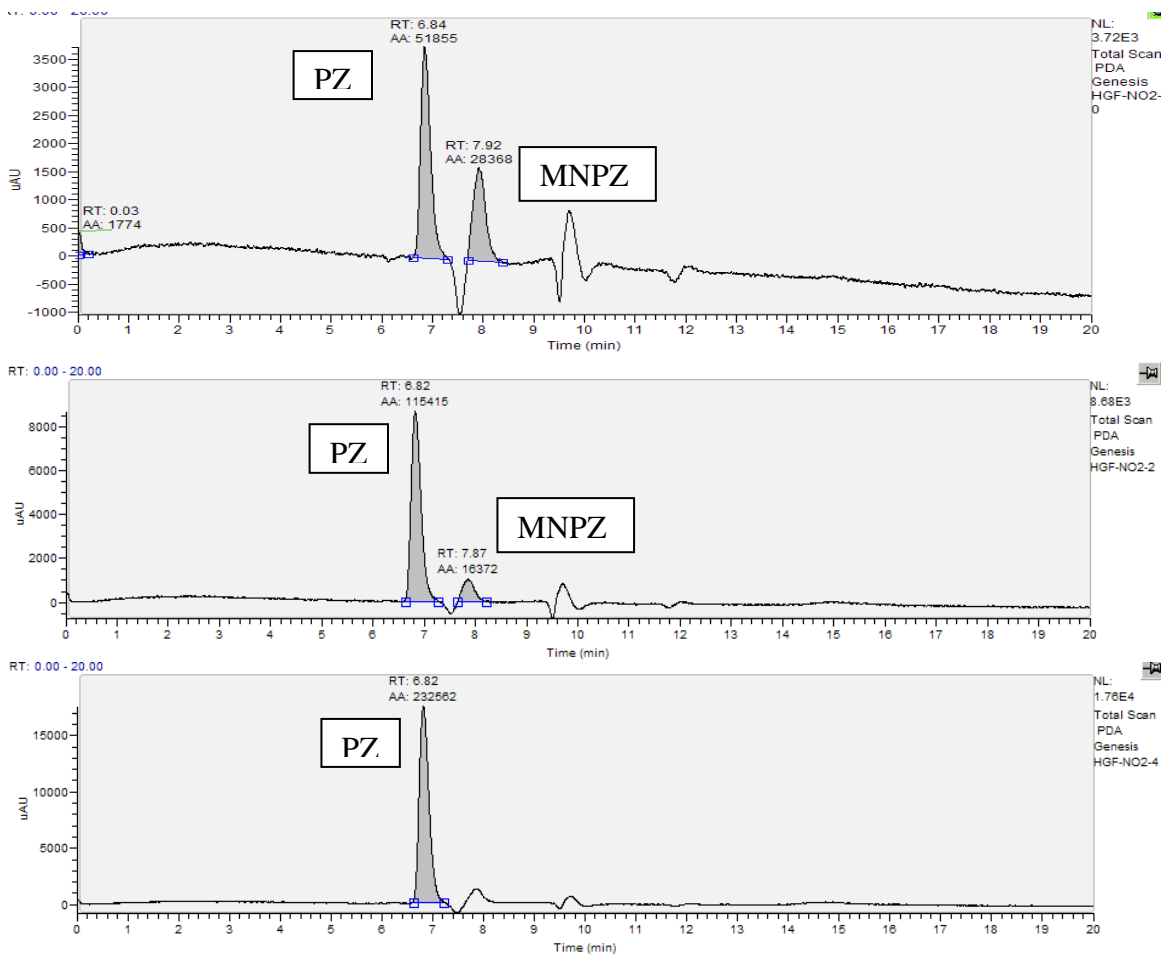


Figure A.23: Chromatogram of reaction products of HGF experiments at the $t=0$, 3, and 5 days of the reaction, analyzed by LC-MS

Figure A.24 contains the results of the same samples as Figure 5 but analyzed by HPLC. HPLC shows good response to standard MNPZ, but as shown in Figure 8, it does not have the accuracy of LC-MS.

HPLC does show the production of an unknown component during the reaction which has a retention time close to that of MNPZ and DNPZ. Since this could be something other than MNPZ or DNPZ, another analytical method (MS) should be used to identify the new product.

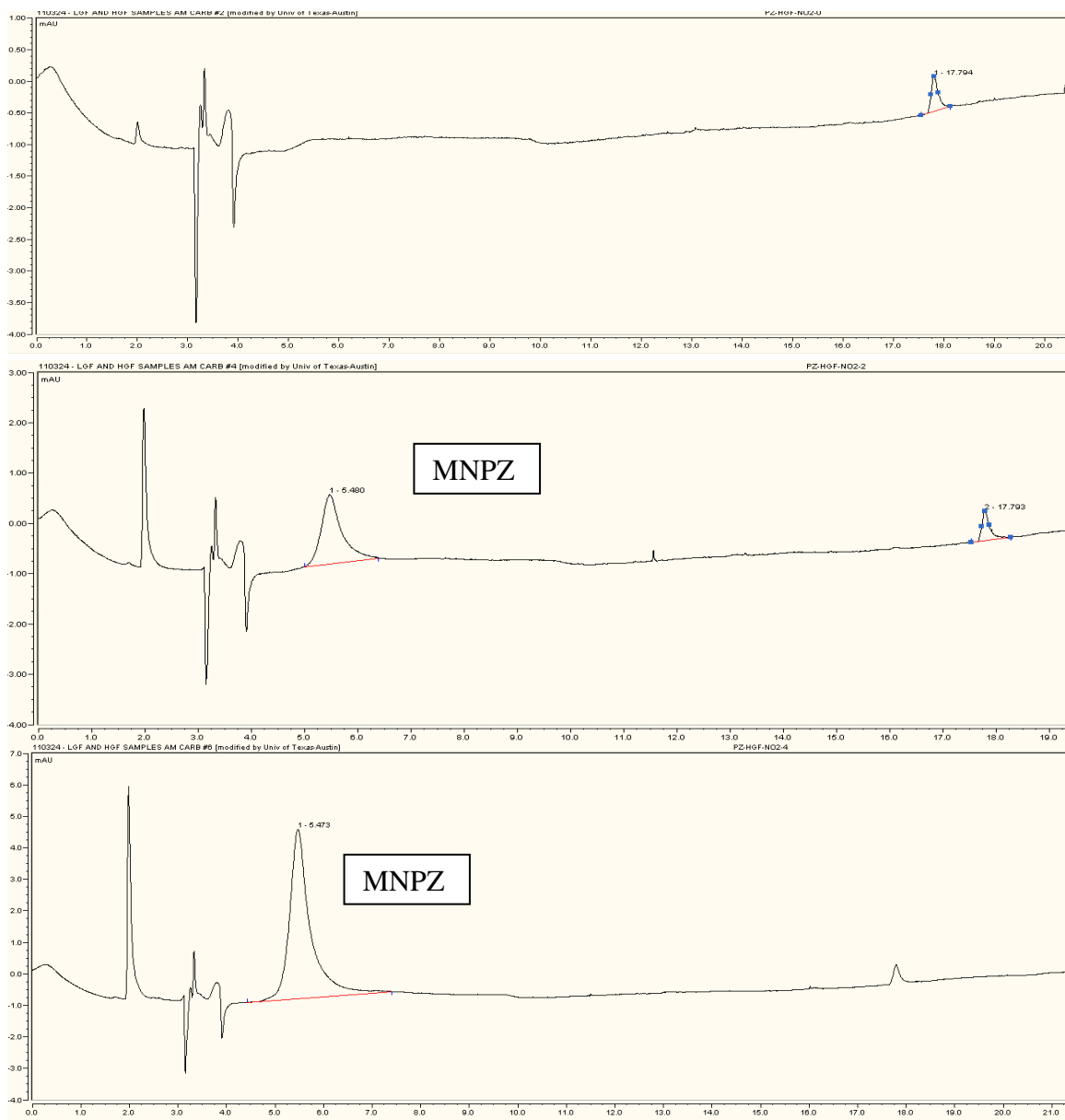


Figure A.24: Chromatogram of reaction products of HGF experiments at t=0, 3, and 5 days, analyzed by HPLC/UV.

The same analysis has been done for the low gas flow experiment (Figures A.25, A.26).

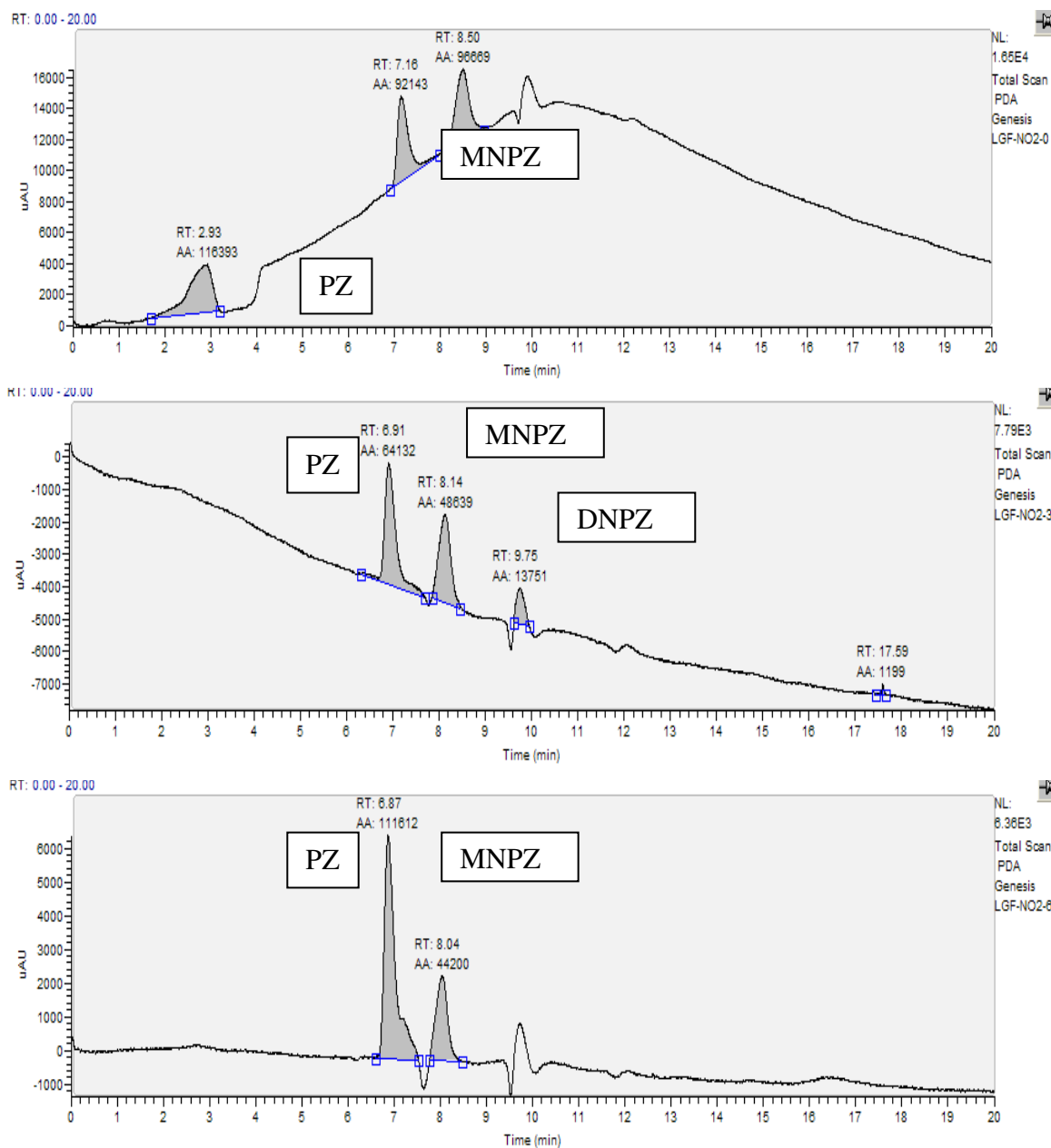


Figure A.25: Chromatogram of reaction products of LGF experiments at the t=0, 3, and 15 days of reaction, analyzed by LC-MS. as before, show the times.

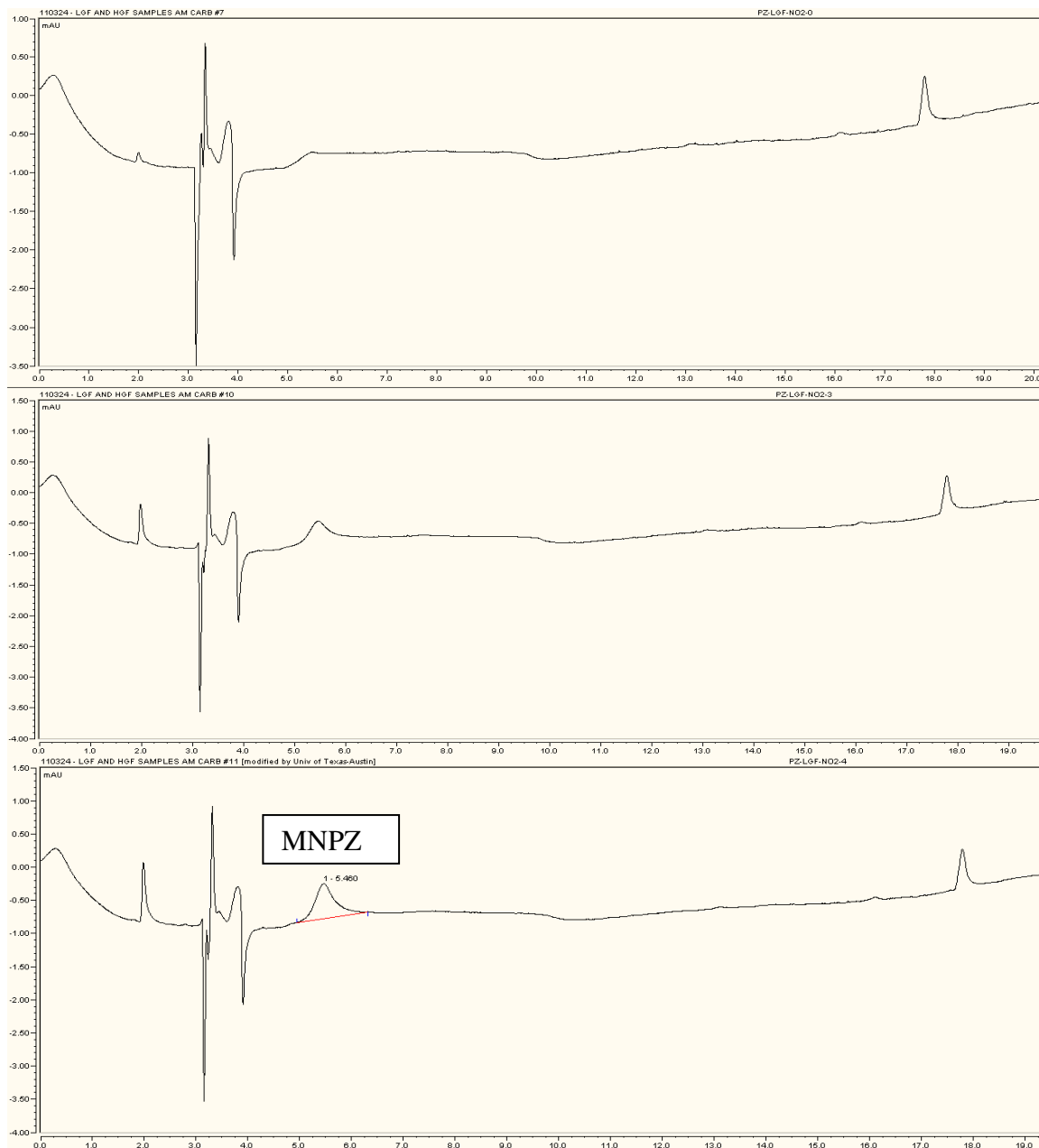


Figure A.26: Chromatogram of reaction products of LGF experiments at the t=0, 3, and 15 days of reaction, analyzed by HPLC.

Appendix B

B.1 DATA FOR REACTION RATE OF NITRITE CONSUMPTION DURING THE REACTION WITH PZ

Reaction conditions: 50 mmol/kg Nitrite, 0.3 mole CO₂/Equiv N						
Clear glass reactor, exposed to the light						
Time (days)	PZ concentration: 8m			PZ concentration: 2m		
	20 °C	60 °C	75 °C	20 °C	60 °C	75 °C
	Nitrite(mmol/kg)	Nitrite(mmol/kg)	Nitrite(mmol/kg)	Nitrite(mmol/kg)	Nitrite(mmol/kg)	Nitrite(mmol/kg)
0	52.3	53.33	52.12	50.03	50.03	50.03
1	51.29	33.42	21.16	49.23	47.76	43.14
2	51.1	23.5	18.1	50.49	48.6	41.8
3	51.02	17.3	10.3	48.67	47.2	36.62
4	52.13	9.64	4.8	49.16	39.5	30.38
5	50.126	9.6	3.95	48.5	37.23	24.01
6	51.27	9.55	3.56	No Data	No Data	No Data

Reaction conditions: 8 m PZ, 0.3 mole CO₂/Equiv N, T=60 °C Starting reactions with different nitrite concentrations				8 m PZ, T=60 °C Clear glass reactor in water bath, exposed to the light		8m PZ, T=90 °C Performed in Autoclave		
				Using 2 M H₂SO₄ to adjust the pH	Using Formaldehyde as catalyst	50 mmol/kg Nitrite, 0.3 mole CO₂/Equiv N		
Time (days)	Nitrite (mmol/kg)	Nitrite (mmol/kg)	Nitrite (mmol/kg)	Nitrite (mmol/kg)	Nitrite (mmol/kg)	Time (days)	Nitrite (mmol/kg)	MNPZ (mmol/kg)
0	5	22.3	51.33	50.69	50.29	0	43.1	0
1	2.77	15.25	42.41	33.78	34.53	0.04	28.67	30.28
2	1.65	8.2	33.6	35.36	21.13	0.08	21.46	31.31
3	No Data	No Data	No Data	29	90.21	0.17	15.67	27.37
4	1.36	5.5	17.9	27.7	4.13	0.21	11.92	26.85
5	0.78	4.15	13.4	28.9	4.09	0.25	9.81	24.00
6	No Data	No Data	No Data	29.07	5.65	0.5	6.51	23.00
7	No Data	No Data	No Data	26.8	4.63	1.17	5.32	12.33

B.2 HIGH TEMPERATURE EXPERIMENTAL DATA

Reaction conditions: 8m PZ, 50 mmol/kg Nitrite, 0.3 mole CO₂/Equiv N; performed in closed cylinder in the oven						
Time (days)	100 °C		135 °C		150 °C	
	Nitrite (mmol/kg)	MNPZ (mmol/kg)	Nitrite (mmol/kg)	MNPZ (mmol/kg)	Nitrite (mmol/kg)	MNPZ (mmol/kg)
0.00	45.63	0.00	45.63	0.00	45.63	0.00
0.04	32.51	9.65	43.69	40.32	0.94	39.66
0.13	21.91	20.90	No Data	No Data	No Data	No Data
0.21	14.25	25.91	2.70	37.82	0.66	26.26
0.29	10.12	26.73	1.53	32.58	0.66	25.04
0.63	8.58	28.12	1.36	14.69	0.62	4.03
1.00	4.66	16.41	1.31	1.77	0.46	0.00
7.00	2.09	11.13	0.56	0.00	0.44	0.00
15.75	0.54	6.64	0.35	0.00	0.29	0.00

Reaction conditions: 8m PZ, 50 mmol/kg Nitrite, 0.2 mole CO₂/Equiv N; performed in closed cylinder in the oven						
Time (days)	T=100 °C		T=135 °C		T=150 °C	
	Nitrite (mmol/kg)	MNPZ (mmol/kg)	Nitrite (mmol/kg)	MNPZ (mmol/kg)	Nitrite (mmol/kg)	MNPZ (mmol/kg)
0.00	45.68	0.00	45.68	0.00	45.68	0.00
0.02	30.17	0.00	26.06	0.00	18.05	42.88
0.08	No Data	No Data	22.26	46.71	16.1	34.81
0.17	No Data	No Data	12.98	43.45	14.68	31.31
0.33	No Data	No Data	5.69	39.32	6.75	21.86
0.50	No Data	42.3	3.49	30.27	No Data	No Data
1	7.77	27.58	0.41	4.03	0.08	4.78
2	3.2	24.97	No Data	3.93	No Data	0.00
3	1.86	22.74	0.09	3.16	0.02	0.00

Reaction conditions: 8m PZ, 50 mmol/kg Nitrite, 0.1 mole CO₂/Equiv N; performed in closed cylinder in the oven						
Time (days)	T=100 °C		T=135 °C		T=150 °C	
	Nitrite (mmol/kg)	MNPZ (mmol/kg)	Nitrite (mmol/kg)	MNPZ (mmol/kg)	Nitrite (mmol/kg)	MNPZ (mmol/kg)
0.00	45.63	0.00	45.63	0.00	45.63	0.00
0.02	No Data	No Data	37.69	8.78	28.81	3.41
0.04	42.07	0.00	29.79	14.08	26.62	22.89
0.13	No Data	35.87	11.62	33.61	25.38	37.95
0.21	No Data	No Data	8.62	42.84	8.52	34.07
0.33	35.96	No Data	4.29	37.26	4.45	32.66
0.50	28.87	35.87	3.44	5.38	4.29	0.18
1.00	23.22	41.55	0.34	5.70	1.47	0.06
2.00	10.42	36.15	0.16	4.17	1.67	0.00
3.00	6.73	30.07	No Data	3.66	0.47	0.00

Reaction conditions: 2m PZ, 50 mmol/kg Nitrite, 0.3 mole CO₂/Equiv N; performed in closed cylinder in the oven						
Time (days)	T=100 °C		T=135 °C		T=150 °C	
	Nitrite (mmol/kg)	MNPZ (mmol/kg)	Nitrite (mmol/kg)	MNPZ (mmol/kg)	Nitrite (mmol/kg)	MNPZ (mmol/kg)
0.00	48.70	0.00	48.70	0.00	48.70	0.00
0.04	25.60	4.50	14.40	31.75	1.55	34.29
0.08	20.48	10.33	2.30	29.27	0.47	33.47
0.13	15.53	15.67	1.80	29.96	No Data	No Data
0.17	15.46	20.79	1.63	29.09	0.46	32.04
0.50	14.94	26.88	1.52	27.92	0.45	23.43
1.00	11.87	40.22	1.43	24.61	0.44	12.73
2.00	10.32	36.66	0.34	12.31	0.2	7.05

REFERENCES

- Addison, C. "Chemistry in Liquid Dinitrogen Tetroxide." Part I of "Chemie in Nichtwasaerigen Ionisierenden Losungsmateln"; *Vieweg: Braunschweig*, 1967; 1: 111.
- Anderson JD Austern MH. "Measurement of Z' couplings at future hadron colliders through decays to τ leptons." *Phys Rev*. 1992;6:290–302.
- Andrzejewski P, Kasprzyk-Horden B, Nawrocki J. "N-nitrosodimethylamine (NDMA) formation during ozonation of dimethylamine-containing waters." *Water Res*. 2008; 42:863–870.
- Archer MC, Wishnok JS. "Quantitative Aspects of Human Exposure to Nitrosamines." *Food Cosmet Toxicol*. 1975; 15:233.
- Biggs D, and Williams D.H.L. "Kinetics and Mechanism of the Fischer-Hepp Rearrangement and Denitrosation part V. the Mechanism of Denitrosation." *J. Chem. Soc. Perkin Trans*. 1975; 2: 107.
- Bleazard M, Jones GR. "Nitrosamine inhibition." *United States Patent*. Application No. 5,223,644; 1993.
- Cachaza JM, Casado J, Castro A, Lopez MA. "Kinetic studies on the formation of nitrosamines I." *J Cancer Res Clinical Onc*. 1978; 91(3).
- Cannon WN. (Cumberland, IN). Application Number: 06/495273. *Patent* 4501608, 1985.
- Castegnaro M, Eisenbrand G, Ellen L, Keffer D, Klein E.B, Sansone D, Spincer, and Telling G. "Laboratory Decontamination and Destruction of Carcinogens in Laboratory Wastes: Some N-Nitrosamines." *IARC, Scientific Publications No. 43*, World Health Organization, Geneva, Switzerland, Web, Eds, 1982.
- Challis BC, and Butler A. R. "Substitution at an Amino Nitrogen in the Chemistry of the Amino Group," *Wiley Interscience New York*, 1968; R6: 277-345.
- Challis BC, and Kyrtopoulos SA. "Rapid formation of carcinogenic N-nitrosamines in aqueous alkaline solutions." *Br J Cancer*. 1977; 35 (5): 693-696.
- Challis BC, Edwards A, Hunma RR, Kyrtopoulos SA, Outram JR. "Rapid formation of N-nitrosamines from nitrogen oxides under neutral and alkaline conditions." *IARC. Sci Publ*. 1978; 19: 127-42.
- Challis BC, and Outram JR. "The chemistry of nitroso-compounds. Part 17. Formation of N-nitrosamines in solution from dissolved nitric oxide in the presence of hydriodic acid or metal iodides." *Chem Soc, Perkin Trans*. 1979; 2:693–699.
- Challis, B.C., and Outram JR. "Formation of N-nitrosamines and N-nitramines by gaseous nitrogen dioxide." *Acta Cient. Compostelana*. 1982. 19(1-2): p. 153-66.

- Choi Y, Kang J, Park JHY, Lee Y, Choi J, Kang Y. "Polyphenolic flavonoids differ in their antiapoptotic efficacy in hydrogen peroxide-treated human vascular endothelial cells." *J Nutr.* 2003; 133:985–991.
- Cooney RV, Hatch-Pigott V, Ross P, Ramseyer J. "Carcinogenic N-nitrosamine formation: A requirement for nitric oxide." *J Envir Sci Health. Part A*, 1992;27(3): 789-801.
- Crosby T, and Sawyer R. "N-Nitrosamines: A Review of Chemical and Biological Properties and their Estimation in Foodstuffs, in C.O. Chichester." *Advances in Food Research.* 1976; 22: 1-56.
- Cullinane JT, Rochelle GT. "Kinetics of Carbon Dioxide Absorption into Aqueous Potassium carbonate and Piperazine." *Ind Eng Chem Res.* 2007; 45(8):2531–2545.
- Doyle M, Terpstra W, Pockering A, and LePoire M. "Hydrolysis, Nitrosyl Exchange, and Synthesis of Alkyl Nitrites." *J. Org. Chem.* 1983; 48(20): 3379-3382.
- Fridman A, Mukhametshin F M, and Novikov S S. "Advances in the Chemistry of Aliphatic N-nitrosamines." *Russ.Chem.Rev.Eng. Transl.* 1971; 40: 34.
- Fukushima N, Edegger B, Muthukumar VN, Gros G. "Evaluation of matrix elements in partially projected wave functions." *Phys Rev.* 2005; 2; 505–14.
- Gray P. and Yoffe AD. "The reactivity and structure of nitrogen dioxide." *Chem. Rev.* 1955; 55. 1069-1154
- Greenblatt M, Mirvish S, and So B.T. "Nitrosamine Studies: Induction of Lung Adenomas by Concurrent Administration of Sodium Nitrite and Secondary Amines in Swiss Mice." *J. Nati. Cancer Inst.* 1971; 46: 1029-1034.
- Hisatune I C. "Thermodynamic Properties of some Oxides of Nitrogen." *J. Phys. Chem.*, 1961; 65: 2249. Jones K, Bailoar JC, Emeleus HJ, Nyholm RE. "Comprehensive Inorganic Chemistry." *Pergamon*, 1973; 2: 323–356.
- Kalatzis E, Ridd JH. "Nitrosation, Diazotisation, and Deamination. Part XII. The Kinetics of N-nitrosation of N-methylaniline." *J Chem Soc B.* 1966; 2325–2328.
- Keefer LK, Roller PP. "N-Nitrosation by Nitrite Ion in Neutral and Basic Medium." *Science.* 1973; 181:1245–47.
- Kemi., "Summary Risk Assessment Report of Piperazien." *Swedish Chemical Inspectoratte.* 2003
- Kemi., "Summary Risk Assessment Report of Piperazien." *Swedish Chemical Inspectoratt.*, 2005
- Kirsch M, Fuchs A, De Groot H. "Regiospecific Nitrosation of N-terminal-blocked Tryptophan derivatives by N₂O₃ at Physiological pH." *JBC.* 2003; 278: 11931–11936.

- Kirsch M, Korth H, Sustmann AR, De Groot H. "Carbon Dioxide but Not Bicarbonate Inhibits N-Nitrosation of Secondary Amines: Evidence for Amine Carbamates as Protecting Entities." *Chem Res Toxic.* 2000; 13(6):451–461.
- Kunisaki N, Hayashi M. "Formation of N-Nitrosamines from Secondary Amines and Nitrite by Resting Cells of Escherichia coli B." *App Envir Microbio.* 1979; 37(2):279–282.
- Lijinsky W, Conrad E, Van de Bogart R. "Nitrosamines formed by drug/nitrite interactions." *Nature (Lond.)*. 1972; 239:165–167.
- Love L.A, Lijinsky W, Keefer L, and Garcia H. "Chronic Oral Administration of 1-nitrosopiperazine in High Doses to MRC Rats." *Z. Krebsforsch.* 1977; 69-73.
- Lovejoy DJ, Vosper AJ. "Dinitrogen trioxide. Part VI. The reactions of dinitrogen trioxide with primary and secondary amines." *J Chem Soc A.* 1968; 2325-2328.
- Lv Cl, Liu YD, Zhong RG. "Theoretical investigation of N-Nitrosodimethylamine formation from Dimethylamine nitrosation catalyzed by carbonyl compounds." *J Phy Chem A.* 2009; 113(4): 713–718.
- Magee PA, Barnes JM. "Toxic liver injury. The metabolism of dimethylnitrosamine." *Biochem J.*, 1956; 64: 676–682.
- Masuda M, Mower HF, Pignatelli B, Celan M, Friesen MD, Nishino H, Ohshima H. "Formation of N-nitrosamines and N-nitramines by the reaction of secondary amines with peroxyxynitrite and other reactive nitrogen species: comparison with nitrotyrosine formation." *Chem Res Toxic.* 2000; 13(4): 301-8.
- Mirvish SS. "Kinetics of dimethylamine nitrosation in relation to nitrosamine carcinogenesis." *J Natl Cancer Inst.* 1970;44(3): 633–639.
- Mirvish SS, Wallcave L, Eagen M. "Ascorbate-Nitrite Reaction: Possible Means of Blocking the Formation of Carcinogenic N-Nitroso Compounds." *Science.* 1972; 177(4043): 65–68.
- Mirvish SS. "Formation of N-nitroso compounds: chemistry, kinetics, and in vivo occurrence." *Toxicol Appl Pharmacol.* 1975 Mar;31(3):325–351.
- Mitch WA, Sedlak DL. "Factors controlling nitrosamine formation during wastewater chlorination." *Water Supply*, 2002; 3:191–198.
- Mizgireuv I, Majorova IG, Gorodinskaya VM. "Carcinogenic effect of N-nitrosodimethylamine on diploid and triploid zebrafish." *Toxicol Patho.* 2004; 32: 514–518.
- MSDS, "Piperazine" SC-212561, *Santa Cruz Biotechnology, Inc.*, 2010.
- Oae S, Kim Y. H, Fukushima D, and Shinhama K. "New Syntheses of Thionitrites and their Chemical Reactivities" *J.Chem. Soc.* 1978; 913-017.

- Osterdahl BG, Ellander B. "Determination of N-mononitrosopiperazine and N,N'-dinitrosopiperazine in Human Urine, Gastric Juice and Blood." *J Chromatogram.* 1983; 278: 71.
- Parts L and Miller J T. "Reaction of Nitrosonium Nitrite with Isobutylrnr at 77-195 °K." *J. Phys. Chem.*, 1969; 73(9): 3088-3097.
- Polo J and Chow Y L. "Efficient Photolytic Degradation of Nitrosamines." *J. Nat. Cancer. Inst.* 1976; 56: 997.
- Ridd J H. "Nitrosation, Diazotisation and Deamination." *Rev. chem. Soc.* 1961; 15: 418.
- Russelles D, Onalod R, Exvan PE. "A Mechanism for the Reaction of Diethylamine with Nitric Oxide." *J. American Chem Soc.* 1961; 83; 4337-39.
- Sander J, LaBar J, Ladenstein M, and Schweinsberg F. "N-nitroso Compounds in the Environment." *IARC.* 1975; 123.
- Schmahl D, and Thomas C. "Erzeugung von Lungen- und Lebertumoren bei Mäusen mity Dinitrosopiperazin." *Z. Krebsforsch.* 1965; 67: 11-15.
- Sexton A. "Amine Oxidation in CO₂ Capture Processes." The University of Texas at Austin. Ph.D. Dissertation. 2008.
- Smith AS, Loeppky RN. "Nitrosative Cleavage of Tertiary Amines." *J Am Chem Soc.* 1967; 89(5):1147-1157.
- Tanaka H, Ando A, Ogura K, Ide S, Iida M, Oho K, Ozaki S, Iwamura K, Yamazaki A, Nakamura M, Maekawa T, Terumichi Y, and Tanaka S. " Electron Cyclotron Current Drive at the Second Harmonic in the WT-3 Tokamak." *Phys. Rev.* 1988; 60; 1033-1036.
- Tannenbaum SR, Wishnok JS, and Leaf CD. " Inhibition of Nitrosamine Formation by Ascorbic Acid", *American Journal of Clinical Nutrition.* 1991; 53: 247-.
- Thomas, C. "Zur Morphologie der Nasenhahentumoren bei der Ratte." *Z. Krebsforsch.* 1965; 67: 1-10.
- Trams A, and Kunkel H. A. "Keine MutationsaufllÄ sung durch V-Nitrosopiperidin und A'jV-Dinitrosopiperazin bei Escherichia coli." *Naturwissenschaften.* 1965; 52: 650-651.
- Tricker A.R, Kumar R, Siddiqi M, Khuroo M.S, and Preusmann R. "Endogenous Formation of N-nitrosamines from Piperazine and their Urinary Excretion Following Anthelmintic Treatment with Piperazine Citrate." *Carcinogenesis.* 1991; 12(9): 1595- 1599.
- Veleminsky J, and Gichner T. "The Mutagenic Activity of Nitrosamines in Arabidopsis thaliana." *Mutation Res.* 1968; 5: 429-431.

- Walash ML, Belal F, Ibrahim F, Hefnawy M, and Eid M. " LC determination of dinitrosopiperazine in simulated gastric juice." *Journal of Pharmaceutical and Biomedical Analysis*. 2001; 26(5-6): 1003-1008.
- Weisburger J. H, Weisburger E. K, Mantel N, Hadidian Z, and Fredrickson T. "New Carcinogenic Nitrosamines." *Naturwissenschaften*. 1966; S3: 508.
- White EH and Feldman WR. "The Nitrosation and Nitration of Amines and Alcohols with Nitrogen Tetroxide". *J. Am. Chem. Soc.* 1957; 79: 61.
- Williams D H. "S-Nitrosation of Thiourea and Thiocyanate ion." *J. Chem. Soc. Perkin Trans.* 1977; 2: 128.
- Williams D H. "S-Nitrosation and the Reactions of S-Nitroso Compounds." *Phys. Org. Chem.* 1983; 19: 381.
- Winter JW, Paterson S, Scobie G." Nitrosamine Generation from Ingested Nitrate Via Nitric Oxide in Subjects With and Without Gastroesophageal Reflux." *Gastroenterology*. 2007; 133: 164-174.
- Yang L, Chen Z, Shen J, Xu Z, Liang H, Tian J, Ben Y, Zhai Y, Shi L, and Li X. "Reinvestigation of the Nitrosamine-Formation Mechanism during *Ozonation*, *Environ. Sci. Technol.* 2009, 43 (14), 5481–5487
- Zabezhinskii M A. "On the Carcinogenic Effect of -Dinitrosopiperazine on Mice." *Vop. Onkol.* 1969; 75: 104-106.
- Zhao Y, Boyd J, Hruddy SE, and Li X. " Characterization of new nitrosamines in drinking water using liquid chromatography tandem mass spectrometry." *Environ. Sci. Technol.* 2007; 40; 7636–7641.
- Ziebarth D, Bogovski P, and Walker AE." N-nitroso Compounds in the Environment." *IARC*. 1975; 137.

Vita

Mandana Ashouripashaki graduated from the University of Tehran with a Bachelors Degree in Chemical Engineering in 1996. During her career, she worked in both academic and industrial fields as an instructor and process engineer. She got a Master's degree in Environmental and Water Resources Engineering from The University of Texas at Austin in 2008. She entered the Chemical engineering graduate program at the University of Texas at Austin in spring 2010.

This thesis was typed by author.